DIFFERENT BIOMASS CONVERSION STRATEGIES FOR VALUABLE CHEMICALS PRODUCTION

Llorenç Gavilà Terrades

Llorenç Gavilà Terrades

Different biomass conversion strategies for valuable chemicals production

Doctoral thesis

Supervised by:

Dr. Magdalena Constantí Garriga

Dr. Francesc Medina Cabello

Departament d'Enginyeria Química

UNIVERSITAT ROVIRA i VIRGILI

Tarragona

2017

UNIVERSITAT ROVIRA i VIRGILI

ESCOLA TÈCNICA SUPERIOR D'ENGINYERÍA QUÍMICA
DEPARTAMENT D'ENGINYERIA QUÍMICA

Av. Dels Països Catalans, 26
43007, Tarragona (Spain)
Tel. +34 977 55 96 03 / 04
e-mail: secdeq@etsequ.urv.es

Dr. Magdalena Constantí Garriga and Dr. Francesc Medina Cabello,

CERTIFY:

That the present study, entitled "Different biomass conversion strategies for valuable chemicals production", presented by Llorenç Gavilà Terrades for the award of the degree of Doctor, has been carried out under our supervision at the Chemical Engineering Department of this university.

Tarragona, 6th July 2017

Doctoral Thesis Supervisors

Dr. Magdalena Constantí Garriga

Dr. Francesc Medina Cabello

ACKNOWLEDGEMENTS

First of all I would like to thank my supervisors Dr. Magda Constantí and Dr. Francesc Medina, for trusting and giving me the opportunity to carry out my PhD in their groups. Also for their time during this three years. I also would like to thank the Martí Franqués fellowship for the financing support.

This doctoral thesis cannot be understood as the work of a sole person, in countless aspects many people has contributed to this work, so here I would to thank some of this people.

En Tarragona, me gustaría agradecer a todo el grupo de Catheter, así como a Interfibio por abrirme las puertas de su laboratorio y dejarme aprender en ellos. Muchas de estas enseñanzas se deben a Mayra y Antón, sin los cuáles ni esta tesis sería lo que es ni yo sería lo que soy. También la ayuda de Susana en todo momento ha contribuido a que esta tesis se acabara. Abel también ha sido un gran apoyo en el ámbito personal durante este tiempo. Las comidas y los cafés se han hecho mucho más amenos gracias a gente coma Quique, Paco Ana, y Suso. Finalmente, los escaladores Niko y Antonio, grupo que pese a haberse constituido un poco tarde han sido un gran apoyo en el último año.

Molta gent des de la distància ha sigut un gran suport durant estos tres anys. Victorio i Carlos, tot i la distància s'han sentit prop quan ha sigut necessari. Gran mención a Rafa y Migue por su paciencia durante estos tres años y los muy buenos ratos juntos.

En el poble, a garrot i pa dur al complet per estar sempre ahí i tindre sempre cervesa i cassalla fresca. També vull agrair a tota la meva família en lo personal, particularment als meus pares per el seu esforç fins arribar a ací.

Finalment, a Patri per la seva infinita paciència i comprensió, no ha segut fàcil estar al meu costat durant este temps, però ho has estat. Gràcies.

INDEX

LIST OF ABBREVIATIONS

DP - degree of polymerisation
SE - steam explosion
AFEX - ammonia fiber explosion
THF - tetrahydrofuran
ILs - ionic liquids
DBU - 1,8-diazabicyclo-[5.4.0]-undec-7-ene
PLA - poly-lactic acid
HMF - 5-hydroxymethylfurfural
FDCA - furandicarboxylic acid
DMF - 2,5 dimethylfuran
DHH - 2,5-dioxo-6-hydroxyhexanal
FA - furfural
PeD - pentanediol
SILs - switchable ionic Liquids
AD - arundo donax
LAB - lactic acid bacteria
MEA - monoethanol amine
AD - arundo donax
SCB - sugar cane bagasse
IPA - isopropanol
PFTE - polyfluoroethylene
HPLC - high pressure liquid chromatography
RID - refractive index detector
TOF - time of flight
ESI - electrospray ionization
TOC - total organic carbon
WSC - water soluble compounds
FTIR - fourier transform infrared
ATR - attenuated total reflection
XRD - X ray diffraction
CECT - colección española cultivos tipo
HEPES - 4-(2-hydroxyethyl)-1-piperazineethanesulfonic acid
CI - crystallinity index
MS - mass spectroscopy
OP - optically pure
CMF - 5-chloromethylfurfural
MMF - methoxymethylfurfural
AMF - 5-acetoxymethylfurfural
^{1}H-NMR - hydrogen nuclear magnetic resonance

GPC - gel permeation chromatography
UV - ultra violet
ACN - acetonitrile
DS - degree of substitution
FFA - furfuryl alcohol
THFA - tetrahydrofurfuryl alcohol
BET - Brunauer–Emmet–Teller
TPR - temperature-programmed reduction
TGA - thermogravimetric analysis
GC - gas chromatography
IUPAC - international union of pure and applied chemistry
EDX - electron dispersive X ray
JCPDS - Joint Committee on Powder Diffraction Standards
TPD-NH3 -thermal programmed desorption of ammonia

Chapter 1:

Introduction

1. BIOMASS AND BIOREFINERY SCOPE

Biomass is the most visible and available resource on earth, everywhere, every day biomass can be seen. Hence, it make sense to transform it into valuable outputs. Since primitive times, biomass transformation mainly consisted on burning it in order to obtain heat. Nowadays it still remains its main usage. However, chemical treatment of biomass opens a whole range of possibilities for biomass utilisation. For instance, pulp and paper industry has a long tradition of biomass modification in order to mainly obtain paper from wood. However depending on the pulping method, some of the side streams might be as well transformed (valorised), i.e. burning lignin to obtain heat, ferment hemicellulose to obtain ethanol… This can be seen as the origin of "modern" biorefinery concept.

Nonetheless, biomass utilisation as feedstock for chemical production did not have much sense back in the past centuries, since petrol shortage was not even questioned. However, nowadays, it seems that biomass conversion to valuable fuel and chemical products (current biorefinery definition) is gaining more attention due to a compendium of circumstances. Among them we can find autarkical political interests, environmental concerns, and the need of finding an alternative to petrochemical resources. Then in the past years the biorefinery concept has drawn substantial attention.

Before going into further detail, few words about the biomass concept. The term biomass is often defined as "the biodegradable fraction of products, wastes and residues with biological origin, from agriculture (including vegetable and animal substances), forestry and related industries including fisheries and aquaculture, as well as the biodegradable fraction of industrial and municipal waste".[1] However, in this thesis the word biomass would solely refer to vegetal biomass, concretely vegetal biomass coming from wood or energy crops.

Vegetal biomass is also referred as lignocellulose. Lignocellulose is claimed to be the most abundant available raw material on earth. For instance, according to FAOSTAT, 2800 MT/year of agricultural residues remain unexploited. Vegetal biomass is constituted by cellulose, hemicellulose, lignin, and a heterogeneous compendium of minor compounds, commonly denoted as extractives (see Scheme 1.1 for illustrative view). The content of each strongly depends on the biomass source, and defines most of the physico-chemical properties of the biomass sample.

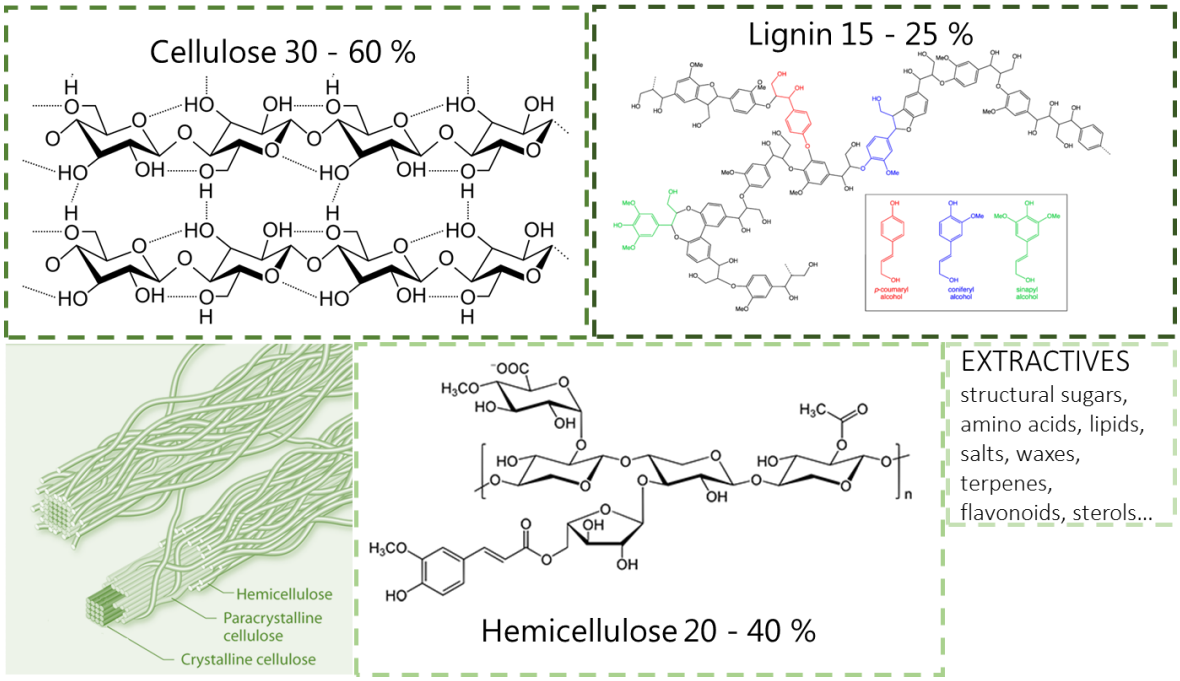

Scheme 1.1. Illustrative image of vegetal biomass components.

Cellulose is a linear polymer formed by units of glucose linked to each other through β-(1,4)-glycosidic bonds. One glucose molecule is axially turned 180º respect to the following, so the monomeric unit is often defined as the cellobiose unit (two linked glucose molecules). These polymeric chains are packed together forming microfibrils, among them, intramolecular and intermolecular hydrogen bonds strengthen its structure.[2] In addition, the supramolecular structure of cellulose is divided into areas of high order (crystalline) and low order (amorphous).[3] The presence of one or another is claimed to deeply impact on cellulose chemical robustness.[4] While amorphous cellulose is more accessible and simpler to hydrolyze, taking profit of crystalline cellulose is more challenging.

Hemicellulose is a highly branched heterogeneous amorphous polymer made of pentoses (xylose and arabinose), hexoses (glucose, mannose and galactose), and acid sugars (glucuronic and galacturonic acids). Despite its composition depends on the biomass source, normally, the major monomers found in hemicellulose are arabinose and xylose.

Lignin is a complex aromatic amorphous polymer, among its constituents phenyl propanoid precursors can be found (p-coumaryl, coniferyl, and sinapyl alcohol are shown in Scheme 1.1 as an example).

In summary, vegetal biomass is a complex heterogeneous matrix constituted by a wide variety of monomers. In a biorefinery context, vegetal biomass is meant to be upgraded into valuable fuel or chemical products. Since biomass has low density,

when compared to petroleum feedstocks, any biomass conversion technology should aim to take profit of all biomass fractions and do it in a sustainable way.

Two different strategies are used when converting biomass, one would basically aim to produce, from vegetal biomass, products which already have a place in the market; while the second aims to produce strategic molecules with a high potential for further conversions into monomers or chemicals. This strategic molecules receive the name of building blocks. Several studies have reviewed the potential of the desirable building blocks.[5–9] Normally, atom efficiency, functional versatility, and reactivity are the main principles for the successful election of the targeted building block.

In a biorefinery scheme these transformations can be classified in three different categories:

i) **Thermochemical**, which treats the whole biomass fraction at relatively high temperatures producing solid, liquid or gaseous products depending on the elected temperature.
ii) **Microbial**, this approach has a long use-history (i.e. breweries, bread…), microbial transformation mainly convert sugars into low molecular weight acids or alcohols, this conversions normally require a pretreatment in order to make sugar accessible to microorganisms.
iii) **Chemical-catalytic**, this processes usually target a single or a small range of products, and normally starts from a single biomass fraction or even an already biomass-based building block.

At this point, is worth taking a closer look to the different conversion strategies and the current state of the art of each.

1.1 Thermochemical biomass conversion

As previously mentioned, **burning** wood was and still is the main usage of vegetal biomass.[10] This represents around 10 % of the world energy consumption.[11] Over decades the efficiency of this process has been improved and still nowadays a lot of research on this topic is going on. We refer some nice reviews for more details of biomass combustion.[12–15]

A second thermochemical conversion is **pyrolysis**. Biomass pyrolysis can be defined as chemical decomposition, under heat influence (400 – 500 ^{o}C), in the absence of oxygen. Also, pyrolysis has been used, from ages, for charcoal production. However, in the last years pyrolysis for liquid products production has also been targeted. Many factors influence the product and process performance i.e. feedstock, catalyst,

additives, pressure… However, temperature and residence time are the main important factors, strongly influencing the ratio of obtained gas, solid, and liquid products. Again, we refer to expert reviewers for more detail.[16–19]

Finally, biomass **gasification** aims to convert solid biomass into a gas phase with high chemical energy by reaction at high temperatures (*ca.* 600 - 1500 ºC). Afterwards the obtained gas can be used directly as fuel[12,20] or condensed into valuable chemicals throughout catalytical assisted reactions e.g. Fischer-Tropsch or equivalent processes.[21]

Thermochemical conversions of biomass are promising strategies, and most likely would be required in the future for integrated biorefineries in one way or another. Albeit, in this thesis we would not address any critical aspect of thermochemical biomass conversions, hence, we refer the interested reader, to the above mentioned references for more information about thermochemical biomass conversions.

1.2 Pretreatment methods

Contrary to thermochemical conversion methods, most of the times biological and chemical methods do require of some treatment before the "transformation" itself. Although pretreatment itself cannot be classified as a pure transformation, sometimes pretreatment leads to direct transformation of some biomass fraction (see scheme 1.2 for an illustrative picture).

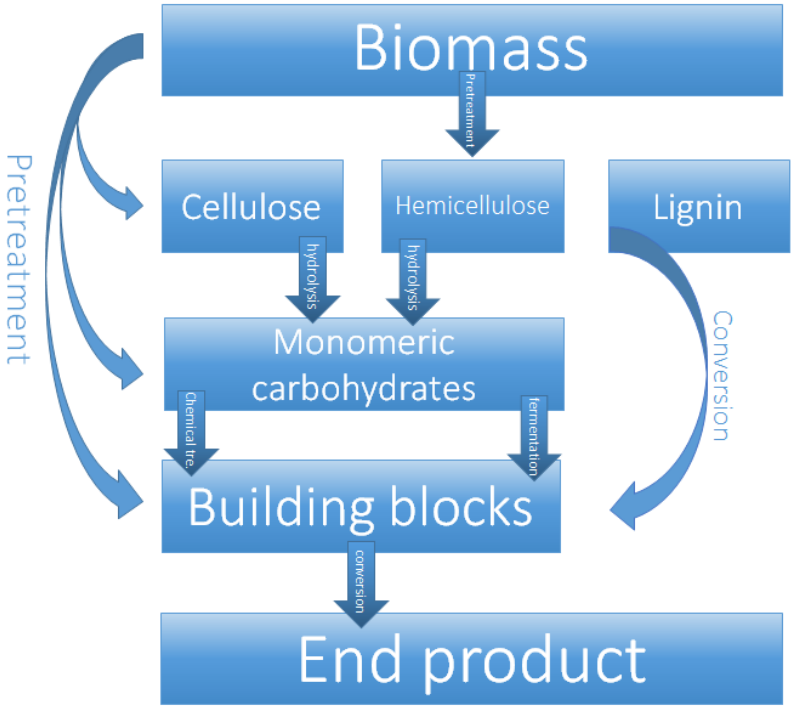

Scheme 1.2. Illustrative scheme of the overall biomass conversion strategies.

The beauty of biomass conversion into valuable chemical products, most of the times, relies on a proper combination of pretreatment method and transformation or even the blend between pretreatment and transformation.

The main objective of pretreatment is to permit the access to the different biomass fractions in order to facilitate i) the saccharification of cellulose (and hemicellulose if possible) into fermentable sugars or ii) the chemical conversion of some of the fraction (or solubilized molecules) into a valuable building block. Generally, due to the intimate association existing between the three main fractions of biomass the accessibility to polysaccharides is not trivial. When pretreatment aims to obtain separately the three different biomass process (or at least isolate one of them), receives the name of fractionation.

Generally, the election of the pretreatment method strongly depends on the physical nature, chemical composition, and textural properties of the biomass feedstock. Also the desired fraction and the extent of changes that are desired on each fraction has to be taken into account prior any election. So, the election of the appropriate fractionation technique not only depends on the available feedstock, but also of the type of process (or usage) that follows fractionation. Yet, this are some of the requirements than an ideal fractionation method should meet:[22,23]

1) Overcome biomass recalcitrance, facilitating the access of each fraction for the further transformation technique (ideally this would include cellulose decrystallization)
2) Allow the recovery of all fractions facilitating the utilisation of each
3) Avoid inhibitory products formation (for microbial biomass conversion approaches)
4) Be cost–effective and have a low energetic demand, while minimize waste generation

Since pretreatment methods are vital for any microbial biomass conversion and for chemical-catalytic approaches, here we would shortly describe some of them in order to give an appropriate background to the reader.

1.2.1 Milling

It is one of the most important physical treatments, and aims to, at least, reduce particle size. When treatment hardness increases, reduction of cellulose crystallinity and degree of polymerisation (DP) can also be achieved. By doing this the surface area of the feedstock increases, and thus, accessibility to the different biomass' fractions. Albeit, increasing hardness deeply impacts on the operational costs of the process, since concise milling methods such as ball milling are required in order to

reduce cellulose crystallinity. Interestingly, combining biomass milling with catalytic amounts of mineral acid leads to a complete soluble biomass fraction as reported by Meine et.al. (mechanocatalytic depolymerisation).[24]

1.2.2 Steam explosion (SE)

Biomass is treated with a high pressure water steam at high temperature (170 to 220 ºC) for a short time, and then it is rapidly depressurized (so-called explosion). This results in partial to almost solubilisation of hemicellulose, while lignin is removed and redistributed to some extent.[25] Producing then, a more digestible substrate with higher reactivity (surface area) towards further transformation reactions. In order to improve steam explosion efficiency, acid (normally SO_2 or H_2SO_4) is also added to the substrate (impregnated), reducing residence time and severity of the treatment.[23] However this increases reactor corrosion and an additional separation step is required.

1.2.3 Ammonia fiber explosion (AFEX)

Similarly to SE, in AFEX biomass is exposed to liquid anhydrous ammonia under high pressure and temperatures ranging from 160 to 180 ºC, and then the pressure is quickly released, thus rapidly vaporizing the ammonia. Compared with SE more solid fraction is recovered, achieving almost complete recovery of solids. The recovered solid also presents higher digestibility, meaning lower crystallinity and DP for cellulose, and lignin and hemicellulose partial cleavage. Even AFEX decreases severity when compared to SE, still presents problems such as ammonia recovery, which increases operational costs.

1.2.4 Super critical CO_2 explosion

Super critical carbon dioxide is used as solvent for biomass, CO_2 combines with the present water forming carbonic acid, and then CO_2 is suddenly released producing fibers explosion. This technique when compared to SE, operates at lower temperatures, and reduces operational costs when compared to AFEX. However lignin is barely affected during these treatments, and the high reactor costs also impede and straight forward scale-up.

1.2.5 Liquid hot water extraction

In this treatment biomass is soaked in water, which is heated at high temperatures (150 - 240 ºC) while the pressure is kept above water saturation point, maintaining, thus, water in liquid state. This process is also referred as auto-hydrolysis, because no chemicals are added. Rather, the acetyl moieties of hemicellulose, which are initially cleaved, enable hemicellulose dissolution. Temperature and residence time

are claimed to deeply impact on solids recovery and potential degradation of sugars.[26] The large amounts of water required and the energy needed for this processes are its main drawbacks.

1.2.6 Alkaline hydrolysis

By using alkaline solution, mainly sodium or calcium hydroxide, lignin and hemicellulose bonds are degraded to some extent. Thus basically solubilizing hemicellulose and some part of lignin (depending on the process conditions).[27] Long reaction times and the formation of salts during the process (which may incorporate into the produced solid and thus disturbing the following step) are some of the inconveniences of this treatment.

1.2.7 Acid hydrolysis

This method was already studied 100 years ago, and has a long tradition in biomass transformation industry. See table 1.1 (adapted from reference 28) for an historical overview of biomass acid hydrolysis process. Acid hydrolysis can achieve complete biomass dissolution, however it requires the use of concentrated acid and is associated to large formation of degradation products. These disadvantages together with the large use of acids (and associated waste/recovery/corrosion problems) have historically hampered large scale exploitation of these technologies. For more details of acid treatments we refer to a comprehensive review by Rinaldi and Schüth.[28] .

Table 1.1 (Adapted from reference 28). Acid processes used as biomass treatments.

Year	Process	Catalyst	T(ºC)
1923	Scholler	Dilute H_2SO_4	170
1937	Bergius	Conc. HCl	25
1945	Madison	Dilute H_2SO_4	180
1960	Noguchi	Gaseous HCl	45
1978	Grethlein	Dilute H_2SO_4	240
1981	Hoechst	Anhydrous HF	40
1985	Two-stage	Dilute H_2SO_4	170 (1^{st} stage)
			190 (2^{nd} stage)

In the last years, combining acid hydrolysis with other technologies in order to improve the existing methods (an example would be the above mentioned mechanocatalytic depolymerization) is gaining more attention.

In this line, in 2007 Orozco et. al.[29] reported for the first time combination of dilute acid treatment of cellulose and microwaves. They studied grass (and cellulose) dissolution with aqueous phosphoric acid, achieving 90 % of glucose yield at 175 ºC and 2.5 % w/w acid. They claimed that reaction rates were increased during microwave treatments, attributing this enhancement to the ability of microwave fields to disrupt cellulose hydrogen-bond matrix, as well as microwave ability to increase the rate of reactant and product diffusion. Although microwave intrinsic benefits still are a controversy,[30] since the publication of the paper by Orozco et. al., microwave popularity for biomass treatment did not stop growing. Microwave heating it has also been combined to other pretreatment methods such, alkaline hydrolysis or pretreatment with ionic liquids. We refer the reader to Chapter 10 of "Production of biofuels and chemicals with microwave"[31] for a more extend description of the state of the art for biomass microwave processing.

1.2.8 Organic solvation (Organosolv) treatment

An interesting method, which takes advantage of the different solvation properties of organic solvents, enabling selective dissolution of certain biomass' fractions. Among common solvents acetone, methanol, ethanol, or tetrahydrofurfuryl alcohol (THF) can be found. The advantages of these treatments are the ease of solvent recovery (usually organic solvent present high vapour pressure and can be readily distilled off), as well as the relatively simple recovery of the solvated fractions (normally by antisolvent addition). However due to high volatility of these organic solvents, process pressure dramatically increases and, thus, increasing reactor costs. Even this method is still under development, an interesting approach was studied in Leitner's group where they selectively extracted hemicellulose and lignin in a biphasic system with water (0.1 M oxalic acid)/2-methyltetrahydrofuran.[32,33]

1.2.9 Ionic liquids (ILs) treatment

Analogously to Organoslov methods, ionic liquids solvation properties are used for biomass fractionation processes. Shortly, ILs are salts with low melting point (normally below 100 ºC). In contrast to organic solvents, ILs do have low vapour pressure, then permitting low pressure processes. There is a wide range of ILs, and their properties can be accurately tuned for the desired solvation abilities by properly electing the anion and cation. First wood dissolution with ILs was reported by Fort et. al.[34] in 2007 (although a Finnish patent was already submitted)[35], since then interest in wood dissolution with ionic liquids vividly increased.[36–40]

ILs are one of the most promising techniques, however there are still some aspects that needs to be addressed (in order to be economically viable) prior its industrial application; such:

1) Reducing ILs production cost
2) Enabling efficient recycling of ILs
3) Increasing water tolerance (since intrinsic water content of biomass feedstocks)
4) Increase solid loading (biomass/ILs ratio)
5) Developing biocompatible ILs (for further microbial conversion steps)
6) Reasonable treatment conditions (time and temperature)

Again we refer the expert reader to specialized books in order to get more insights about the current state of the art.[41]

Interestingly, an alternative to common ILs was presented by Jessop et. al. They found a solvent capable to reversibly switch from non-ionic solution to an ionic liquid upon exposition to an acid gas such carbon dioxide.[42] In this publication they exposed a 1:1 mixture of a superbase such as DBU (1,8-diazabicyclo-[5.4.0]-undec-7-ene) and alcohol such as1-hexanol, to gaseous flow of CO_2, and at room temperature this liquid mixture was turned into an ionic liquid. Furthermore, when the ionic liquid was exposed to nitrogen bubbling this was readily turned back into a liquid solution. After this finding, different imaginative application of the so-called **switchable ionic liquids** (SILs) have been presented.[43–47] Interestingly, SILs were also used for biomass treatments, albeit, initially long times were required for extraction of lignin and hemicellulose.[48,49] However, modifying SIL properties, fractionation was achieved in presence of water, without agitation and at short treatment times.[50] So if we recall the above mentioned requirements for ILs exploitation for biomass treatments, some were already met by using SIL (water tolerance and reasonable working conditions), although some needs to be addressed (biocompatibility, reuse…).

1.3 Microbial biomass conversions

The flagship of microbial biomass transformation process is bioethanol production, and probably is the first thing that comes to everybody's mind when we talk about fermentative conversion of biomass derived products. Indeed, nowadays bioethanol is used to fuel cars, but more commonly as a fuel blend in certain countries. However there are many controversies regarding the actual production of bioethanol, since the current biomass' feedstocks consist of edible sources, and, thus, compete with food. When edible biomass is used as feedstock, biomass can be directly fermented

since it just consist on starch or sugars, then it does not require any sophisticated pretreatment (and that is why, it was the first one to be implemented). However, moving forward, and using, at least, the cellulosic fraction of biomass is a must (second generation biorefinery).[51] Hence, appropriate pretreatment methods are needed, in order to facilitate the production of fermentable sugars from non-edible biomass sources.

Normally, ethanol fermentation is carried out by yeast (*Saccharomyces cerevisiae*). During ethanol fermentation, one mole of glucose (C6) is converted into two moles of ethanol (C2) and two moles of carbon dioxide. During fermentation, not only glucose can be converted, hexoses are also readily fermented. Otherwise conversion of pentoses is more challenging and is gaining a lot of attention in order to improve economic viability of second generation biorefinery.

Analogously to ethanol, more chemicals can be produced through microbial fermentation. Depending on the employed microorganism different compounds can be targeted, having biogas or hydrogen as gas fuels or more complex molecules such as itaconic, succinic, or glutamic acids as valuable building blocks.

Another interesting chemical compound that is gaining more importance is **lactic acid**. Lactic acid (2-hydroxypropanoic acid) has traditionally been employed in pharmaceutical and alimentary industry. Recently, lactic acid has gained more importance in industry because its usage as a precursor for poly-lactic acid (PLA) production. PLA, a thermoplastic aliphatic polyester, is becoming a highly consumed bioplastic. European demand for PLA in 2008 was 25 000 tons per year, and could potentially reach 650 000 tons per year in 2025.[52] Lactic acid is produced either by chemical synthesis or fermentative processes. Chemical based synthesis involves the use of petrochemical resources and leads to a racemic mixture of lactic acid. However, high isomeric purity of lactic acid is desired in order to obtain good physical properties of the further produced PLA.[53] Rather, using fermentative processes, glucose can be transformed into almost isomerically pure lactic acid.[54] Even microbial fermentation is the preferred synthetic way for lactic acid production, again, we face the same problem that for bioethanol production: the need to employ a sustainable feedstock. As just mentioned above, the shift from first generation biofuels towards second generation biofuels, comes together with the need of moving towards cheaper and sustainable raw materials for fermentative processes.

1.4 Chemical-catalytic biomass conversion

Microbial biomass transformation methods rely on microbial ability to transform sugars into concrete molecules. Hence the number of produced chemicals is restricted to countable number of products (even if genetic modification of microbial strains is increasing the range of products that can be produced through fermentation).

Chemical-catalytic transformation can vastly increase the range of products that can be obtained from biomass. Chemical-catalytic biomass transformation can either transform one biomass fraction into a valuable building block or upgrade an already biomass-produced building-block. Most of the chemical-catalytic biomass conversion strategies aim to obtain either fuels (or fuels additives)[7,55] or building block molecules.[6,8] Catalytic transformation of platform molecules into eiter liquid fuels or building blocks appears an interesting route for biomass exploitation. However, biomass platform molecules are highly oxygenated compounds, then high oxygen removal is needed for fuel production (hydrogenation, dehydration, hydrogenolysis…). Also, molecular weight enhancement is eventually needed (C5 or C6 building blocks at most), reaching molecules in the range of C10-C20 if the fuel is to be used for diesel engines; hence, C-C coupling reactions are also needed. Eventually isomerization reactions are also involved, e.g. glucose-fructose isomerisation. Finally for building blocks upgrading, oxidation reactions are also sometimes required. So if we take into account the high number of required reactions together with the broad range of available feedstocks, a countless number of reactions are involved. Here we would briefly refer about the current state of the art of the chemical conversions involved in this thesis experimentation. The interested reader can refer to several reviews for additional information[6,8,55–59].

1.4.1 Cellulose hydrolysis

As described in section 1.2.7, cellulose can be hydrolysed in acidic conditions. For cellulose hydrolysis the glycosidic bond which links glucoses units needs to be cleaved. A short reaction scheme can be seen in scheme 1.3 (reproduced from reference 28). Two different pathways are proposed, although pathway II needs stronger evidences to be proven. Shortly, the hydronium ion approaches the oxygen of the glycosidic bond and either protonates it (pathway I), or protonates the oxygen present in the glucose ring (pathway II). Then is formed an acyclic (pathway I) or cyclic (pathway II) carbocation which reacts with water (step 3) reestablishing the anomeric position and regenerationg the hydronium ion.

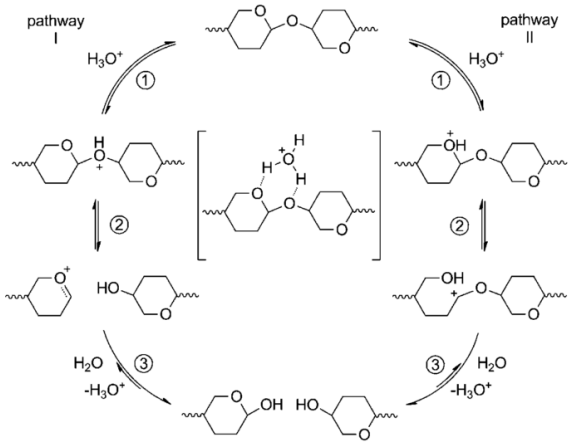

Scheme 1.3 (adapted from reference 28). Mechanism of acid hydrolysis of glycosidic bond. (The authors omitted hydrogen and hydroxyl groups, which are not involved in the hydrolysis, for clarity).

By breaking the glycosidic bond present in cellulose, the cellulose chains are shortened and eventually glucose units are produced. However, while this process is occurring, the produced sugars are simultaneously being degraded (most likely dehydrated). Although hydrolysis and sugar degradation rates depend on the employed conditions, for most of the conventional processes both degradation rates are in the same order of magnitude.[28] Resulting, then, in low selectivity towards glucose, which actually hampers biomass exploitation for chemicals production. However, the current development of solid acid catalyst for cellulose hydrolysis might overcome the above mentioned problems, we refer the review by Hunag and Fu for a comprehensive understanding of the solid acid catalyst employed for cellulose hydrolysis.[60]

1.4.2 Glucose dehydration

The dehydration of glucose in acidic conditions leads to the formation of 5-hydroxymethylfurfural (HMF) (*via* glucose-fructose isomerization). HMF is considered one of the most versatile building blocks that can be produced from biomass, since it is a significant intermediate with enormous potential. For instance in polymer science[61] or as fuel additives[62] thanks to its derivatives furandicarboxylic acid (FDCA) and 2,5 dimethylfuran (DMF), respectively.

However, HMF readily rehydrates in hydrothermal aqueous acidic conditions (most commonly employed working conditions) forming levulinic and formic acid. Furthermore, HMF can also rehydrate forming 2,5-dioxo-6-hydroxyhexanal (DHH) which favours the formation of condensation products (normally referred as humins).[63,64] More mechanistic insights about humins formation would be discussed in chapter 2. As an alternative, biphasic solvent systems [65,66] or organic solvents[67–69] have been developed to improve HMF yield.

1.4.3 Hemicellulose hydrolysis

Acid hydrolysis using mineral acids such as sulfuric, hydrochloric, nitric, or phosphoric acids readily cleaves the glycosidic bonds of hemicellulose. The reaction products are mainly monomeric sugars (majorly xylose). Hydrolysis is performed between 80 and 150 ^{o}C, and the amount of acid used is normally ranging 0.1 - 0.5 M. Hydrolysis yields range from 70 to 95% in released sugars.[70] Albeit hemicellulose is readily hydrolysed few industrial processes focus on the sole hemicellulose monosaccharaides production, rather further processes such as pentose dehydration are employed in industry. Being furfural formation one of the most important chemical compound derived from biomass nowadays.

1.4.4 Pentose dehydration

When pentoses are hydrothermally treated in acidic conditions, furfural (FA) is readily produced. Pentoses dehydrate similarly to hexoses (glucose) *via* cyclodehydration. Although, the precise order of the different dehydration steps is not known for certain. Different strategies are employed in industry, in order to avoid FA condensation into humins (similar to HMF condensation described in 1.4.2), for instance FA steam striping.[71]

Thus, FA is a low cost, polyfunctional substrate produced entirely from biomass. FA can be used for the production of numerous bulk and fine chemicals, for an illustrative view see scheme 1.4 (reproduced from reference 71). We refer the interested reader to reference 71 for detailed information about the chemical reactions that FA can undergo in order to form the depicted compounds.

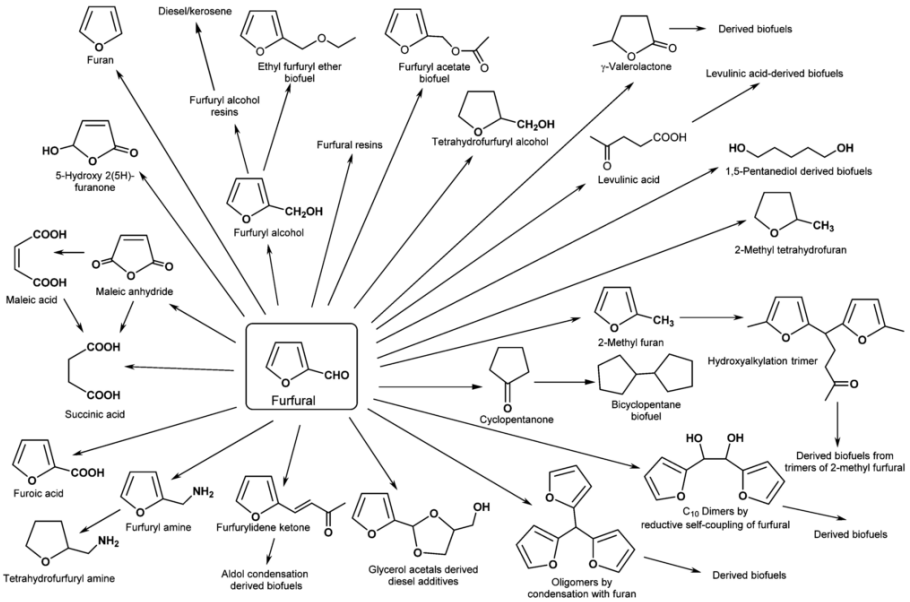

Scheme 1.4 (adapted from reference 71). Furfural derived chemicals.

Among this reactions, hydrogenation is probably one of the most important in industry for FA related chemical compounds production.[72] A wide range of products can be produced *via* hydrogenation of FA, e.g. furfuryl alcohol, tetrahydrofurfurylalcohol, methylfuran, tetrahydromethylfuran, cyclopentanone or open ring product such as different pentanediols. The production of these different products mostly depends on the reaction conditions and on the nature of the catalyst used. Among this products, straight chain diols are valuable targets due to its use as monomers and resin precursors. Production of diols from FA requires hydrogenation of the aldehyde group, double bond hydrogenation and dissociation of C-O present in the furan ring.

However, due to the high amount of competitive reactions that FA can undergo the direct use of FA as starting material still remains a challenge. Tomishigue's group has been intensively researching on diols production from renewable sources, and has successfully developed a two steps system, using Pd-Ir-ReOx/SiO_2 as catalyst, which achieved 71 % yield of 1,5-Pentanediol (1,5-PeD), which until now is the greatest yield of 1,5-PeD achieved from FA.[73] Despite the great potential of this bifunctional catalyst, both of the active sites are based on precious metals, which highly impacts on the cost of this technology and limits its application in a biorefinery scenario. Thus the development of a non-noble metal catalyst for diols production from FA is still needed.

1.5 Aim of the thesis

So far, here, current state of the art of biomass and biorefinery has been presented. It is a broad topic in constant development with numerous cases of success and failure. Also, in this thesis, some of the topics that are up-to-date being under development are addressed, related to biomass fractionation technologies, microbial conversions and chemical-catalytic conversions.

By the present thesis we aim to present different strategies for the whole picture of biomass conversion i) producing fermentable sugars from both cellulose and lignocellulose and prove their viability for microbial conversion; ii) developing an integrated strategy to produce a valuable building block from lignocellulose; and iii) upgrading a building block such as furfural to an end product like 1,5-pentanedienol. Then, this thesis is divided in three parts.

Chapter 2 is focussed on the production of fermentable sugars (glucose) from, cellulose, pulp produced with switchable ionic liquid, and biomass. So, in this section the fractionation of two types of biomass is studied (*Saccharum officinarum* bagasse and *Arundo donax*) using switchable ionic liquids. Afterwards the dilute acid hydrolysis of cellulose, the different obtained pulps and the raw biomass is studied using a microwave reactor. And finally the obtained hydrolysate is fermented by *Lactobacillus delbrueckii* in order to prove that the obtained glucose can be efficiently converted to optically pure lactic acid (a valuable building block with a growing demand for bioplastics production).

In **chapter 3,** a new approach for biomass conversion into building blocks is presented. First, instead of using bare cellulose as feedstock, a cellulose derivate such as cellulose acetate is produced (from different biomass sources, i.e. cellulose, Organocat[33] pulp, and Beech wood). Afterwards, these cellulose acetates are submitted to dilute acid hydrolysis (batch and flow) and a HMF derivative (5-acetoxymethylfurfural) is produced. 5-acetoxymethylfurfural is a versatile building block, analogous to HMF, which can be derived into numerous valuable chemical compounds (for bioplastics or fuel applications for instance).

Finally, in **chapter 4** the upgrading of furfural, a strategic building block, into a straight chain diol is studied. For this, a Co-spinel is first characterised and afterwards its catalytic properties are studied in a batch reactor. Different reduction temperatures for catalyst, reaction times, hydrogen loading pressure and reaction temperatures are tested. As a result, for the first time a noble-metal free catalyst is employed for the production of 1,5-pentanediol (which has an extended use as monomers and resin precursors) from furfural.

2. References

1 EU, *Renewable energy directive (2009/28/EC)*, .

2 C. Loerbroks, R. Rinaldi and W. Thiel, *Chemistry*, 2013, **19**, 16282–94.

3 D. Klemm, B. Heublein, H. Fink and A. Bohn, *Angewandte*, 2005, **44**, 3358–3393.

4 S. Haghighi, A. Hossein Golfeshan, M. Tabatabaei, G. Salehi Jouzani, G. H. Najafi, M. Gholami and M. Ardjmand, *Renew. Sustain. Energy Rev.*, 2013, **27**, 77–93.

5 T. and P. G. Werpy, *Natl. Renew. Energy Lab.*, 2004, 76.

6 P. Gallezot, *Chem. Soc. Rev.*, 2012, **41**, 1538–1558.

7 M. J. Climent, A. Corma and S. Iborra, *Green Chem.*, 2014, **16**, 516.

8 A. Corma, S. Iborra and A. Velty, *Chem. Rev.*, 2007, **107**, 2411–2502.

9 J. J. Bozell and G. R. Petersen, *Green Chem.*, 2010, **12**, 539.

10 J. Chow, R. J. Kopp and P. R. Portney, *Science*, 2003, **302**, 1528–31.

11 W. van Swaaij, S. Kersten and W. Plaz, *Biomass power for the world*, Pan Stanford Publishing, 2015.

12 A. C. Caputo, M. Palumbo, P. M. Pelagagge and F. Scacchia, *Biomass and Bioenergy*, 2005, **28**, 35–51.

13 B. M. Jenkins, L. L. Baxter, T. R. J. Miles and T. R. Miles, *Fuel Process. Technol.*, 1998, **54**, 17–46.

14 A. Demirbas, *Prog. Energy Combust. Sci.*, 2004, **30**, 219–230.

15 R. Saidur, E. A. Abdelaziz, A. Demirbas, M. S. Hossain and S. Mekhilef, *Renew. Sustain. Energy Rev.*, 2011, **15**, 2262–2289.

16 F. Shafizadeh, *J. Anal. Appl. Pyrolysis*, 1982, **3**, 283–305.

17 S. Yaman, *Energy Convers. Manag.*, 2004, **45**, 651–671.

18 D. Mohan, C. U. Pittman and P. H. Steele, *Energy and Fuels*, 2006, **20**, 848–889.

19 H. Yang, R. Yan, H. Chen, C. Zheng, D. H. Lee, V. Uni, N. D. V, R. V March, V. Re, M. Recei and V. September, *Energy and Fuels*, 2006, **20**, 388–393.

20 P. McKendry, *Bioresour. Technol.*, 2002, **83**, 55–63.

21 M. J. A. Tijmensen, A. P. C. Faaij, C. N. Hamelinck and M. R. M. Van Hardeveld, *Biomass and Bioenergy*, 2002, **23**, 129–152.

22 P. Alvira, E. Tomás-Pejó, M. Ballesteros and M. J. Negro, *Bioresour. Technol.*, 2010, **101**, 4851–4861.

23 M. H. L. Silveira, A. R. C. Morais, A. M. Da Costa Lopes, D. N. Olekszyszen, R. Bogel-Lukasik, J. Andreaus and L. Pereira Ramos, *ChemSusChem*, 2015, **8**, 3366–3390.

24 N. Meine, R. Rinaldi and F. Schüth, *ChemSusChem*, 2012, **5**, 1449–1454.

25 X. Pan, D. Xie, N. Gilkes, D. J. Gregg and J. N. Saddler, *Appl. Biochem.*

Biotechnol., 2005, **121–124**, 1069–1079.

26 M. Laser, D. Schulman, S. G. Allen, J. Lichwa, M. J. Antal and L. R. Lynd, *Bioresour. Technol.*, 2002, **81**, 33–44.

27 M. M. Ibrahim, W. K. El-Zawawy, Y. R. Abdel-Fattah, N. A. Soliman and F. A. Agblevor, *Carbohydr. Polym.*, 2011, **83**, 720–726.

28 R. Rinaldi and F. Schüth, *ChemSusChem*, 2009, **2**, 1096–107.

29 A. Orozco, M. Ahmad, D. Rooney and G. Walker, *Process Saf. Environ. Prot.*, 2007, **85**, 446–449.

30 C. O. Kappe, B. Pieber and D. Dallinger, *Angew. Chemie - Int. Ed.*, 2013, **52**, 1088–1094.

31 Z. Fang, R. L. Smith and X. Qi, *Production of Biofuels and Chemicals with Microwave*, 2015.

32 T. vom Stein, P. M. Grande, H. Kayser, F. Sibilla, W. Leitner and P. Domínguez de María, *Green Chem.*, 2011, **13**, 1772.

33 P. M. Grande, J. Viell, N. Theyssen, W. Marquardt, P. Domínguez de María and W. Leitner, *Green Chem.*, 2015, **17**, 3533–3539.

34 D. A. Fort, R. C. Remsing, R. P. Swatloski, P. Moyna, G. Moyna and R. D. Rogers, *Green Chem.*, 2007, **9**, 63–69.

35 Dissolution method-US20080023162, 2008, 1.

36 A. S. Amarasekara and O. S. Owereh, *Ind. Eng. Chem. Res.*, 2009, **48**, 10152–10155.

37 R. D. Sun, N., Rahman, M., Qin, Y., Maxim, M.L., Rodriguez, H., Rogers, *Green Chem.*, 2009, **5**, 646–655.

38 C. Li, B. Knierim, C. Manisseri, R. Arora, H. V. Scheller, M. Auer, K. P. Vogel, B. A. Simmons and S. Singh, *Bioresour. Technol.*, 2010, **101**, 4900–4906.

39 N. Sun, H. Rodríguez, M. Rahman and R. D. Rogers, *Chem. Commun. (Camb).*, 2011, **47**, 1405–1421.

40 H. Wang, G. Gurau and R. D. Rogers, *Chem. Soc. Rev.*, 2012, **41**, 1519–1537.

41 R. Bogel-łukasik, *Ionic liquids in the biorefinery concept: challenges and perspectives*, Royal Society of Chemistry, 2016.

42 P. P. G. Jessop, D. J. D. Heldebrant, X. Li, C. A. C. Eckert and C. C. L. Liotta, *Nature*, 2005, **436**, 1102.

43 Y. Yoshida and G. Saito, *Phys. Chem. Chem. Phys.*, 2010, **12**, 1675–1684.

44 Y. Himeda, N. Onozawa-Komatsuzaki, H. Sugihara and K. Kasuga, *Organometallics*, 2007, **26**, 702–712.

45 M. L. Stone, C. Rae, F. F. Stewart and A. D. Wilson, *Desalination*, 2013, **312**, 124–129.

46 Q. Zhang, N. S. Oztekin, J. Barrault, K. De Oliveira Vigier and F. Jérôme, *ChemSusChem*, 2013, **6**, 593–596.

47 Ionic liquids for solubilizing polymers. WO2008043837A1, 2008.

48 I. Anugwom, P. Mäki-Arvela, P. Virtanen, S. Willför, P. Damlin, M. Hedenström and J.-P. Mikkola, *Holzforschung*, 2012, **66**, 809–815.

49 I. Anugwom, P. Mäki-Arvela, P. Virtanen, S. Willför, R. Sjöholm and J.-P. Mikkola, *Carbohydr. Polym.*, 2011, **87**, 2005–2011.

50 I. Anugwom, V. Eta, P. Virtanen, P. Mäki-Arvela, M. Hedenström, M. Yibo, M. Hummel, H. Sixta and J.-P. Mikkola, *Biomass and Bioenergy*, 2014, **70**, 373–381.

51 P. S. Nigam and A. Singh, *Prog. Energy Combust. Sci.*, 2011, **37**, 52–68.

52 D. A. H. L Nattrass, *http//www. nnfcc.co.uk/publications/nnfcc-renewable-chemicals-factsheet-lactic-acid . Accessed 3 Jun 2016*, 2010.

53 A. J. R. Lasprilla, G. a R. Martinez, B. H. Lunelli, A. L. Jardini and R. M. Filho, *Biotechnol. Adv.*, 2012, **30**, 321–328.

54 K. Madhavan, N. R. Nair and R. P. John, *Bioresour. Technol.*, 2010, **101**, 8493–8501.

55 G. W. Huber, S. Iborra and A. Corma, *Chem. Rev.*, 2006, **106**, 4044–4098.

56 M. J. Climent, A. Corma and S. Iborra, *Green Chem.*, 2011, **13**, 520–540.

57 J. C. Serrano-Ruiz and J. A. Dumesic, *Energy Environ. Sci.*, 2011, **4**, 83–99.

58 S. G. Wettstein, D. Martin Alonso, E. I. Gürbüz and J. a. Dumesic, *Curr. Opin. Chem. Eng.*, 2012, **1**, 218–224.

59 D. Esposito and M. Antonietti, *Chem. Soc. Rev.*, 2015, **44**, 5821–5835.

60 Y.-B. Huang and Y. Fu, *Green Chem.*, 2013, **15**, 1095–1111.

61 A. F. Sousa, C. Vilela, A. C. Fonseca, M. Matos, C. S. R. Freire, G.-J. M. Gruter, J. F. J. Coelho and A. J. D. Silvestre, *Polym. Chem.*, 2015, **6**, 5961–5983.

62 Y. Román-Leshkov, C. J. Barrett, Z. Y. Liu and J. a Dumesic, *Nature*, 2007, **447**, 982–985.

63 S. K. R. Patil and C. R. F. Lund, *Energy and Fuels*, 2011, **25**, 4745–4755.

64 S. K. R. Patil, J. Heltzel and C. R. F. Lund, *Energy and Fuels*, 2012, **26**, 5281–5293.

65 J. N. Chheda, Y. Roma and J. A. Dumesic, *Green Chem.*, 2007, **9**, 342–350.

66 B. Saha and M. M. Abu-Omar, *Green Chem.*, 2014, **16**, 24–38.

67 R. Weingarten, A. Rodriguez-Beuerman, F. Cao, J. S. Luterbacher, D. M. Alonso, J. A. Dumesic and G. W. Huber, *ChemCatChem*, 2014, **6**, 2229–2234.

68 L. Shuai and J. Luterbacher, *ChemSusChem*, 2015, **9**, 133–155.

69 M. A. Mellmer, C. Sener, J. M. R. Gallo, J. S. Luterbacher, D. M. Alonso and J. A. Dumesic, *Angew. Chemie - Int. Ed.*, 2014, **53**, 11872–11875.

70 F. Martel, B. Estrine, R. Plantier-Royon, N. Hoffmann and C. Portella, *Top. Curr. Chem.*, 2010, **294**, 79–115.

71 R. Mariscal, P. Maireles-Torres, M. Ojeda, I. Sádaba and M. López Granados,

Energy Environ. Sci., 2016, **9**, 1144–1189.

72 D. Sun, S. Sato, W. Ueda, A. Primo, H. Garcia and A. Corma, *Green Chem.*, 2016, **18**, 2579–2597.

73 S. Liu, Y. Amada, M. Tamura, Y. Nakagawa and K. Tomishige, *Green Chem.*, 2014, **16**, 617–626.

Chapter 2:

Bacterial D-lactic acid production from different biomass sources

1. INTRODUCTION

Different chemical compounds have been identified as profitable products which can be obtained from biomass.[1] Among them, lactic acid (2-hydroxypropanoic acid) is a highly demanded chemical. Lactic acid has traditionally been employed in pharmaceutical and alimentary industry. Nonetheless since polylactic acid (PLA) demand rise, together with the interest in biopolymers, lactic acid demand did not stop growing, as an example PLA European demand can reach 650 000 tons/year in 2025.[2] Lactic acid can be produced either by chemical synthesis or fermentative processes. While chemical based synthesis involves the use of petrochemical resources and leads to a racemic mixture of lactic acid, when using fermentative processes, biomass can be used as feedstock and isomerically pure lactic acid can be produced.[3] High isomeric purity of lactic acid is required in order to obtain good physical properties of the further PLA.[4]

The current limitation of fermentative processes is the raw material source. Nowadays the shift from first generation biofuels towards second generation biofuels, comes together with the need of moving towards vastly available and sustainable raw materials for fermentative process. Nevertheless, the required pretreatment method is the current bottleneck. Thus, a lot of efforts are being done in order to establish a reliable pretreatment process to facilitate the biomass digestion by lactic acid bacteria.[5]

Woody biomass is an abundant raw material, vastly available in nature. Each of the three main components of woody biomass, namely lignin, hemicelluloses and celluloses are themselves valuable resources, if being selectively separated.[6] Kraft pulping is undoubtedly the most popular method in paper mills. Even Kraft pulping endless advances have been constantly improving its efficiency and reducing the emission of environmental pollutants, its intrinsic usage of toxic and hazardous chemicals will always remain a burden for complete green processing.[7] Hence, new and economically attractive fractionation methods are being studied in order to regenerate pulp and paper industry. Kemira patent of wood dissolution in ionic liquids became public in 2008.[8] In the meanwhile, Fort *et al.* reported dissolution of wood in ionic liquids (ILs) in 2007,[7] since then, ionic liquids have been intensively studied as efficient solvents for woody biomass fractionation. ILs have tuneable physicochemical properties, high boiling points and, usually, great thermal stability. Therefore, controlling ILs properties, different aims concerning biomass dissolution can be achieved: from dissolving cellulose[9] or lignin[10], to accurately fraction biomass into its components.[11] Switchable ionic Liquids (SILs) have been studied as fractionation solvents for woody biomas.[12] SILs are solvents capable of ionic/non-ionic switching by addition or of a trigger, commonly an acid gas.[13] Thus, the advantage of SILs in front of common ILs, basically relies on their ability to switch,

at will, from ionic molten salt to a liquid solution. This can be of a particular interest for separation, purification and reuse for pulping purposes.

After pulping, most of biomass application for chemical production rely on enzymatic saccharification of cellulose, producing fermentable sugars which are finally converted by bacteria to the desired end product, e.g. the well-known bioethanol. However, it is claimed that the high enzyme cost and strict control of temperature and pH required by enzymes, are responsible for the vast majority of the operational costs when scaling-up of these processes.[14]

Thereby, in the recent years, microwave assisted hydrolysis of cellulose has been purposed as a stimulating alternative.[15] Microwave treatment is reported to hydrolyze cellulose efficiently thanks to the formation of hot spots, which break up the crystalline structure and increase the degradation of the material.[16,17]

In this chapter, first, dilute acid treatment of crystalline cellulose assisted by microwave heating is studied as first approach for microbial production of lactic acid from biomass. Then, we study the fractionation of two different biomass sources: sugar cane bagasse (SCB), produced massively; and *Arundo donax* (AD) or giant cane, which has been posed as one of the energy crops in Mediterranean areas. For this, a SIL based on an organic super base, 1,8-diazabi-cyclo-[5.4.0]-undec-7-ene (DBU); an amine, monoethanol amine (MEA); and SO_2 as switching gas was used. Afterwards, in order to prove the suitability of the produced pulp for a whole biorefinery scheme, pulp was hydrolysed with dilute acid assisted by microwave and further fermented by lactic acid bacteria (LAB).

2. METHODOLOGY

2.1 Materials and methods

Commercial microcrystalline cellulose powder (Sigma-Aldrich) was used in cellulose hydrolysis experiments. SILs were prepared from DBU, MEA, and SO_2 by previously reported methods.[12] Briefly, an equimolar mixture of DBU and MEA was added into a three-neck round bottom flask. Acid gas was then bubbled through the mixture under rigorous stirring. The exothermic reaction was occurring until the reaction to form the SIL was finished. *Arundo donax* and sugar cane bagasse (*Saccharum officinarum* bagasse) were kindly provided by colleagues from the mechanical engineering department in URV, Tarragona. The samples were grounded using a 4 mm sieve and dried at 60 ºC prior its utilization. 2-propanol, sulphuric acid and the rest of reagents were bought at Sigma-Aldrich. The enzymatic kit for determination of L-lactic acid was purchased from Oenolab diagnostics.

2.2 Pulping of *Arundo donax* and sugar cane bagasse with switchable ionic liquids

A total of 2 grams of *Arundo donax* (AD) or sugar cane bagasse (SCB) was mixed with 10 grams of SIL and 6 mL of distilled water. The samples were irradiated, in a 100 ml PFTE reactor, with a microwave system (Milestone ethos-touch control) at 120 ºC or 160 ºC 1 or 2 hours with a maximum power of 400 watts without any agitation. The desired temperature was quickly reached due to the ionic nature of the solvent mixture. Thus microwave irradiation seems a reasonable way to heat up this type of solvent mixtures. Once the reaction finished, the reaction mixture was allowed to cool down to *circa* 80 ºC and vacuum filtered, and the solid fraction (pulp) was thoroughly washed with warm (60 ºC) isopropanol (IPA). Then the recovered liquid (SIL+IPA) was mixed and more IPA was added to reach a final volume of 80 mL, here due to the antisolvent effect, another solid fraction was recovered from the SIL, i.e. the extracted part from the wood by SIL. This solid fraction was centrifuged, filtered, washed, dried and weighted. While the mixture SIL+ IPA was separated with a rotary evaporator (see scheme 2.1 for an overall view of SIL treatment). For the reuse experiments, to the recovered SIL + water, additional water was added to reach a final weight of 16 g and the 2 grams of fresh sample was added. Sample names were given "SIL#" according to appearance order in Table 2.1 and named as assigned thereafter.

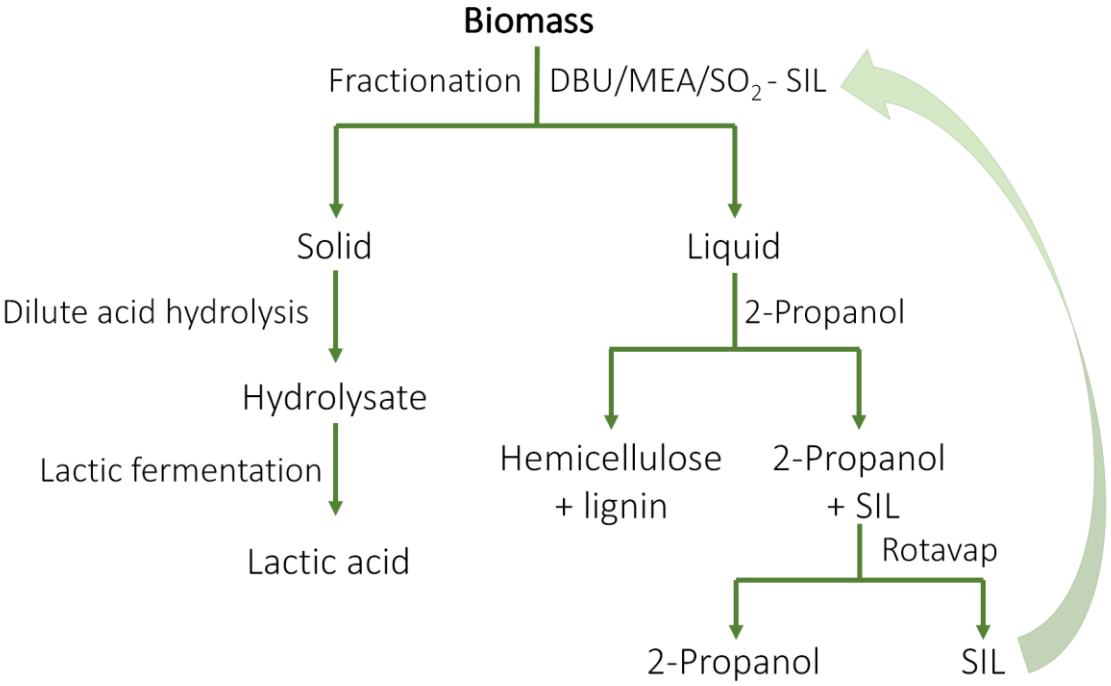

Scheme 2.1. Scheme of biomass pulping with SILs.

2.3 Hydrolysis experiments

Despite similarities between samples, cellulose and AD, SCB and the prepared pulps were not hydrolysed in the same conditions (or microwave set-up). This differences were only due to time lapses between the two experiments. Raw biomass and the prepared pulps were not impregnated with sulphuric acid prior hydrolysis due to the non-homogeneous nature of these samples (when compared to commercial available powder microcrystalline cellulose).

2.3.1 Cellulose hydrolysis

Cellulose was impregnated with sulphuric acid at 3 % wt. then the samples were dried overnight at 100 ºC. All hydrolysis experiments were carried out in a PFTE reactor loading 1 g of impregnated cellulose and 20 mL of deionized water. The samples were irradiated at 400 watts with a microwave system (Milestone ethos-touch control) at 120 ºC for 4 hours, 2 hours and 30 minutes. The hydrolysis experiments were done in triplicate and the results expressed as mean and standard deviation.

2.3.2 Dilute acid hydrolysis of AD, SCB and the prepared pulp

The recovered pulp, AD, and SCB were hydrolysed in a Milestone Synthwave microwave reactor. A total of 1 gram of dried sample was placed in a 30 mL glass tube and mixed with 20 mL of a solution 0.05 M of sulphuric acid (10 % wt. corresponding to the solid sample) and irradiated 15 minutes at 160 ºC under 400 rpm stirring.

2.4 Characterisation of cellulose, AD, SCB and pulp hydrolysates

After hydrolysis, the liquid fraction was separated from the solid fraction by vacuum filtration. The hydrolysate was measured by HPLC system (HPLC Agilent 1100 series) with ICSep ICE-COREGEL 87H3 as column, using RID as detector. The aqueous mobile phase was deionized and its pH was adjusted to 2.2 with H_2SO_4. The HPLC column operated at 50 ºC with a mobile phase flow of 0.6 mL/min. Each analysis injected 20 μL of sample and was analysed during 60 min. Commercial compounds were used as standards for calibration and quantification. Eventually, glucose, lactic acid, levulinic acid, and HMF were confirmed using mass spectrometry. The chromatographic system was an Agilent 1200 liquid chromatography coupled to 6210 Time of Flight (TOF) mass spectrometer with an ESI interface, using the same column as above HPLC analysis. The mobile phase was deionized and its pH was adjusted to 2.2 with formic acid. The rest of conditions were the same as for the HPLC analysis in order to obtain equivalent retention times.

And the concentration of total carbon hydrolysed into the liquid phase was determined by Total Organic Carbon (TOC) Analyser (Shimadzu, TOC-L CSN). The concentration of the generated compounds was calculated in gC/L in order to express clearer the contribution of each to the total organic carbon (TOC). Unidentified compounds were expressed as water soluble compounds (WSC).

2.5 Characterization of the recovered solid fractions.

The recovered pulp, AD, and SCB were submitted to acid hydrolysis for determination of the cellulose content, while the amount of hemicelluloses was determined by acid methanolysis. The lignin content was determined using a modified Klason lignin method.[18] Additionally, FTIR spectra of the recovered pulp, AD, and SCB. The FTIR spectra were recoded with a Jasco FT/IR-600 Plus equipped with ATR Specac Golden Gate. The spectra was recorded with 64 scans using 4 cm^{-1} resolution.

While, different FTIR bands were followed in order to understand the extraction of the different fractions for SIL pulping, they are resumed in the following table:

Table 2.1. Monitored bands for the lignin and hemicellulose decay after pulping

Wavenumber (cm^{-1})	Assignation	Reference
2850	methoxyl C-H lignin stretching	(Collier et al. 1997)[19]
1740	carbonyl C=O stretching of acetyl groups in hemicellulose	(Bodirlau et al. 2008)[20]
1595	aromatic skeletal vibrations + C=O stretching syringyl and guaiacyll lignin	(Schwanninger et al. 2004)[21]
1510	aromatic lignin C=C skeletal stretching	(Li et al. 2010)[22]
1460	asymmetrical C-H lignin bending	(Collier et al. 1997)[19]
1370	symmetrical C-H lignin bending	(Collier et al. 1997)[19]
1234	C–O stretching in lignin and hemicellulose	(Li et al. 2010)[22]

Cellulose hydrolysis experiments were monitored by X-ray diffraction (XRD). Furthermore, the raw AD, some of the obtained pulps and a sample recovered after hydrolysis were characterized by XRD analysis. A Siemens D5000 diffractometer (Bragg-Brentano for focusing geometry and vertical θ-θ goniometer) with an angular 2θ-diffraction range between 5° and 70° was used. The sample was dispersed on a Si (510) sample holder and spectra were collected with an angular

step of 0.05° at 3 s per step of sample rotation. Cu Kα radiation (λ=1.54 Å) was obtained from a copper X-ray tube operating at 40 kV and 30 mA. The crystallinity index (CI) of cellulose was calculated according to the Segal method,[23] and used only for the sake of comparison between the studied samples. Amorphous cellulose, lignin, and hemicellulose contributions have not been taken into account.

2.6 Fermentation of hydrolysates

Lactobacillus delbrueckii delbrueckii, CECT 286, was grown on an impoverished MRS broth (5.0 g/L peptone, 5.0 g/L beef extract, 2.5 g/L yeast extract, 2.0 g/L ammonium citrate, 5.0 g/L sodium acetate, 0.2 g/L $MgSO_4 \cdot 7H_2O$, 0.05 g/L $MnSO_4 \cdot H_2O$, 2.0 g/L K_2HPO_4, 1.0 g/L cysteine hydrochloride, 11 g/L HEPES and 10 mg/L resazurin). A total of 10 mL hydrolysate was mixed with a solution of 12.5 mL containing MRS broth with a concentration such to finally reach the above described concentration and the pH was adjusted at 6.2. The fermentations were carried out in batch reactors of 50 mL, sealed with rubber cap and aluminum seal and afterwards deoxygenated with an argon flow. Resazurin was used as indicator of oxygen presence. The inoculum consisted of 2.5 mL of previously grown *L. delbrueckii*. The fermentation was done at 37 ºC, in duplicate and the results expressed as mean and standard deviation. In order to control the fermentative process, 1 mL of sample was taken periodically. A total of 100 μL was placed in a 96-welled microplate for absorbance measurements at 600 nm with a microplate reader, the rest of sample was filtered with 0.22 μm filters and used for HPLC analysis. In the plots of lactic acid production, the initial concentration of lactic acid from the inoculums was subtracted in order to represent the total lactic acid formed during the fermentative process. L-Lactic acid was measured using the method established from Oenolab enzymatic kit. The optical purity (OP) of D-lactic acid was defined as follows:

$$OP = 100 \times \frac{lactic\ acid - L\text{—}lactic\ acid}{lactic\ acid}$$

3. RESULTS AND DISCUSSION

3.1 Fractionation of *Arundo donax* and Sugar cane bagasse

3.1.1 Sugar cane bagasse

Sugar cane bagasse final mixture of biomass:SIL:H_2O (2:10:6) did not allow a proper soaking of biomass due to the low density of the sample, i.e. the consistency was more a paste-like. So, we hypothesise that probably the microwave treatment was not entirely homogenous through all the sample and that might be the cause of a black final mixture with bad smell (probably decomposed). Additionally, when IPA was added, hemicellulose and lignin could not be recovered from the SIL mixture, this effect was more notable as temperature and treatment time increased

Table 2.2. Conditions for the different prepared pulps and recovered pulp weight after extraction with SIL

Sample	Biomass	SIL	time (h)	T (ºC)	H_2O (g)	SIL* (g)	sample (g)	HC+ lignin (g)	SIL + H_2O (g)
SIL1	SCB	fresh	1	120	6	10	1,77	0,10	11,7
SIL2	SCB	fresh	1	160	6	10	1,43	0,06	10,0
SIL3	SCB	fresh	2	160	6	10	1,22	0,04	9,4
SIL4	AD	fresh	1	120	6	10	1,53	0,17	11,7
SIL5	AD	fresh	1	160	6	10	1,50	0,28	12,5
SIL6	AD	fresh	2	160	6	10	1,58	0,20	12,6
SIL7	AD	SIL5	1	160	4	12	1,51	0,24	9,8
SIL8	AD	SIL7	1	160	6,7	9,3	1,59	0,21	6,8
SIL9	AD	SIL8	1	160	9,5	6,5	1,57	0,17	5,8

*SIL or recovered SIL+H_2O

(Table 2.2 SIL2 and SIL3). Although the extracted material could not be recovered from SIL, the treated wood samples showed differences in the structural analysis (Fig. 2.1). When SCB was treated at 120 ºC during 1 hour, cellulose quantity did not increase; however, some lignin and hemicelluloses were already removed. Nonetheless, already at 160 ºC and 1 hour of treatment cellulose content increased 33 % wt., lignin content decreased almost to the half, and hemicellulose content decreased 25% wt. When SCB was irradiated during 2 hours at 160 ºC, the recovered material was very similar to the sample treated during 1 hour at 160 ºC. FTIR spectra (Fig 2.2) was in agreement with structural analysis: i) 1740 cm^{-1} band disappeared already at 120 ºC showing the ease of acetyl cleavage in hemicelluloses, ii) C-O and C-H stretching bands (2850 and 1234 cm^{-1}, respectively) disappeared gradually with SIL severity extraction, showing hemicellulose and lignin extraction to some extent, and iii) aromatic skeletal vibrations and symmetrical C-H lignin bending bands (1595 and 1370 cm^{-1}, respectively) remained in all the samples, corroborating aromatic functionalities, thus lignin persistence. Briefly, even we think that SIL fractionation of SCB is not feasible due to low sample consistency, which impedes recovery of the extracted material and SIL reuse, the produced pulps were enriched in cellulose and partially freed of lignin.

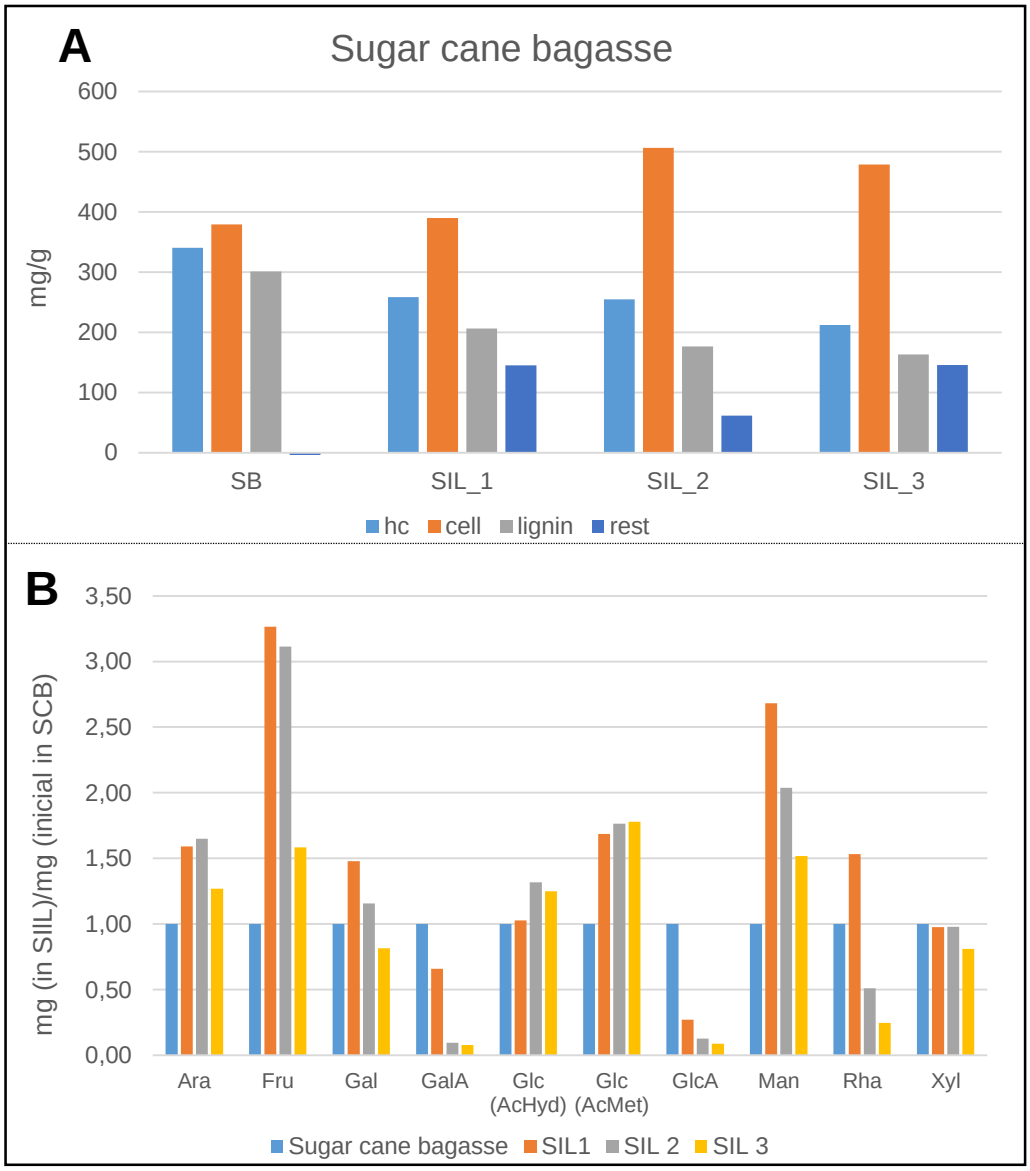

Figure 2.1. Structural analysis of initial SCB and recovered materials after extraction with SIL, (up) for total fractions present and (down) monomers content divided by the initial monomer content of the raw SCB.
Ara: arabinose, Fru: fructose, Gal: galactose, GalA: galacturonic acid, Glc (AcHyd): total glucose (from cellulose and hemicellulose) Glc (AcMet): glucose present in hemicellulose, GlcA: glucuronic acid, Man: mannose, Rha: rhamnose, Xyl: xylose.

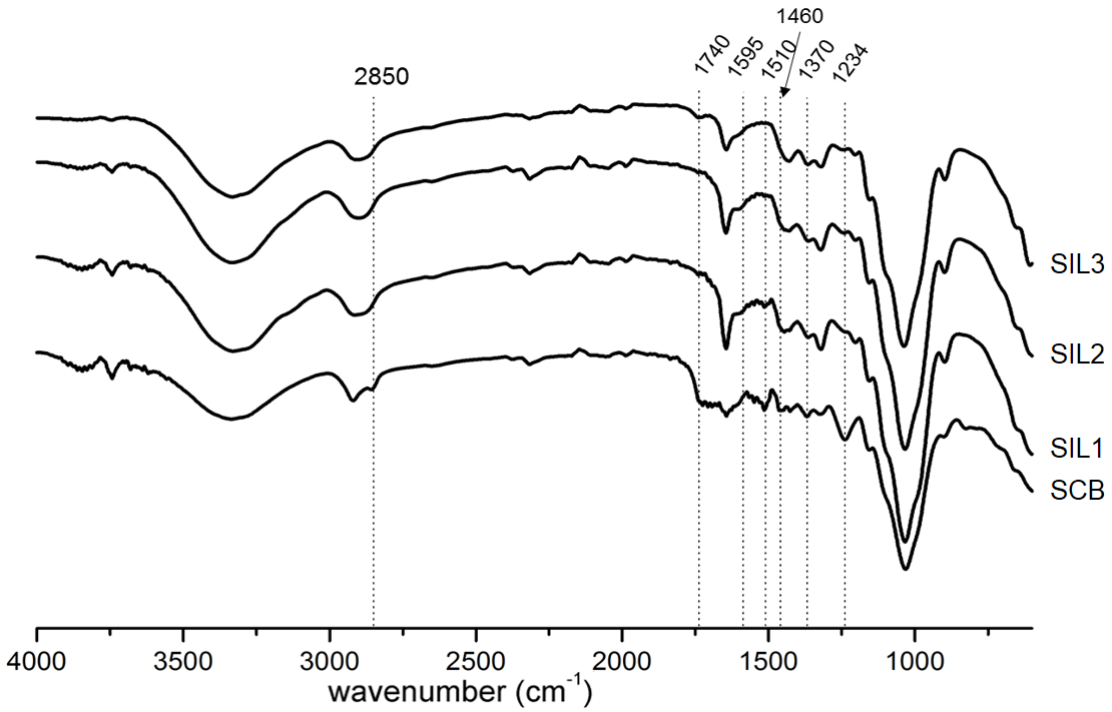

Figure 2.2. FTIR of initial SCB and recovered materials after extraction with SIL.

3.1.2 Arundo donax

When extraction with *Arundo donax* by SIL was performed, the sample was well soaked and the recovered SIL was more looking-like the initial SIL. And when IPA was added most of the extracted components could be recovered (Table 2.1, SIL4-6).

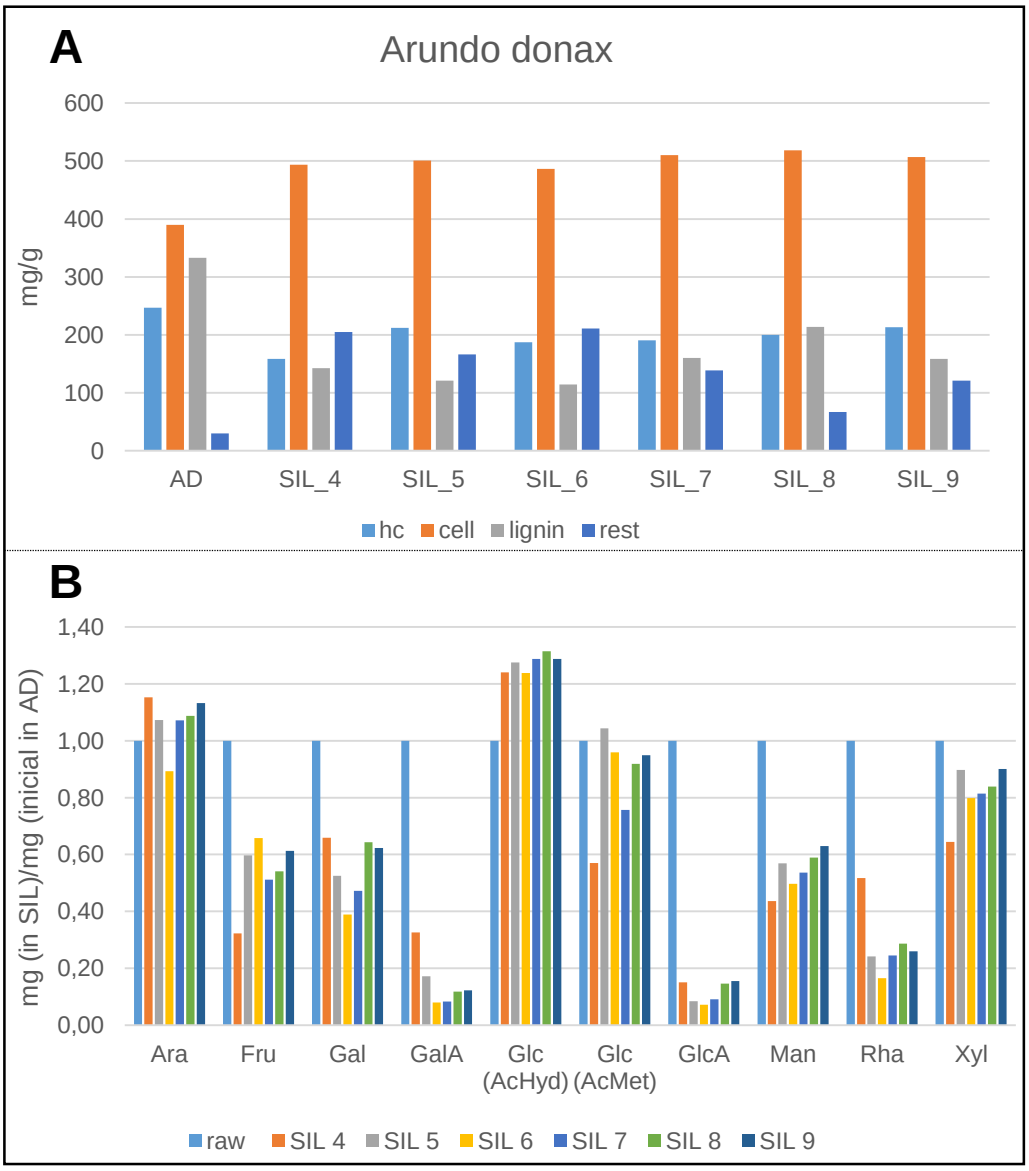

Figure 2.3. Structural analysis of initial SCB and recovered materials after extraction with SIL, (A) for total fractions present and (B) monomers content divided by the initial monomer content of the raw AD.
Ara: arabinose, Fru: fructose, Gal: galactose, GalA: galacturonic acid, Glc (AcHyd): total glucose (from cellulose and hemicellulose) Glc (AcMet): glucose present in hemicellulose, GlcA: glucuronic acid, Man: mannose, Rha: rhamnose, Xyl: xylose.

All conditions tested for AD extraction showed an increase in cellulose content, to at least 20 % wt. Hemicellulose content did not decrease hugely, being always close to 20 % wt. However, near 60 % wt. of lignin was already removed when AD was treated at 120 ºC, and after 2 hours at 160 ºC, 66 % wt. of lignin removal was reached (Fig 2.3). The success of pulping was also monitored by FTIR (Fig. 2.4), where was seen i) 2850, 1740 and 1234 cm^{-1} bands disappeared already at the first extraction ii) 1595 and 1510 cm^{-1} bands disappeared gradually with the increase of severity of the extraction and iii) asymmetrical and symmetrical C-H bending, at 1460 and 1370 cm^{-1} respectively, did not vary along the extraction showing lignin recalcitrance.

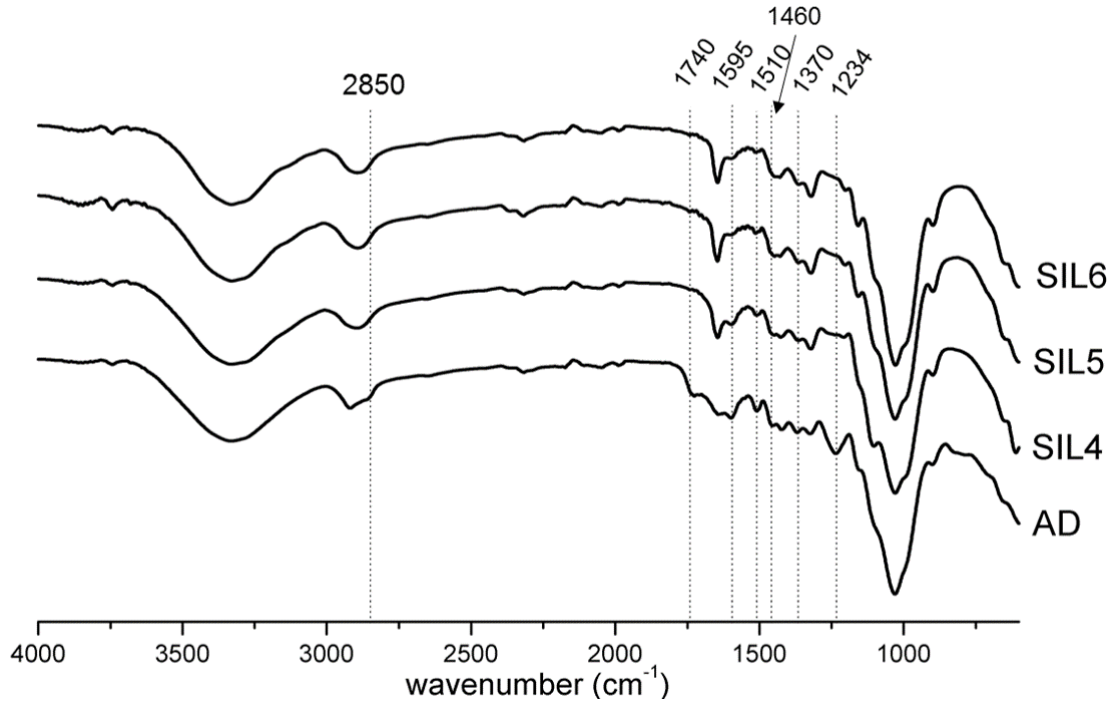

Figure 2.4. FTIR of initial AD and recovered materials after extraction with SIL.

Hence, the reuse of the recovered SIL after extraction and IPA recovery was tested. The necessary amount of water was added to keep 16 g (+2 g of sample) constant for all experiments. SIL reuse is an economical imperative[24] and needs to be addressed for a reasonable ILs exploitation as fractionation solvent.[25] During SIL reuse (Table 2.1, SIL7-9) there was not observed any decay on SIL extraction capacity, producing always pulp with around 50 % wt. of cellulose. Furthermore, lignin removal did not decrease significantly, (Student's t-test at 95% confident limit). For SIL reuse, FTIR spectra (Fig 2.5) of the recovered pulp presented a similar tendency to the above described for AD pulping. XRD data (Fig 2.6) showed that the amount of crystalline cellulose increased after the pulping with SIL. This reinforce the assumption of selective dissolution of lignin and hemicellulose,

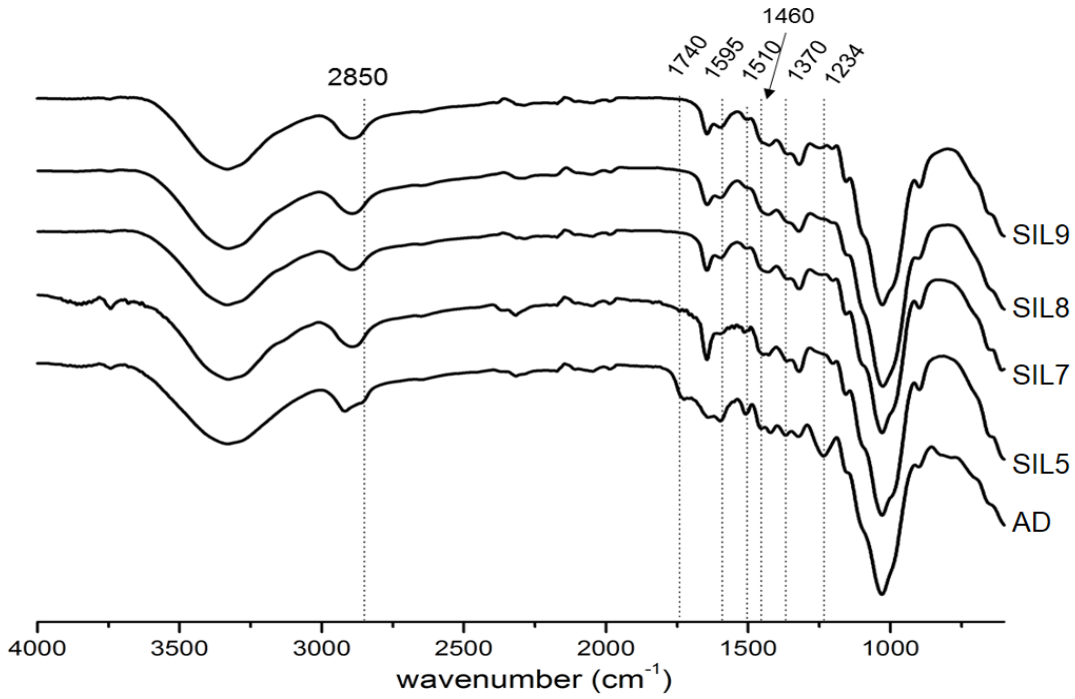

Figure 2.5. FTIR of initial AD and recovered materials after extraction with SIL at 160 ºC and 1 hour of treatment (SIL 5), and reused one (SIL7), two (SIL8) and three (SIL9) times.

resulting in a cellulose's richer pulp. CI values are practically the same for the extraction with fresh SIL (SIL5) and the reused SIL for 3 and 4 runs (SIL 8 and SIL9, respectively).

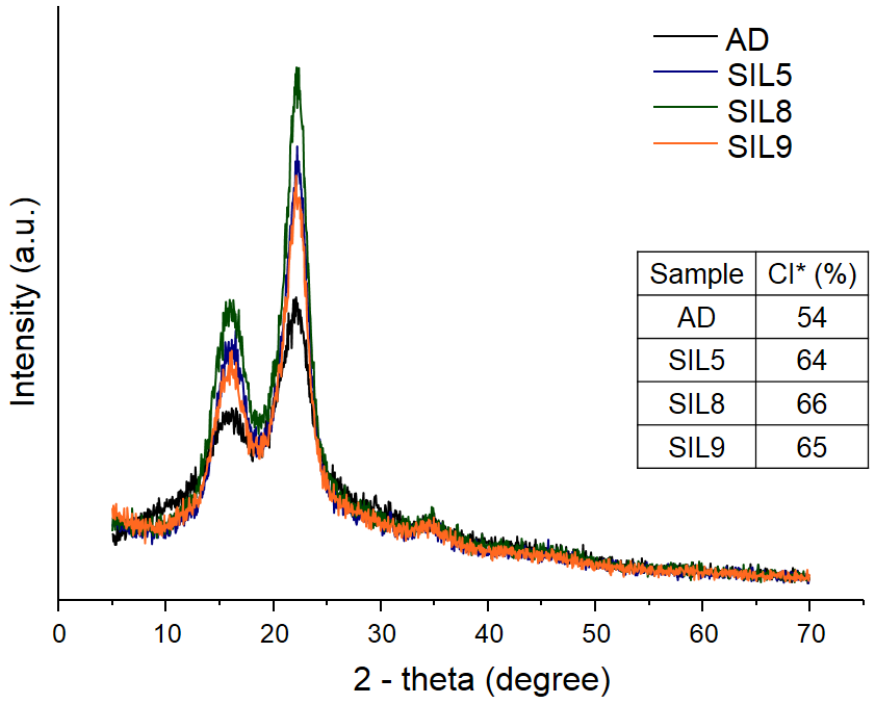

Sample	CI* (%)
AD	54
SIL5	64
SIL8	66
SIL9	65

Figure 2.6. XRD diffraction patterns of AD, SIL 5, SIL8, and SIL9. In the table the CI for cellulose are calculated.

*CI do not aim to be an exact value, they are used just as comparison between our samples.

This corroborated the successes of SIL reuse. In resume, even the extraction of hemicellulose and lignin was not complete, the potential of microwave assisted SIL pulping has been proved. Being able to extract 2/3 of lignin at relatively big particle size (~4 mm) without any mechanical agitation and just 1 hour of treatment time. Additionally, SIL reusability was also demonstrated and SIL pulping ability was not affected during 4 runs.

3.2 Hydrolysis of cellulose, AD, SCB, and produced pulps

Cellulose and woody materials hydrolysis are discussed separately, since the microwave reactors and reaction conditions were not comparable. Also, by discussing them separately more details can be given to each material, depending on its chemical and structural idiosyncrasies.

3.2.1 Hydrolysis of cellulose

During dilute acid hydrolysis of cellulose different competitive reactions take place (Scheme 2.2). Initially, cellulose chains are broken down to glucose oligomer units, which eventually lead to glucose formation.

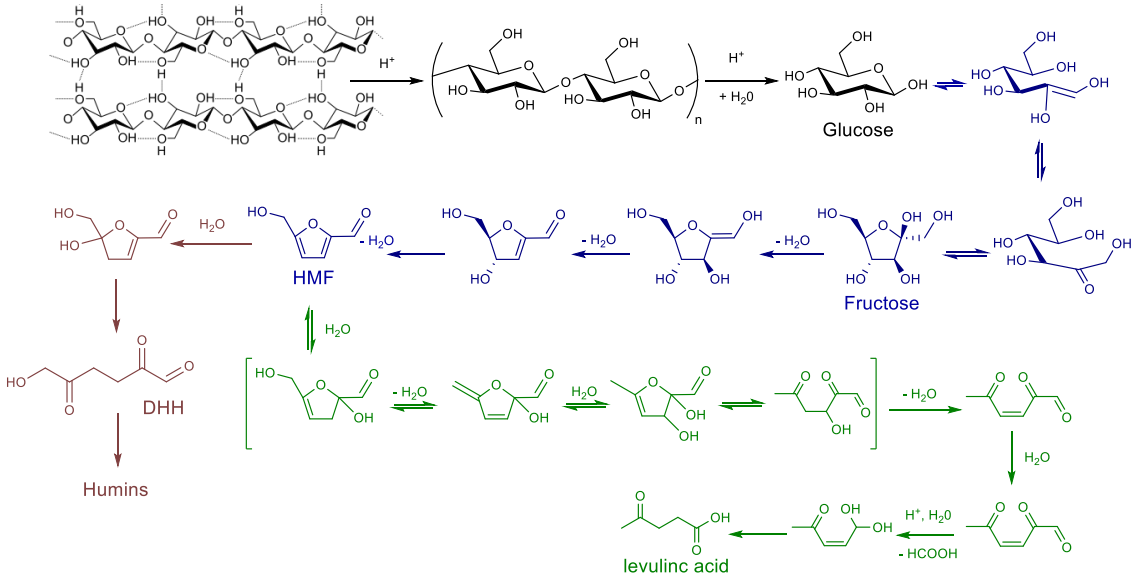

Scheme 2.2. Competitive reactions occurring during cellulose acid hydrolysis. In black, cellulose depolymerisation into glucose; in blue glucose-fructose isomerisation and fructose dehydration to HMF; in red HMF rehydration to DHH (humin precursor); and in green HMF rehydration to levulinic acid.

Glucose can be dehydrated to form 5-hydroxymethylfurfural (HMF), which itself is already a valuable building-block and a desired end product for many research purposes.[26–29] However HMF is not stable under hydrothermally treated acidic aqueous solutions, and rapidly rehydrates forming levulinic and formic acids.[30] Besides the described reactions, when cellulosic materials are submitted to acid hydrolysis, this unavoidably leads to the formation of solid by-products. When these

solid by-products are formed during acid hydrolysis, they are commonly referred as humins. Its formation and growth mechanism is a complex process. Patil and Lund[31] described the sulphuric acid catalysed growth of humins starting from HMF, they showed that at low temperatures (118 - 135 ºC) HMF condensation is acid driven, while at higher temperatures just hydrothermal conditions are enough to form condensed products. In their study they also observed that levulinc acid does not condense, being then, HMF the main responsible of humins growth. However, HMF does not simply condense, rather, through a partial rehydration HMF forms 2,5-dioxo-6-hydroxyhexanal (DHH), which due to its higher aldehyde content favours polymerisation.

The achieved conversions and the obtained products after cellulose hydrolysis with 3 % wt. H_2SO_4 as catalyst at 120 ºC are shown in Fig 2.7.

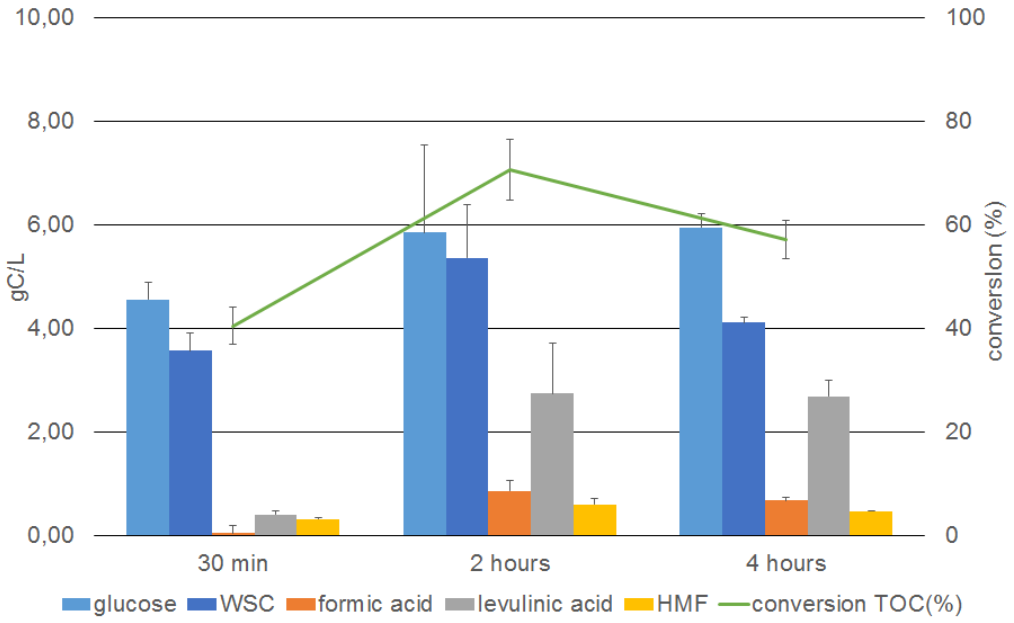

Figure 2.7. Achieved conversions (green line) and the obtained products (bars) after hydrolysis. Conditions: 3 % wt. as catalyst, 120 ºC and 400 watts of microwave irradiation power. WSC: water soluble content – referred to the unidentified formed products.

Besides glucose, which was the main product in all cases, HMF, levulinic and formic acids were detected after hydrolysis. To verify the detection of the obtained products a punctual HPLC-MS analysis of a sample was undertaken, in Table 2.3 the retention times of the different determined compounds can be seen. The close relation between theoretical and calculated exact mass together with the match between retention times is a solid evidence for the accurate compound identification. The observed products correspond to the above discussed mechanism of cellulose hydrolysis. At 30 minutes just 40 % of cellulose was converted, and the major detected compound was glucose (51 % of the total TOC). When increasing irradiation time, the obtained amount of glucose was similar between 2 and 4 hours (*ca.* 6 gC/L).

Table 2.3. Retention times corresponding to the detected compounds by RID and TOF detectors and the detected exact mass by TOF compared with the theoretical exact mass.

	R_t TOF (min)	R_t RID (min)	$[M+Na]_{theoretical}$ (m/Z)	$[M+Na]_{TOF}$ (m/Z)
Glucose	9.081	9.140	203.0526	203.0528
Lactic acid	12.894	12.916	113.0209	113.0210
Levulinic acid	16.251	16.423	139.0366	139.0366
HMF	33.278	33.173	149.0209	149.0210

However, more carbon compounds were present in solution at 2 hours (e.g. higher TOC conversion) than when the treatment went on 4 hours. We initially attributed this to the formation of insoluble condensation products, e.g. the feared humins. In order to study this hypothesis, an FTIR spectra of the recovered solid was measured (Fig 2.8).

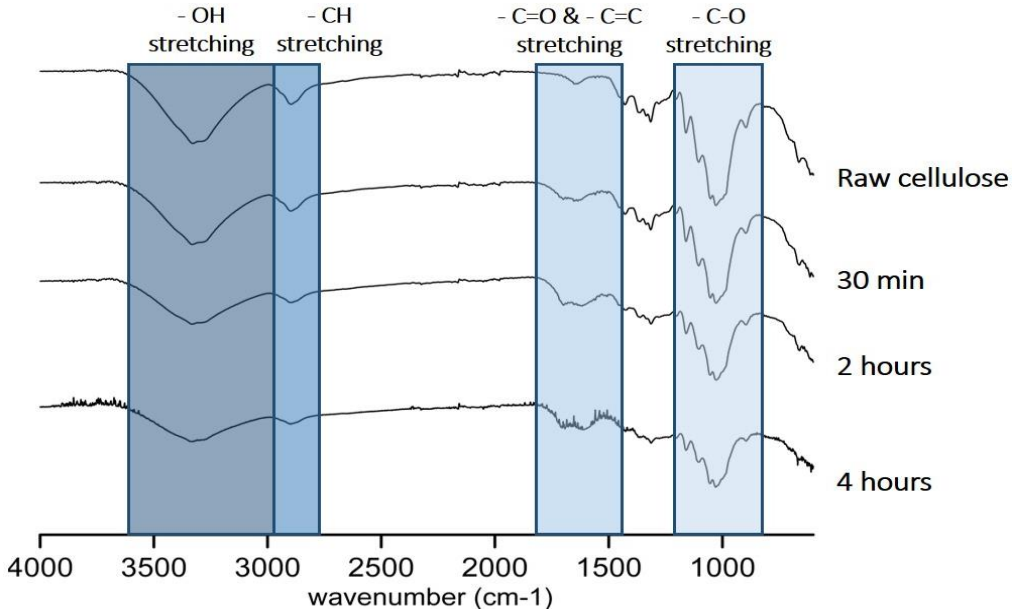

Figure 2.8. FTIR spectra of cellulose and recovered solid phases after treatment with 3% wt. H_2SO_4 at different treatment times.

The degradation of axial -OH bonds (3332 cm^{-1}), responsible of structural robustness of cellulose, increased over microwave irradiation time. Additionally, bands corresponding to C-H (2893 cm^{-1}) and C-O (1000 cm^{-1} zone) stretching decreased their intensity over time, while –C=O (1696 cm^{-1}) and C=C stretching bands (1609 cm^{-1}) appeared more notoriously.

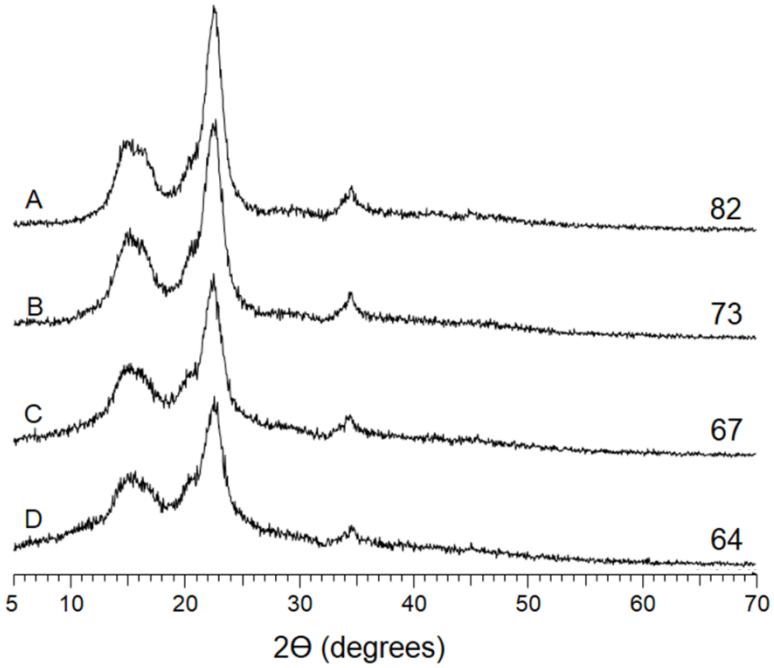

Figure 2.9. XRD spectra of cellulose and solid residues with calculated CI. A raw cellulose; B treated after 30 min; C 2h; and D 4 h.

The presence of double bonds bands (C=O and C=C), which increased along with treatment time, indeed certifies the formation of humins, as reported by Patil and Lund[31]. Finally, in order to follow cellulose degradation, XRD analysis of the remaing solid materials after hydrolysis were measured (Fig. 2.9). Degradation of crystalline cellulose increased over time. Highly crystalline cellulose, with CI = 82 %, was degraded achieving CI values of CI 64 % after 4 hours of treatment.

3.2.2 Hydrolysis of AD, SCB, and pulps

When SCB, AD, and the different produced pulps were treated with sulphuric acid and microwaves for 15 min, up to 75 % of the sample (weight) was already hydrolysed (see figure 2.10).The produced compounds were the commonly known wood hydrolysis products.[32] Namely glucose, HMF, levulinic, and formic acids coming from cellulose together with xylose and furfural coming from the hemicellulose fraction. Dehydration of glucose,[33] was found to some extent in the solution medium. However, HMF concentration was relatively low, since HMF is readily rehydrated to form levulinic and formic acids,[31] which were in turn observed. Formic acid to levulinc acid ratio was not 1:1, according to literature this can be attributed to formic acid production through another reaction pathway rather than HMF rehydration, i.e. furfuryl alcohol formation.[34] The non-identified water soluble compounds were in the range for 30-40 % gC/L for most of the cases. We assumed them to be a compilation of oligomers, unidentified products, and low molecular weight humins (which would give TOC signal).

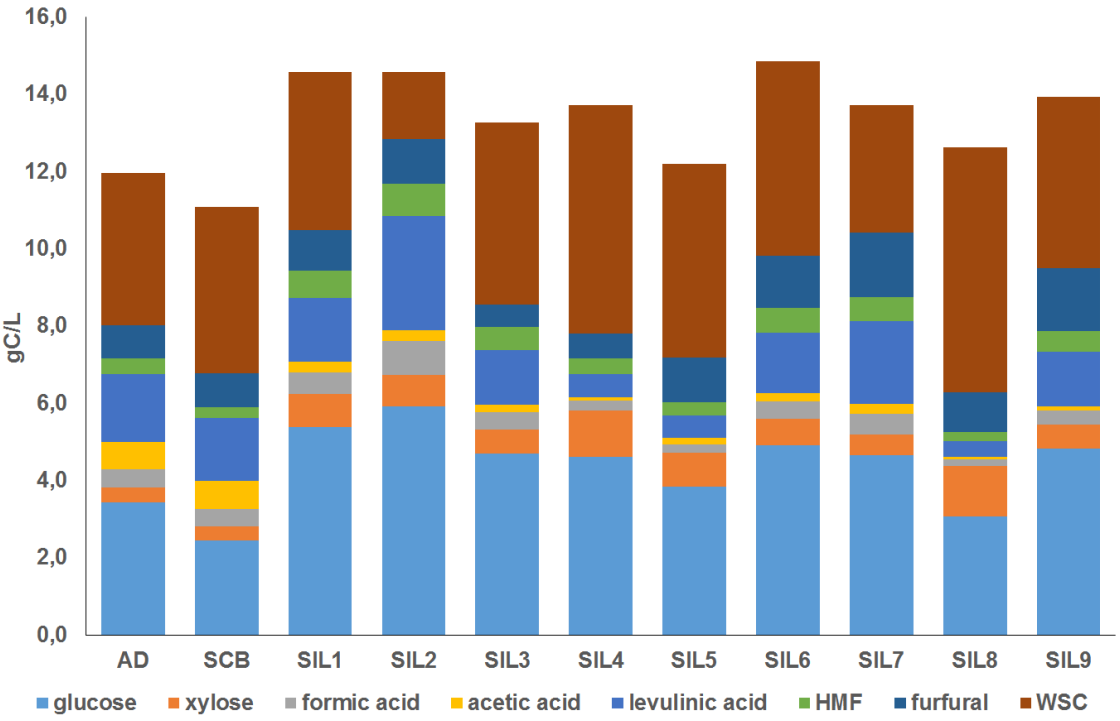

Figure 2.10. Obtained compounds after hydrolysis at 160 ºC during 15 min with 10 % wt. H_2SO_4.

In order to study the further fermentation of obtained products, we aimed to obtain glucose as a major product, which was the case for all the hydrolysis. Glucose concentration ranged from 7.73 g/L (3.09 gC/L) for SCB hydrolysis to 12.89 g/L (5.16 gC/L) for SIL3 pulp hydrolysis. Although there was not a linear tendency between cellulose content in the initial wood material and final glucose concentration, it was generally observed more glucose for the produced pulps rather than the initial SCB or AD. This might indicate that is not just cellulose content which influences wood and pulp hydrolysis, but also parameters such disruption of wood structure, which has already been reported for SIL treatments[35] and is to be expected at hydrothermal conditions. It is also important to notice that major presence of acetic acid, which might require higher alkali quantities prior bacterial fermentation and cause inhibition for bacterial growth,[36] is just found in SCB and AD hydrolysis. This comes in agreement with the FTIR spectra which showed carbonyl band, 1740 cm^{-1}, disappearance already at milder conditions. Also, xylose, coming from hemicellulose hydrolysis was found in solution, ranging from 1 (0.4 gC/L) to 3 g/L (1.2 gC/L) depending on the sample. Finally, furfural as dehydration product of xylose was also present. In order to better understand the nature of the hydrolysis residues, and figure out a potential use of such byproducts, an FTIR spectrum of these residues was also recorded (Fig. 2.11). Despite no major information can be given because the fingerprint area (1500-900 cm^{-1}) of humins and lignin can coincide, already few bands can be allotted at first sight, i) carbonyl band (1740 cm^{-1}) which disappeared after SIL pulping (above discussed) was again present

in the recovered materials, indicating a possible humin nature (aldehyde moiety coming from condensated HMF[31]) and ii) the band at 1510 cm^{-1} which was previously assigned to C=C aromatic stretching, and it decreased along severity of the extraction with SIL, was again notorious, hence, showing the aromatic nature of recovered products. This hypothesis was also supported by XRD diffraction of the recovered materials after hydrolysis (Appendix I, Fig A1) which did not show any crystalline phase of cellulose, proving that crystalline cellulose was fully degraded. Hence, we assumed these materials to be a mixture of humins and possibly some lignin remain, this mixture in a possible integration scheme might be valorised for instance through gasification.[37,38]

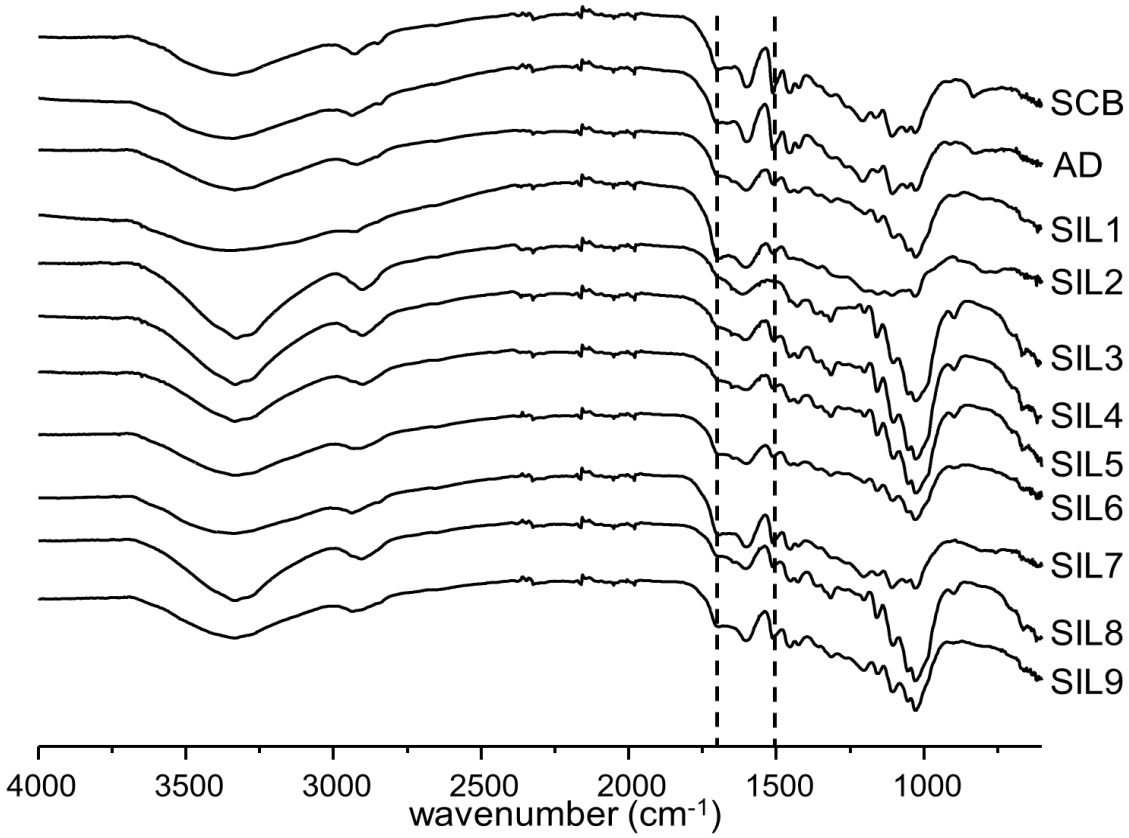

Figure 2.11. Obtained compounds after hydrolysis at 160 ºC during 15 min with 10 % wt. H_2SO_4 as catalyst.

3.2.3 Comparison of cellulose, pulp and biomass hydrolysis

Despite different composition of commercial cellulose, the produced pulps, and raw biomass; the major compound found in solution after hydrolysis was glucose. Also glucose degradation products were found to some extent (mechanism described in Scheme 2.2). So the more complex matrix of biomass and pulp did not impede glucose formation. The main difference between cellulose and woody hydrolysates was pentose, together with its dehydration product furfural, and acetic acid presence. However, no major solubilized lignin monomers were detected in solution. So, in principle all of the produced hydrolysates could be tested for fermentation with microorganisms.

3.3 Fermentation of hydrolysates

The hydrolysates of cellulose, pulp and crude wood had similar amount of glucose. When the hydrolysates were used as a source of sugars for lactic acid fermentation, all the present glucose was degraded within one day, as example Fig 2.12 is added, the rest of fermentation graphs are shown in appendix (A2-A12 figures).

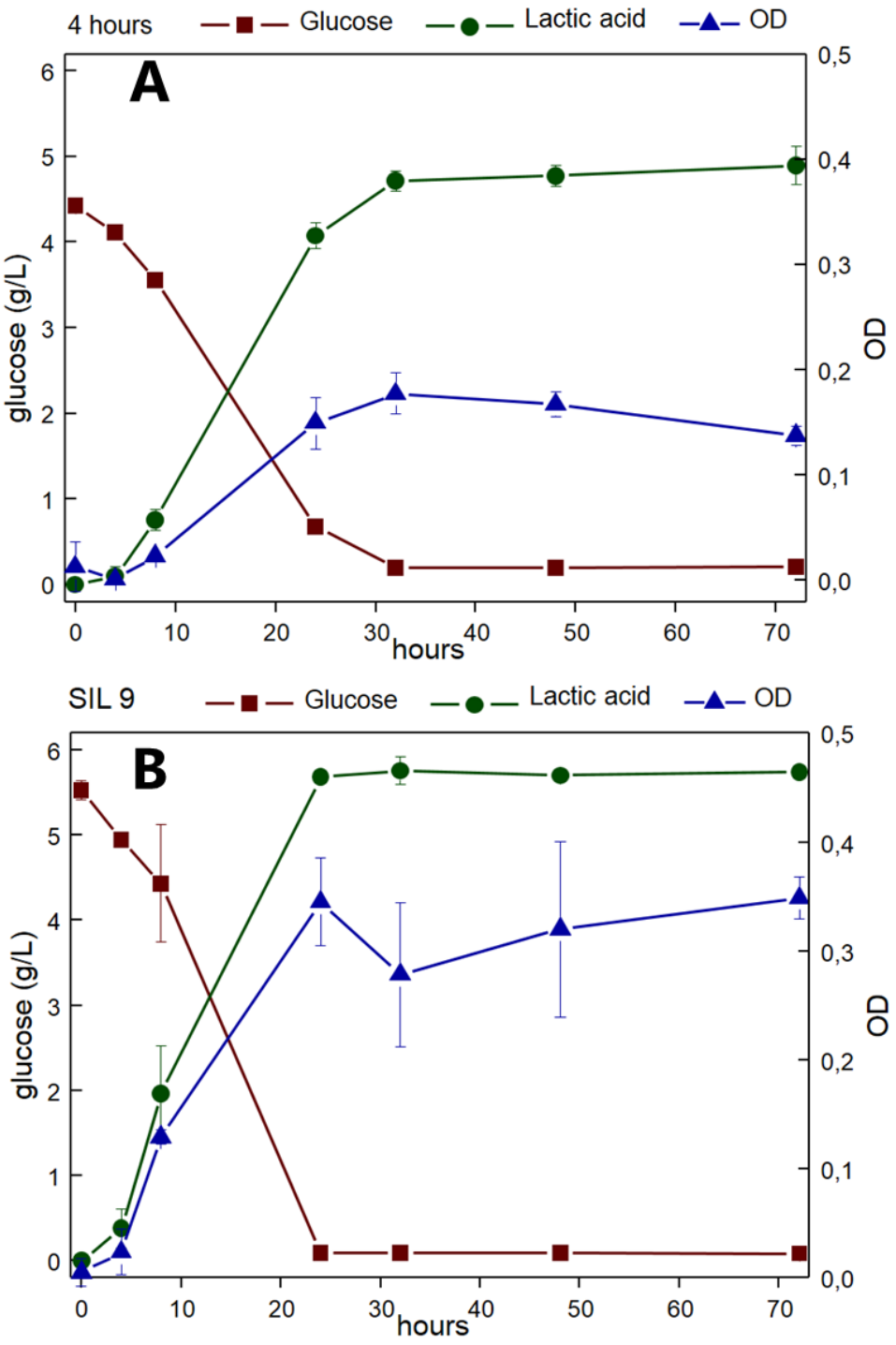

Figure 2.12. Lactic acid production by *L. delbrueckii* from cellulose hydrolysate after 4 hours of treatment (A) and from SIL9 hydrolysate (B).

So, the presence of furanic compounds, which are reported as inhibitory compounds for lactic acid bacteria[39], did not impede lactic acid bacteria growth. Neither the potential presence of traces of SIL obstructed bacterial growth, posing SIL fractionation as a good pulping method prior bacterial fermentation. In addition, table 2.4 shows that initial glucose concentration was almost the same to final lactic acid concentration. Taking into account glucose and lactic acid molecular weight, this basically means that homolactic fermentation occurred, e.g. one glucose

Table 2.4. Glucose, lactic acid concentration, and optical density of bacterial media before (0 h) and after (72 h) fermentation with lactic acid bacteria and optical purity of obtained D-lactic acid.

	Fermentation time (hours)	Glucose (g/L)	Lactic acid (g/L)	Lactic acid OP (%)	Optical density (a.u.)
AD	0	4.6 ± 0.5	0	-	-
	72	0.1 ± 0	4.4 ± 0.2	100 ± 0	0.23 ± 0.05
SCB	0	4.51 ± 0.52	0	-	-
	72	0.1 ± 0	4.18 ± 0.32	100 ± 0	0.21 ± 0.03
SIL1	0	5.15 ± 0.12	0	-	-
	72	0.1 ± 0	5.22 ± 0.16	100 ± 0	0.24 ± 0.05
SIL2	0	5.31 ± 0.07	0	-	-
	72	0.1 ± 0	5.21 ± 0.15	100 ± 0	0.32 ± 0.01
SIL3	0	5.45 ± 0.14	0	-	-
	72	0.1 ± 0	5.33 ± 0.14	100 ± 0	0.25 ± 0.03
SIL4	0	5.74 ± 0.22	0	-	-
	72	0.1 ± 0	5.61 ± 0.26	99.4 ± 0.8	0.38 ± 0.03
SIL5	0	5.37 ± 0.08	0	-	-
	72	0.08 ± 0	5.60 ± 0.06	97.3 ± 3.8	0.30 ± 0.05
SIL6	0	5.74 ± 0.07	0	-	-
	72	0.09 ± 0	5.89 ± 0.17	100 ± 0	0.35 ± 0.07
SIL7	0	5.24 ± 0.03	0	-	-
	72	0.09 ± 0	5.47 ± 0.02	100 ± 0	0.39 ± 0.02
SIL8	0	4.59 ± 0.20	0	-	-
	72	0.05 ± 0.07	4.72 ± 0.23	98.1 ± 2.7	0.22 ± 0.03
SIL9	0	5.53 ± 0.11	0	-	-
	72	0.09 ± 0	5.74 ± 0.05	99.3 ± 1.0	0.35 ± 0.02
2 hours	0	4.36 ± 0.05	0	-	-
	72	0.14 ± 0.04	4.89 ± 0.24	98.7 ± 2.2	0.25 ± 0.01
4 hours	0	4.42 ± 0.09	0	-	-
	72	0.20 ± 0.01	4.90 ± 0.22	99.5 ± 0.9	0.14 ± 0.01

molecule was transformed into two lactic acid molecules. It was also observed that *Lactobacillus delbrueckii* just transformed glucose into lactic acid, while xylose concentration did not vary along the fermentation (data not shown). Also, table 2.4 shows that in all cases the obtained lactic acid was mainly D-lactic acid, not having an optical purity (OP) below 98 %. This is of a particular importance when the obtained lactic acid is to be employed for PLA production, since physico-chemical properties of the final polymer will strongly depend on OP of the initial lactic acid[4]. The difference between the lactic acid obtained quantities just depended on the initial glucose content, so the greater glucose presence, the more lactic acid produced, without any impact on OP. So, here we showed that *Lactobacillus delbrueckii* not only selectively degrades glucose coming from cellulose hydrolysis,[40] but, also, is able to grow and ferment selectively glucose into optically pure lactic acid in the presence of xylose and other by-products coming from wood. This fact is important because no separation step is needed. Thus after pulp hydrolysis microbial fermentation can be directly performed.

4. Conclusions

As mentioned in the introduction moving away from edible biomass sources is strongly recommended for a sustainable development of biorefinery. For this, different processes need to be developed, a reliable fractionation method, a cost efficient technology for hydrolysis and a proper microbial strain choice for fermentation of the hydrolysates. In this chapter the usage of a biocompatible and reusable ionic liquid, SIL, has been demonstrated. Pulping of biomass with SIL, increased cellulose quantity, removed majorly lignin, and facilitated biomass' hydrolysis. Afterwards acid hydrolysis of cellulose, wood, and the produced pulps was carried out, obtaining glucose as the main formed product in the hydrolysate. Without any further separation or purification step, the hydrolysate was fermented by lactic acid bacteria, producing optically pure D-lactic acid. This proves, both, SIL suitability for pulping prior hydrolysis and lactic fermentation; and lactic acid bacteria suitability for fermentation of complex hydrolysates media, producing optically pure D-lactic acid.

5. References

1 G. W. Huber, S. Iborra and A. Corma, *Chem. Rev.*, 2006, **106**, 4044–4098.

2 D. A. H. L Nattrass, *http//www. nnfcc.co.uk/publications/nnfcc-renewable-chemicals-factsheet-lactic-acid . Accessed 3 Jun 2016*, 2010.

3 K. Madhavan, N. R. Nair and R. P. John, *Bioresour. Technol.*, 2010, **101**, 8493–8501.

4 A. J. R. Lasprilla, G. a R. Martinez, B. H. Lunelli, A. L. Jardini and R. M. Filho, *Biotechnol. Adv.*, 2012, **30**, 321–328.

5 R. Kumar, S. Singh and O. V Singh, *J. Ind. Microbiol. Biotechnol.*, 2008, **35**, 377–391.

6 I. Anugwom, V. Eta, P. Virtanen, P. Mäki-Arvela, M. Hedenström, M. Yibo, M. Hummel, H. Sixta and J.-P. Mikkola, *Biomass and Bioenergy*, 2014, **70**, 373–381.

7 D. A. Fort, R. C. Remsing, R. P. Swatloski, P. Moyna, G. Moyna and R. D. Rogers, *Green Chem.*, 2007, **9**, 63–69.

8 Dissolution method-US20080023162, 2008, 1.

9 R. P. Swatloski, S. K. Spear, J. D. Holbrey and R. D. Rogers, *J. Am. Chem. Soc.*, 2002, **124**, 4974–4975.

10 S. G. Khokarale, T. Le-That and J.-P. Mikkola, *ACS Sustain. Chem. Eng.*, 2016, **4**, 7032–7040.

11 R. D. Sun, N., Rahman, M., Qin, Y., Maxim, M.L., Rodriguez, H., Rogers, *Green Chem.*, 2009, **5**, 646–655.

12 I. Anugwom, P. Mäki-Arvela, P. Virtanen, S. Willför, R. Sjöholm and J.-P. Mikkola, *Carbohydr. Polym.*, 2011, **87**, 2005–2011.

13 G. Philip, J. David, A. Charles and L. Charles, *Nature*, 2005, **436**, 1102.

14 C.-H. Zhou, X. Xia, C.-X. Lin, D.-S. Tong and J. Beltramini, *Chem. Soc. Rev.*, 2011, **40**, 5588–617.

15 Z. Fang, R. L. Smith and X. Qi, *Production of Biofuels and Chemicals with Microwave*, 2015.

16 H. Peng, H. Chen, Y. Qu, H. Li and J. Xu, *Appl. Energy*, 2014, **117**, 142–148.

17 R. J. Chimentão, E. Lorente, F. Gispert-Guirado, F. Medina and F. López, *Carbohydr. Polym.*, 2014, **111**, 116–24.

18 P. J. Hatfield, R.D., Jung, H.G., Ralph, J., Buxton, D.R., Weimer, *J. Sci. Food Agric.*, 1994, **65**, 51–58.

19 W. Collier, V. F. Kalasinsky and T. P. Schultz, *Holzforschung*, 1997, **51**, 167–168.

20 R. Bodirlau, C. A. Teaca and I. Spiridon, *BioResources*, 2008, **3**, 789–800.

21 M. Schwanninger, J. C. Rodrigues, H. Pereira and B. Hinterstoisser, *Vib. Spectrosc.*, 2004, **36**, 23–40.

22 C. Li, B. Knierim, C. Manisseri, R. Arora, H. V. Scheller, M. Auer, K. P. Vogel, B. A. Simmons and S. Singh, *Bioresour. Technol.*, 2010, **101**, 4900–4906.

23 L. Segal, J. J. Creely, A. E. Martin and C. M. Conrad, *Text. Res. J.*, 1959, **29**, 786–794.

24 N. V Plechkova and K. R. Seddon, *Chem Soc Rev*, 2008, **37**, 123–150.

25 N. Sun, H. Rodríguez, M. Rahman and R. D. Rogers, *Chem. Commun. (Camb).*, 2011, **47**, 1405–1421.

26 J. N. Chheda, Y. Roma and J. A. Dumesic, *Green Chem.*, 2007, **9**, 342–350.

27 L. Lai and Y. Zhang, *ChemSusChem*, 2011, **4**, 1745–1748.

28 M. E. Zakrzewska, E. Bogel-Łukasik and R. Bogel-Łukasik, *Chem. Rev.*, 2011, **111**, 397–417.

29 R. Van Putten, J. C. Van Der Waal, E. De Jong, C. B. Rasrendra, H. J. Heeres and J. G. De Vries, *Chem. Rev.*, 2013, **113**, 1499–1597.

30 B. Girisuta, L. P. B. M. Janssen and H. J. Heeres, *Ind. Eng. Chem. Res.*, 2007, **46**, 1696–1708.

31 S. K. R. Patil and C. R. F. Lund, *Energy and Fuels*, 2011, **25**, 4745–4755.

32 R. Rinaldi and F. Schüth, *ChemSusChem*, 2009, **2**, 1096–107.

33 T. Wang, M. W. Nolte and B. H. Shanks, *Green Chem.*, 2014, **16**, 548–572.

34 L. Yang, G. Tsilomelekis, S. Caratzoulas and D. G. Vlachos, *ChemSusChem*, 2015, **8**, 1334–1341.

35 I. Anugwom, P. Mäki-Arvela, P. Virtanen, S. Willför, P. Damlin, M. Hedenström and J.-P. Mikkola, *Holzforschung*, 2012, **66**, 809–815.

36 E. Palmqvist and B. Hahn-Hägerdal, *Bioresour. Technol.*, 2000, **74**, 25–33.

37 T. M. C. Hoang, L. Lefferts and K. Seshan, *ChemSusChem*, 2013, **6**, 1651–1658.

38 M. P. Pandey and C. S. Kim, *Chem. Eng. Technol.*, 2011, **34**, 29–41.

39 M. A. Abdel-Rahman, Y. Tashiro and K. Sonomoto, *J. Biotechnol.*, 2011, **156**, 286–301.

40 L. Gavilà, M. Constantı and F. Medina, *Cellulose*, 2015, **22**, 3089–3098.

Chapter 3:

Cellulose acetate as an entry point for continuous furan production

1. INTRODUCTION

Large biomass exploitation for chemicals and fuel production is still awaiting integrate processing.[1] One of the main problems is the scarce solubility of biomass.[2] Cellulose, which is the most studied fraction for fuels and chemical production,[3,4] is generally insoluble in common solvents and its solubilization can only be achieved using complex solvent systems, including the still expensive ionic liquids (ILs).[5] The strong H-bond network that involves unprotected hydroxyls groups is responsible for the scarce solubility of cellulose.[6] Protection or partial protection of this biopolymer disrupts the natural H-bond network, thereby modifying solubility properties. Such strategy has a long tradition and first cellulose derivatives, e.g. nitrocellulose, were already discovered back in the 19th century. Since then a wide range of functional groups has been used to modify the hydroxyl moieties in cellulose, including nitrates, nitrites, xanthates, formates and acetates.[7]

The readily available cellulose acetate has been widely used in industry due its low price. Cellulose acetate is prepared from pure cellulose, however its preparation has been also reported from crude biomass.[8] Cellulose acetate solubility in organic solvents depends on the number of hydroxyl moieties substituted by acetyl groups, commonly referred as degree of substitution (DS). In general, common solvents like tetrahydrofuran, methyl acetate, acetone or dioxane, can be used for DS higher than 2. However, cellulose acetate characterized by a lower DS can only be dissolved by fewer solvents,[9] including for instance acetic acid.

In the area of chemical conversion of cellulose into platform chemicals, almost no reports have appeared using cellulose acetates as the starting material. In turn, different products have been targeted on the basis of unprotected carbohydrates.[10] Among them, 5-hydroxymethylfurfural (HMF), the product of hexoses dehydration,[11] is claimed to be one of the most valuable biomass-derived building-blocks, with enormous potential in the field of polymer production[12] or fuel additives[13] thanks to its derivatives furandicarboxylic acid (FDCA) and 2,5 dimethylfuran (DMF), respectively. However, HMF production is still technically challenging when cellulose is used as carbohydrate source. In this case, processes have been traditionally developed using aqueous reaction mixtures, although alternative solvents have been recently proposed with the aim of improving HMF yields.[14] ILs, for instance, have been proven as an efficient medium to depolymerize cellulose and dehydrate the monomers, achieving the production of HMF in 54 % yield.[15] Nevertheless, despite the great potential, the industrial application of ILs is still costly, as mentioned just above.

The use of alternative solvent systems has also opened the way to the synthesis of interesting HMF derivatives. Methoxymethylfurfural (MMF), which can be obtained in 55 % yield by reacting hexoses in methanol in presence of sulfuric acid[16], has been targeted by Avantium as a key intermediate for the production of FDCA. In addition, Mascal et. al. reported the synthesis of 5-(Chloromethyl)furfural (CMF) by reacting cellulose in hydrochloric acid in the presence of lithium chloride while continuously extracting the reaction mixture in dichloroethane[17]. Interestingly, reaction with alkylammonium acetates can be used to transform crude CMF into acetoxymethylfurfural (AMF).[18] The latter has also been proposed as valuable HMF alternative, claiming that the acetyl moiety makes AMF hydrophobic, less reactive, and more versatile in terms of reactivity.[18] Interestingly, production of AMF by continuous reaction of fructose in supercritical acetic acid has been published.[19] However, we realized that the use of similar conditions for the direct conversion of cellulose derivatives into furanic compounds has not been reported, to the best of our knowledge. Indeed, the direct use of polymeric carbohydrates rather than monomers is not trivial, due to solubility issues as well as to the lower yields caused by competitive processes occurring during polysaccharide deconstruction.[10] Hence, in this work, we investigated the depolymerization of cellulose acetate in acetic acid as a new method to produce AMF. Such method takes advantage of the use of an environmentally benign solvent and offers the benefits of a homogeneous process, since cellulose acetate is readily soluble in acetic acid.

2. METHODOLOGY

2.1 Materials

All the chemicals were purchased from Sigma-Aldrich and used as received.

2.2 IR analysis

Infrared spectra were recorded on a ThermoScientific Nicolet iS5 FT-IR spectrometer at a resolution of 4 cm^{-1} and 64 scans.

2.3 NMR analysis

^{1}H spectra were measured on a Bruker Spectrospin 400 MHz Ultrashield Spectrometer in $CDCl_3$, with chemical shifts referenced to the residual solvent signal and using standard instrument conditions (512 scans). The degree of substitution was calculated according to the ^{1}H-NMR signal ratio between the cellulose backbone signals (5.2-3.4 ppm) and the acetyl signals (2.3-1.8 ppm).

2.4 GPC analysis

The number and weight average molecular weight (Mn, Mw) were calculated from molecular weight distributions determined by size exclusion chromatography (SEC) in tetrahydrofuran as solvent on the basis of polystyrene standards (PSS; Mainz).[20] The GPC was run at 25 °C in THF using a column system by PSS (SDV 100/1000/100,000, 8 x 300 mm, 5 mm particle size) with UV (260 nm) and refractive index detection systems.

The number of glucose units per cellulose acetate chain was calculated dividing the average molecular weight (M_n) by the molecular weight of each glucose acetate unit (M_r):

$$N^o\ glucose\ units = \frac{M_n(g/mol)}{M_r(g/mol)}$$

The molecular weight of each glucose acetate unit (Mr) was calculated according to its degree of substitution (DS). The cellulose repeating unit, anyhdroglucose, has a weight of 162 g/mol; each of the 3 free hydroxyl groups can however be acetylated (acetyl group: 43 g/mol). Thus, Mr is calculated as follows:

$$Mr(g/mol) = 159 + 43 \times DS + (3 - DS) \times 1$$

2.5 HPLC analysis

After filtration of the reaction mixture, 100 µL of sample was diluted with 900 µl of a 1:1 mixture of acetonitrile-water. Thus, 20 µL of the resulting solution was injected for analysis. The HPLC analysis was performed using an Agilent 1200 instrument connected to a Hypersil GOLD C8 column, DAD was used as detector and the signal at 260 nm was used for quantification. ACN-water (1:1) was used as the mobile phase with a flow of 0.4 mL/min. The HPLC column was kept at 40 °C, and data acquisition was performed over 20 minutes intervals. Prepared glucose acetate and commercial AMF or HMF were used as standards for the preparation of calibration curves.

AMF yield was calculated correcting the molecular weight of the acetylated anhydroglucose unit with the acetyl content per unit (DS calculated by 1H-NMR):

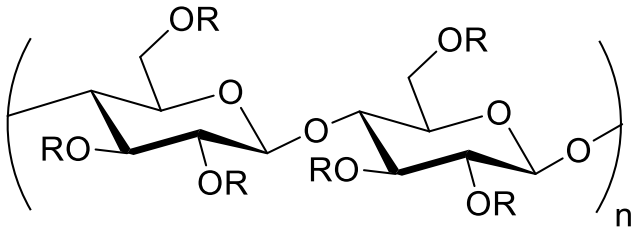

R = $CH_3(C=O)$ or H according to DS

$$Cellulose\ acetate\ unit\ Mr(g/mol) = 159 + 43 \times DS + (3 - DS) \times 1$$

$$AMF\ yield = 100 \times \frac{[AMF]HPLC\ measured\ (g/L)}{[AMF]_{max}\ (g/L)}$$

$$[AMF]_{max}\ (g/L) = \frac{cellulose\ acetate(g) \times 168(g/mol)}{cellulose\ acetate\ M_r(g/mol) \times V(L))}$$

2.6 Glucose acetate synthesis

To a cold mixture of glucose (10 g, 55.5 mmol) and pyridine (30 mL, 373 mmol) acetic anhydride (30 mL, 317 mmol) was added. The mixture was stirred overnight and then transferred to a separation funnel with ethyl acetate (100 mL). The solution was washed with 2 M hydrochloric acid, saturated sodium bicarbonate and brine, dried over sodium sulfate and concentrated.

2.7 Organocat pulp preparation

Organocat pulp was prepared according to the method described by Grande et al.[21] Briefly, in an autoclave, beech wood (25 g) was suspended in water (500 mL). Oxalic acid (2,25 g) was added followed by 2-Methyl tetrahydrofuran (500 mL) and the reaction was stirred at 130 °C for 3 h. The obtained solid was thoroughly washed with water and dried at 80 °C overnight.

2.8 Cellulose acetate synthesis from cellulose

In a round bottom flask, cellulose (2 g, 12 mmol) was suspended in acetic acid (35 mL) and stirred for 1 hour at 55 °C. Then, a mixture of acetic anhydride (10 mL, 105 mmol) and sulfuric acid (0.4 mL, 7.5 mmol) was slowly added, while the mixture was kept at 55 °C for 2 hours.[22] The mixture was thus poured into cold water, the precipitate was filtered, washed and dried at 40 ºC in a vacuum oven.

2.9 Cellulose acetate synthesis from pulp or wood

In a round bottom flask, 2 g of wood or pulp was suspended in acetic acid (35 mL) and stirred for 1 hour at 55 °C. Then, a mixture of acetic anhydride (10 mL, 105 mmol) and sulfuric acid (0.4 mL, 7.5 mmol) was slowly added, while the mixture was kept at 55 ºC for 2 hours.[22] The mixture was poured into cold water, the precipitate was filtered, washed and dried at 40 ºC in a vacuum oven. In order to purify the cellulose acetate, the precipitate was stirred in dichloromethane (30 mL) at 30 ºC for 1 hour; afterwards 2/3 of the solvent was evaporated with a rotary evaporator and poured into 20 mL of ethanol, the precipitate was washed with ethanol and dried at 40 ºC in a vacuum oven.

2.10 General procedure for the acetolysis of cellulose acetate

Solutions of cellulose acetate in acetic acid were prepared under the approximation that all cellulose acetate is composed of triacetylated anhydroglucose units (molar mass: 288 g/mol). The following molarities (mM) and the number of equivalents are therefore calculated with respect to triacetylated anhydroglucose units. Briefly, the corresponding amount of cellulose acetate to reach a final concentration of 5 g/L (17.4 mM) was dissolved in acetic acid and 35 mM of acetic anhydride (2 eq) and 35 mM of acid (2 eq) was added each run, unless otherwise stated. (The same procedure was adapted for non-acetylated cellulose [molar mass: 162 g/mol] as control experiment).

2.10.1 Batch acetolysis

The above mentioned solution (15 mL), was charged in a Teflon lined, stainless steel autoclave (45 ml volume, purchased from Parr Instruments). The autoclave was placed into an oven at the desired reaction temperature and kept for the desired reaction time.

2.10.2 Flow acetolysis

For the continuous flow acetolysis, a commercial reactor (X-Cube Flash, Thales Nano) equipped with a 4 mL hastelloy reaction loop was used. After equilibrating the system at the desired temperature over a period of 2 min, 5 mL of a filtered feed solution were passed through the coil using an HPLC pump. Then, a minimum of 1 mL of sample was collected for analysis. The residence time was controlled by adjusting the flow rate.

For the Crude AMF recovery from the 2h time on stream experiment, the solution was flowed through the reactor at 175 ºC with a flow rate of 0,8 m/L and the

2 hours eluate was collected. The collected solution (96 mL) was poured into ethyl acetate (200 mL) and the solution was washed with saturated sodium bicarbonate (150 mL) and brine (150 mL), dried over anhydrous sodium sulfate, concentrated and dried at 40 ºC in a vacuum oven. 191 mg of crude AMF (see NMR in Appendix I, Fig B1) was recovered.

3. RESULTS AND DISCUSSION

3.1 Commercial cellulose acetate acetolysis in batch reactor

We started testing the reactivity of commercial cellulose acetate in acetic acid in an autoclave reactor.

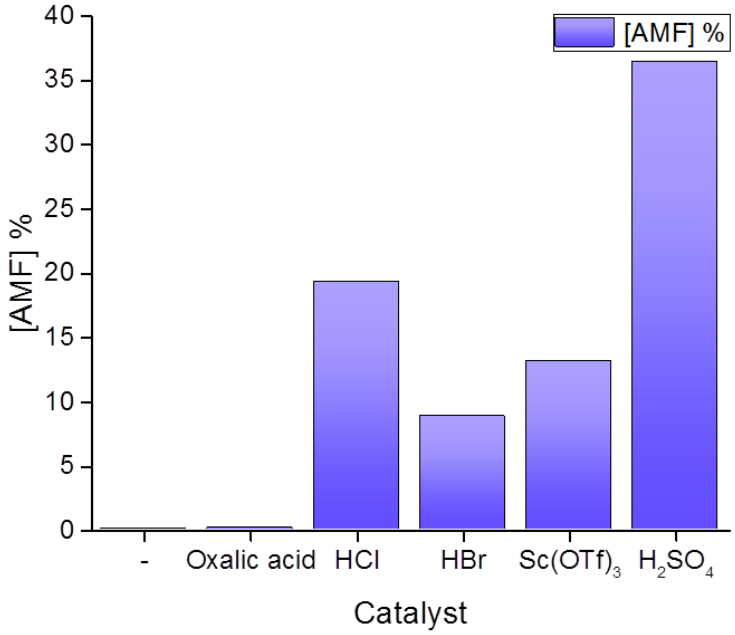

Figure 3.1. AMF yield for the acetolysis of cellulose acetate in the presence of different catalysts. General conditions: cellulose acetate, acetic anhydride, catalyst, 200 °C, 2 hours.

Lewis acids, as well as organic and mineral Brønsted acids are traditionally used for the transformation of unprotected sugars into HMF, and were therefore screened also in the present study (figure 3.1). Initially, all reactions were carried out in presence of 2 equivalents of acetic anhydride, in order to preserve the reaction intermediates and the product in the acetylated state. HPLC was employed for the analysis of the products.

A control experiment was performed in the absence of an additional catalyst, showing no AMF production. In a similar way, the addition of an organic catalyst such oxalic acid, did not result in AMF production, suggesting that stronger acids are required. A Lewis acid such scandium triflate, afforded AMF in 13 % yield. While monoprotic Brønsted acids such as hydrogen chloride and hydrogen bromide,

resulted in the formation of the product in a yield of 19 % and 9 % respectively. Among the different homogenous catalysts screened, sulfuric acid showed the best performance, 36 % AMF yield, suggesting that higher dehydrating properties increase AMF yield. Although initial experiments showed that AMF can be produced in 36 % yield by reaction at 200 ºC for 2 hours in the presence of 2 equivalents of H_2SO_4 (figure 3.1), any attempt to further optimize the reaction was not successful. When increasing the reaction time over 2 hours, AMF yield decreased (figure 3.2A), possibly due to AMF degradation. A drop in AMF yield is also observed when reaction temperature is increased from 200 ºC to 220 ºC, in agreement with the assumption that furfural-based condensation products are more favored at higher temperatures.[23]

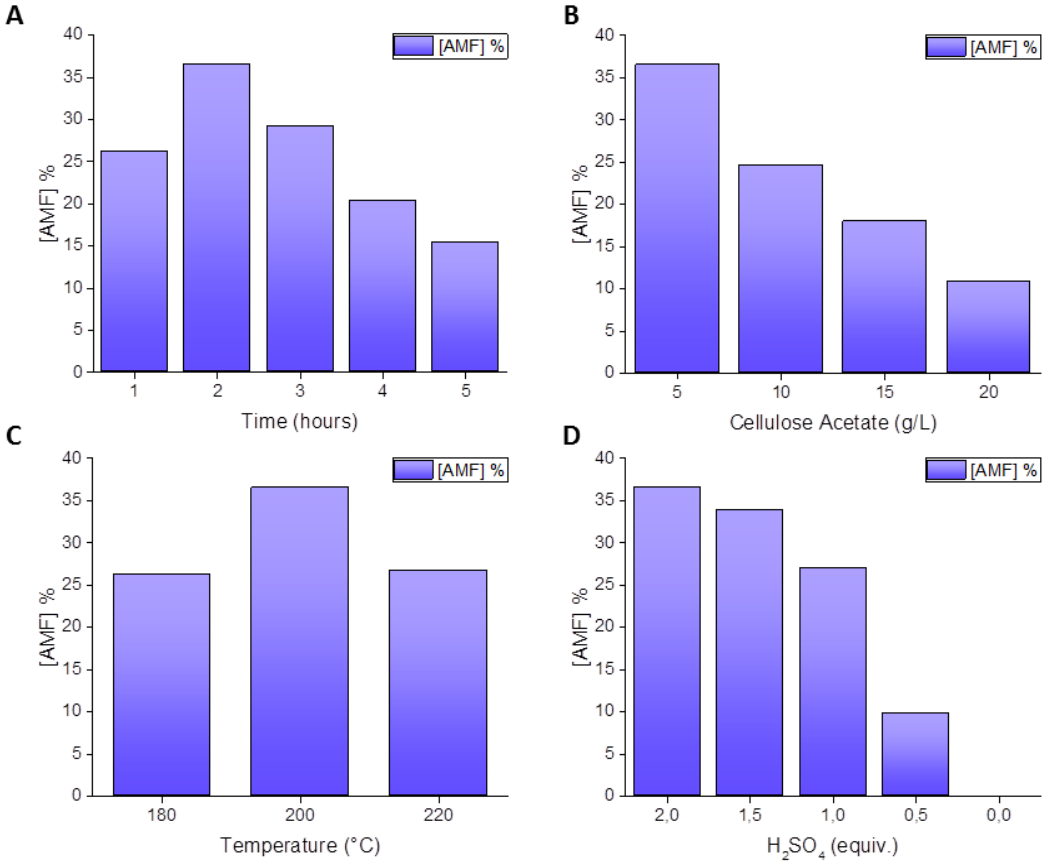

Figure 3.2. AMF yield for the conversion of cellulose acetate in acetic acid and acetic anhydride at different reaction time (A), cellulose acetate concentration (B), temperature (C) and catalyst concentration (D).

For the same reason, increasing the concentration of cellulose acetate, did not increase AMF yield, while decreasing the amount of catalyst led to a decrease in AMF yield (figure 3.2D).

Interestingly, the acetolysis of non-acetylated cellulose was performed as an additional control experiment under optimal conditions (2 eq of H_2SO_4 during 2

hours at 200 °C). In this case, AMF could be obtained in only 4 %, demonstrating the crucial role of acetylation during AMF formation.

During the conversion of acetylated cellulose into AMF, the presence of acetyl groups on the hydroxyl functionality of each glucose unit (defined by the DS) does not prevent product formation. Hence, we speculated that the reaction can possibly proceed via standard cellulose hydrolysis followed by glucose-fructose isomerization (Scheme 3.1). However, for glucose-fructose isomerization to occur, a partial formal deacetylation is required to generate an intermediate in which at least position 1 and 2 on glucose are deprotected. Deacetylation can be the result of acyl transfer mediated by free hydroxyls.

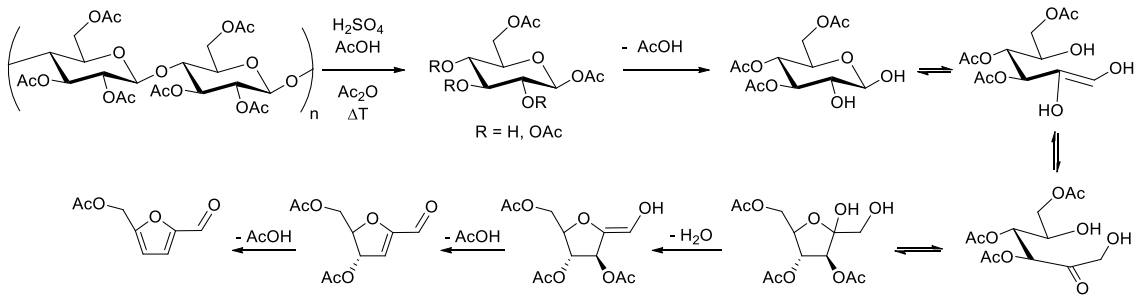

Scheme 3.1. Proposed reaction mechanism for AMF formation.

Alternatively, it could be mediated by traces of water present in the acetic acid, which can act as a nucleophile at high temperatures. In order to better estimate the impact of water and related acetylated species on the reaction, two additional experiments were carried out. Cellulose acetate was reacted at the optimized conditions but in the absence of acetic anhydride, which could act as a water scavenger as well as a capping agent. Alternatively, a second experiment was performed adding a slight water excess to the reaction (10 equivalents), in order to potentially alter the DS. In both cases, we did not observe sensible changes in the yield of AMF, which was obtained in 35 % and 34 % yield for reaction without acetic anhydride and with water respectively. According to these data, we concluded that slight changes in the water content, which may alter the DS in situ, do not play a major role in the reaction, and the use of acetic anhydride can be avoided in general. However, future detailed mechanistic studies will be required to confirm these assumptions.

As mentioned above, the acidic hydrolysis of cellulose acetate in acetic acid results in a light brownish clear solution with a maximum AMF yield of *ca.* 40%. Despite our efforts to identify potential C1-C5 byproducts of the reaction using GC-MS, NMR or HPLC-MS, we could only find traces (< 5%) of acetylated glucose, fructose or levoglucosane, which did not allow us to close a mass balance. Acetic acid is an

additional byproduct of the reaction, which is originated via the cleavage of the acetyl groups and is added to the bulk of the solvent. Interestingly, levulinic acid and formic acid, which are among the most common byproducts reported during the aqueous degradation of HMF, were not observed. Although acetic acid has been reported to reduce the high molecular weight humins formation,[24] we assumed that AMF could condense into soluble low molecular weight humin-like structures. In order to verify this hypothesis, we performed a stability experiment, reacting AMF (3 g/L) in acetic acid (15 mL of) at 220 ºC for 6 hours. Interestingly, in the resulting light brownish clear solution no trace of AMF was detected by HPLC. In turn, when the solution was vacuum dried in the rotary evaporator, a solid black product was obtained. Interestingly, the FTIR spectra of this insoluble product (see Appendix I, Fig B2), resembled the one of humic substances.[25,26] In an integrate process this substances could be valorized either by gasification[27] or liquefaction[28] obtaining syngas and bio-oil, respectively.

3.2 Prepared cellulose acetate acetolysis in batch reactor

So far, we were able to show that AMF can be obtained in good yield using cellulose acetate as the starting material. Interestingly, the latter can be easily obtained by biomass fractionation protocols.[8] Therefore, in order to evaluate the possible integration of this process into a biorefinery scenario, AMF production by treatment of cellulose acetate obtained by different biomass fractionations schemes was evaluated.

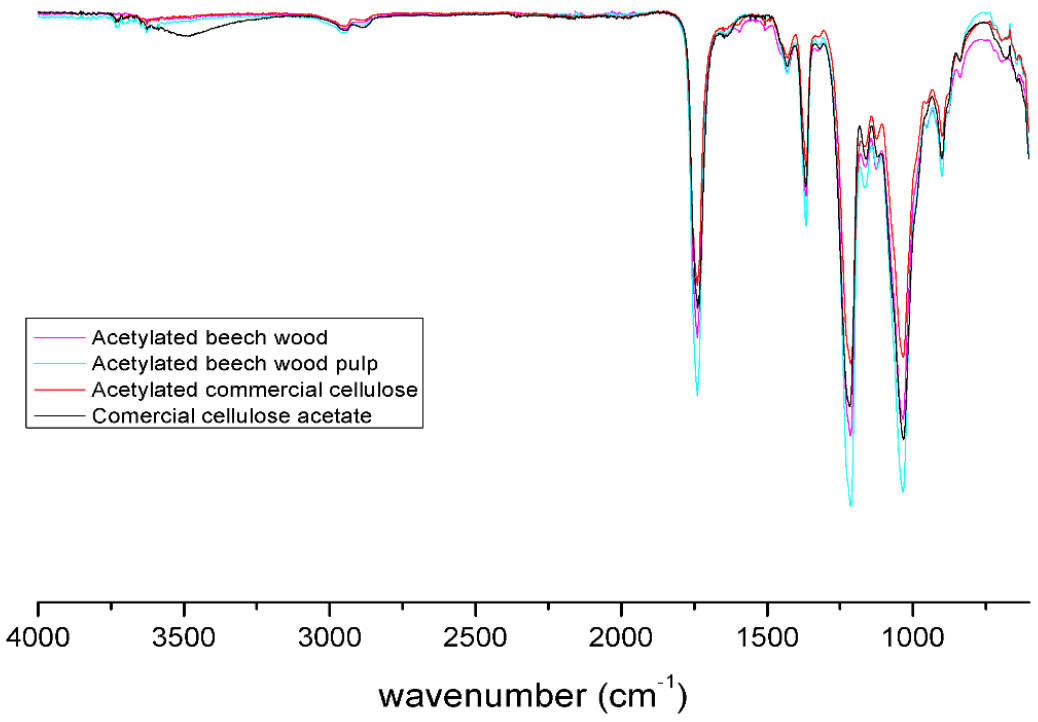

Figure 3.3. FTIR spectra of the acetylated materials and the commercial cellulose acetate.

Commercial cellulose, Organocat pulp[21] and crude beech wood were, therefore, acetylated (FTIR spectra of the produced materials is shown in Fig. 3.3). It can be observed from the FTIR profile that in all cases highly acetylated cellulose materials were obtained (there was no -OH stretch band at 3500 cm^{-1}), being commercial cellulose acetate the only material that exhibited a weak -OH absorption band. This was further confirmed by NMR (See appendix I, Fig B3 - 6), where it was observed that unlike the case of commercial cellulose acetate, cellulose acetates with DS > 2 were obtained (table 1) via acetylation. Moreover, gel permeation chromatography revealed that the molecular weight of the all compounds were in the same range (See GPC in appendix I, Fig B7 – 10). This fact suggests that a previous fractionation of biomass is not required in principle, and acetylation itself could be used as alternative wood pulping method for future exploitation of this process. The conversion of the prepared materials into AMF was tested in an autoclave reactor (table 3.1) for 2 hours at 200 ºC using 2 eq of sulfuric acid as catalyst.

Table 3.1. Properties of the different acetylated materials and corresponding AMF yield after reaction in acetic acid for 2 hours at 200 °C in autoclave, in the presence of sulfuric acid (2 eq).

Substrate	Degree of substitution[a]	Mn (g/mol)[b]	Glucose Units	AMF Yield (%)
Commercial cellulose acetate	1.75	30000	127	36.4
Acetylated cellulose	2.67	10000	36	39.7
Acetylated Organocat pulp	2.74	9000	32	46.9
Acetylated beech wood	2.35	10000	38	36.6

[a]: calculated by NMR; [b]: obtained by gel permeation chromatography

The as-prepared cellulose acetates afforded AMF with yields ranging from 36 % to 47 %. Commercial cellulose acetate resulted in a slight lower yield, while acetylated pulp could be converted with the highest yield. All the prepared materials showed similar molecular weights (M_n), which are smaller compared to commercial cellulose acetate, so, apparently, there is no correlation between M_n and yield. However a slight change in the DS could be observed, ranging from 2.35 for acetylated wood to 2.74 for acetylated pulp. The AMF yield occurred to be higher for higher DS, going from 47 % for acetylated pulp to 37 % in the case of acetylated wood. However, although DS seemed to influence AMF yield, future studies would need to be conducted to fully assess the role of substitution over a broad DS range.

3.3 Commercial cellulose acetate acetolysis in flow reactor

With the aim of increasing AMF yield through fine control of temperature and reaction time, the conversion of cellulose acetate into AMF was tested in a continuous flow reactor. Flow reactors are claimed to have better reproducibility and scalability, safer operability and are generally more viable for high pressure reactions.[29] In this case, we focused initially on acetylated glucose as a model compound, and investigated its conversion at different temperatures (figure 3.4). Noteworthy, AMF could be obtained in 82 % yield at 175 ºC in just 5 min of residence time. However, in line with our previous observations during batch studies, an increase in temperature resulted in deceased AMF yields already at 200 ºC.

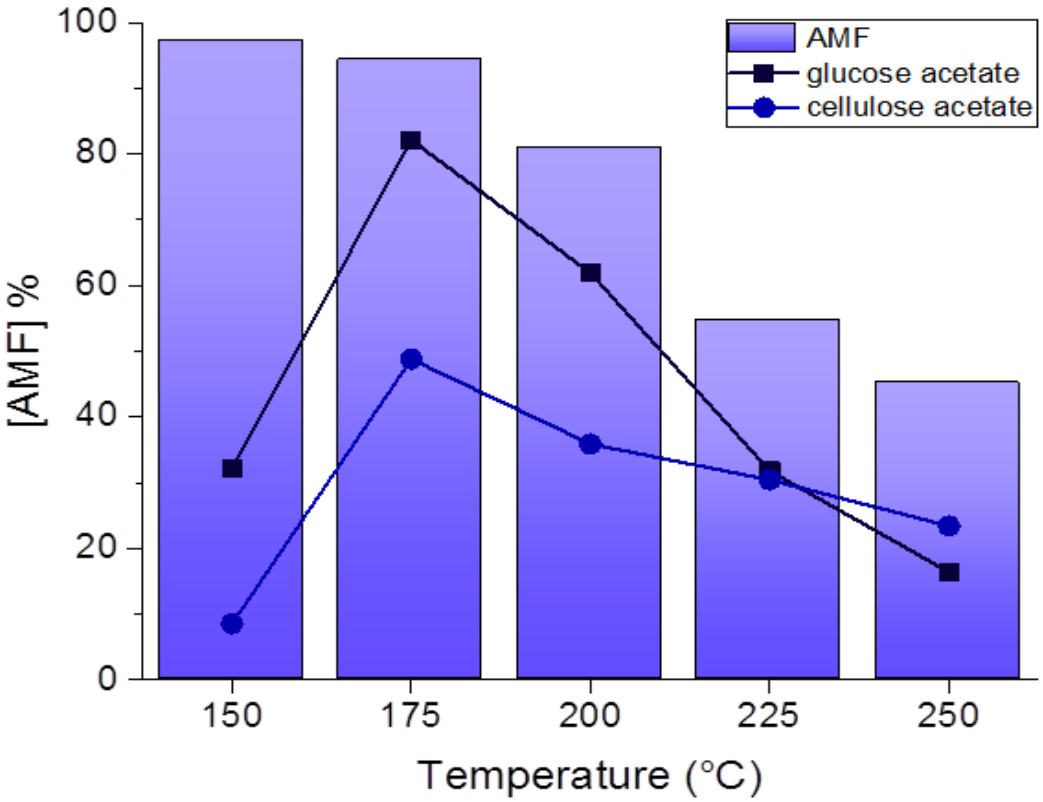

Figure 3.4. AMF recovery experiments (bars) as a function of temperature at 5 minutes residence time, and AMF yield from glucose (dark blue squares) and cellulose acetate (light blue circles) as a function of temperature at 5 minutes residence time. Experiments were conducted in the flow reactor.

In order to shed light into this fact, the stability of AMF under the reaction conditions was tested and appeared to be critical above 200 ºC. In fact, while AMF could be still recovered in 94 % after 5 minutes at 175 °C, its recovery dropped to 55 % and 45 % at 225 or 250 ºC respectively (figure 3.4, solid bars).

Based on these results, the conversion of cellulose acetate was optimized at 49 % yield with a residence time of 5 minutes at 175 ºC (figure 3.4, light blue circles). Interestingly, higher residence time did not increase AMF yield (figure 3.5).

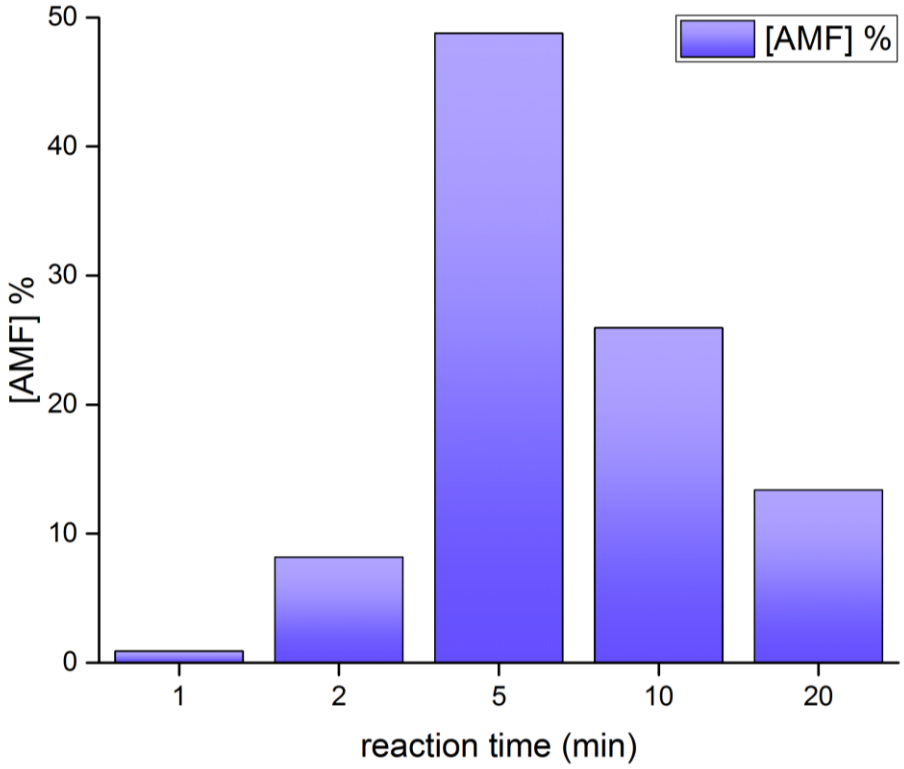

Figure 3.5. AMF recovery experiments as a function of the residence time in the flow reactor at 175 °C. Conditions: cellulose acetate (5 g/L), acetic acid as solvent, Ac_2O (2 eq), H_2SO_4 (2 eq).

Comparing flow reactor and batch results, it is important to emphasize the drastic reduction of the reaction time achieved using continuous processing. We attribute this difference to the lack of a temperature gradient and the reduced heat transfer limitations, which are in turn observed in the batch system. As a result, it was possible not only improve the yields but also reduce the required temperature and the processing time. In order to prove the scalability of this method, a time on stream experiment was performed running the reaction over 2 hours under the optimized conditions. The crude isolated after work up was mainly composed of AMF as confirmed by NMR analysis (see appendix, figure B1). Hence, continuous processing proved to be viable. Furthermore, acetic acid is a convenient solvent for a variety of transformations. For instance, HMF oxidation to FDCA in acetic acid has been recently proposed,[30] pointing to the development of integrated methods for the production of important HMF derivatives (e.g. FDCA) avoiding intermediate AMF separation. Finally, the presence of the acetyl functionality in AMF is expected to influence the reactivity of the furan system and to allow for the selective functionalization of the aldehyde group.

4. CONCLUSIONS

For the first time, we demonstrated that acetolysis of cellulose acetate in the presence of sulfuric acid, is as an efficient method to produce AMF. The proposed method takes advantage of the good solubility of acetylated cellulose in acetic acid, enabling a homogenous process, unlike the case of unprotected cellulose. The strategy works well also when crude acetylated biomass is used as precursor, enabling a simple biorefinery scheme for the direct valorization of biomass into an important value added platform chemical. Finally, due to its homogenous nature, we demonstrated that the method is compatible with continuous processing, opening a new scenario for the preparation of furans from biomass.

5. REFERENCES

1 S. G. Wettstein, D. Martin Alonso, E. I. Gürbüz and J. a. Dumesic, *Curr. Opin. Chem. Eng.*, 2012, **1**, 218–224.

2 R. Rinaldi and F. Schüth, *ChemSusChem*, 2009, **2**, 1096–107.

3 A. Corma, S. Iborra and A. Velty, *Chem. Rev.*, 2007, **107**, 2411–2502.

4 G. W. Huber, S. Iborra and A. Corma, *Chem. Rev.*, 2006, **106**, 4044–98.

5 H. Wang, G. Gurau and R. D. Rogers, *Chem. Soc. Rev.*, 2012, **41**, 1519.

6 D. Klemm, B. Heublein, H.-P. Fink and A. Bohn, *Angew. Chem. Int. Ed. Engl.*, 2005, **44**, 3358–93.

7 T. Liebert, in *Cellulose Solvents: For Analysis, Shaping and Chemical Modification*, 2010, pp. 3–54.

8 D. G. Barkalow, R. M. Rowell and R. a. Young, *J. Appl. Polym. Sci.*, 1989, **37**, 1009–1018.

9 S. Fischer, K. Thümmler, B. Volkert, K. Hettrich, I. Schmidt and K. Fischer, *Macromol. Symp.*, 2008, **262**, 89–96.

10 D. Esposito and M. Antonietti, *Chem. Soc. Rev.*, 2015, **44**, 5821–5835.

11 S. P. Teong, G. Yi and Y. Zhang, *Green Chem.*, 2014, **16**, 2015.

12 A. F. Sousa, C. Vilela, A. C. Fonseca, M. Matos, C. S. R. Freire, G.-J. M. Gruter, J. F. J. Coelho and A. J. D. Silvestre, *Polym. Chem.*, 2015, **6**, 5961–5983.

13 Y. Román-Leshkov, C. J. Barrett, Z. Y. Liu and J. a Dumesic, *Nature*, 2007, **447**, 982–985.

14 M. A. Mellmer, C. Sener, J. M. R. Gallo, J. S. Luterbacher, D. M. Alonso and J. A. Dumesic, *Angew. Chemie - Int. Ed.*, 2014, **53**, 11872–11875.

15 J. B. Binder and R. T. Raines, *J. Am. Chem. Soc.*, 2009, **131**, 1979–85.

16 R.-J. van Putten, J. C. van der Waal, M. Harmse, H. H. van de Bovenkamp, E. de Jong and H. J. Heeres, *ChemSusChem*, 2016, **9**, 1827–1834.

17 M. Mascal and E. B. Nikitin, *Angew. Chemie - Int. Ed.*, 2008, **47**, 7924–7926.

18 E. S. Kang, Y. W. Hong, D. W. Chae, B. Kim, B. Kim, Y. J. Kim, J. K. Cho and Y. G. Kim, *ChemSusChem*, 2015, **8**, 1179–1188.

19 M. Bicker, D. Kaiser, L. Ott and H. Vogel, *J. Supercrit. Fluids*, 2005, **36**, 118–126.

20 H. Namazi and S. J. Rad, *J. Appl. Polym. Sci.*, 2004, **94**, 1175–1185.

21 P. M. Grande, J. Viell, N. Theyssen, W. Marquardt, P. Domínguez de María and W. Leitner, *Green Chem.*, 2015, **17**, 3533–3539.

22 S. S. Z. Hindi and R. A. Abohassan, *Bioresources*, 2015, **10**, 5030–5048.

23 I. Van Zandvoort, Y. Wang, C. B. Rasrendra, E. R. H. Van Eck, P. C. a Bruijnincx, H. J. Heeres and B. M. Weckhuysen, *ChemSusChem*, 2013, **6**, 1745–1758.

24 P. Domínguez de María, *Industrial Biorenewables. A critical viewpoint*, Wiley-VCH Verlag, 2016.

25 S. K. R. Patil and C. R. F. Lund, *Energy and Fuels*, 2011, **25**, 4745–4755.

26 L. Shuai and J. Luterbacher, *ChemSusChem*, 2015, **9**, 133–155.

27 T. M. C. Hoang, L. Lefferts and K. Seshan, *ChemSusChem*, 2013, **6**, 1651–1658.

28 Y. Wang, S. Agarwal and H. J. Heeres, *ACS Sustain. Chem. Eng.*, 2016, **5**, 469–480.

29 M. Trojanowicz, *Talanta*, 2016, **146**, 621–640.

30 B. Saha, S. Dutta and M. M. Abu-Omar, *Catal. Sci. Technol.*, 2012, **2**, 79–81.

Chapter 4:

Co-spinel as an alternative to noble metal catalysts for the one-pot reduction of furfural to 1,5-pentanediol

1. INTRODUCTION

Commonly, the transformation of biomass sources is addressed by targeting a set of molecules that can be further transformed in already applicable compounds or offer a versatile range of applications, the so-called building blocks.[1] Among them, furfural (FA) is one of the few which nowadays is completely produced from renewable sources.[2] FA has an enormous potential for chemical synthesis, and its derivatives have been proposed either as fuels or monomers for biopolymers production.[3-8] Diols, which are among the most appreciated monomers,[9] can be produced *via* furfural hydrogenation.[10]

FA hydrogenation was already reported over copper chromite in 1931 by Adknins and Connor. They reported quantitative conversion of FA to furfuryl alcohol (FFA), and afterwards, in a second reaction, 70 % yield of 1,2-pentanediol (1,2-PeD) and 1,5-pentanediol (1,5-PeD) from FFA.[11] However, both copper and chromium are known for their toxicity and, consequently, the use of these catalysts is often dismissed.

Great efforts are being done in recent years in order to achieve good yield of diols from FA on environmental benign catalysts. Commonly two reaction pathways are employed for these reactions.[9] One combines hydrogenation of FA to tetrahydrofurfuryl alcohol (THFA) followed by hydrogenolysis of THFA to either form 1,2-PeD or 1,5-PeD (Scheme 4.1, route II). The second one proceeds *via* direct ring-opening of FFA, which is often preferred as starting material (Scheme 4.1, route II). Independently of which one is employed, FFA or THFA are usually chosen as starting product.

Due to the high amount of competitive reactions that FA can undergo (Scheme 4.1), the direct use of FA as starting material remains a challenge. Xu et al. reported 1,5-PeD production from FA over a platinum supported inverse Co-spinel, achieving *ca.* 35% yield of 1,5-PeD. They claimed that Co^{3+} acted as active site for adsorption and C=C bond cleavage, while Pt catalysed the following reduction steps.[12] Also, Tomishigue's group has intensively studied diols production from renewable sources and has successfully developed a two steps system, using Pd-Ir-ReO_x/SiO_2 as catalyst, obtaining 71% yield of 1,5-PeD, which until now is the greatest yield of 1,5-PeD achieved from FA.[13] This system takes advantage of Pd-ReO_x catalytic activity for FA hydrogenation into THFA, while Ir-ReO_x catalyses the THFA selective hydrogenolysis into 1,5-PeD. Despite the great potential of this

bifunctional catalyst, both of the active sites are based on noble metals, which highly impacts on the cost of this technology and limits its application in a biorefinery scenario.

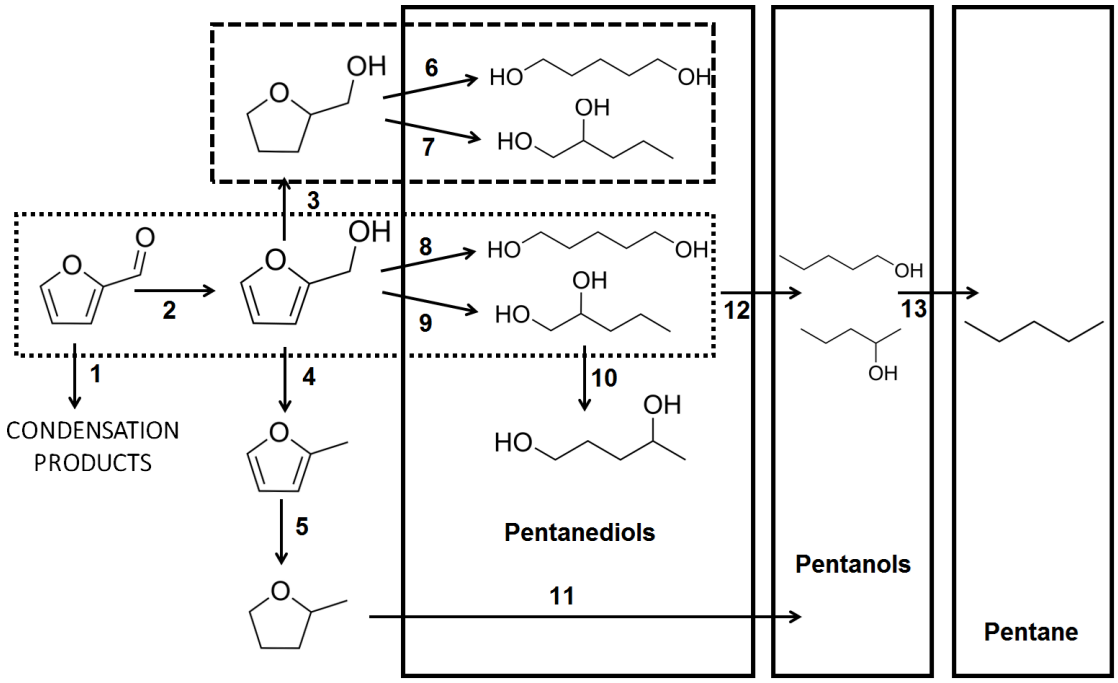

Scheme 4.1. Different products that can be obtained through furfural hydrogenation.

Therefore, in recent years, more efforts are being made in order to develop non-noble metals for FA hydrogenation. Recently, Wu et. al.[14] reported FA hydrogenation to form either FFA or THFA, over bimetallic CuNi nanoparticles (NPs) supported on Mg/Al oxides. Using monometallic catalysts, Audemar et. al.,[15] recently have proposed Co NPs confined in a mesoporous material for practically quantitative hydrogentation of FA to FFA. Lee et. al.[16] successfully applied a Co supported on TiO_2 catalyst for continuous flow FFA hydrogenation on aqueous media, producing 30% of 1,5-PeD. However, to the best of our knowledge there is no report of diols production from FA over non-toxic and non-noble catalysts, for which we have studied the behaviour of Co-Al spinel nanoparticles.

2. METHODOLOGY

2.1 Catalyst synthesis

Aluminium acetylacetonate (99%, Sigma-Aldrich) and cobalt acetate (99,995%, Sigma-Aldrich) were used as received. The precursor solution consisted of a mixture of aluminium acetylacetonate (0.078 mol/L) and cobalt acetate (0.017 mol/L) dissolved in a solution containing 73 %-v of methanol (J.T. Baker) in ion-exchanged water. The Co:Al ratio in the precursor solution was approximately

0.22. The flame spray pyrolysis system used for particle preparation has been described previously.[17] Briefly, the precursor solution was fed through a capillary at a rate of 5 mL/min and atomized with a high-pressure dispersion gas, O_2, at a flow rate of 5 L/min. A premixed methane-oxygen flamelet with gas flow rates of 1 and 2 L/min, respectively, ignited the atomized precursor solution, resulting in the formation of a high-temperature flame, with temperatures in excess of 2000 °C. The produced particles were collected on a Teflon filter (Zefluor, Pall Corporation).

2.2 Catalyst characterization

The X-ray diffraction (XRD) analysis of the cobalt sample was recorded using a Siemens D5000 diffractometer (Bragg-Brentano for focusing geometry and vertical θ-θ goniometer) with an angular 2θ-diffraction range between 5° and 70°. The sample was dispersed on a Si (510) sample holder and spectra were collected with an angular step of 0.05° at 9 s per step of sample rotation. Cu Kα radiation (λ=1.54 Å) was obtained from a copper X-ray tube operated at 40 kV and 30 mA. Diffractograms were fitted using TOPAS software (V4.2, Bruker), fitting were just done tentatively in order to give a better understanding of diffractograms. Raman spectra of the samples was obtained using a T64000 Jobin Ivon spectrometer. The sample was excited using a laser operating at 785 nm and a power of 2mW for 60 s and one scan was recorded.

Specific surface areas were determined by N_2 adsorption at −196 °C using a Quantachrome Autosorb. Samples were previously degassed in situ at 200 °C under vacuum for 16 h. Surface areas were calculated using the Brunauer–Emmet–Teller (BET) method over a p/p_0 range where a linear relationship was maintained.

Temperature-programmed reduction (TPR) experiments were performed in an Autochem II 2920 using 10% H_2 (30 mL/min) in Ar stream. The samples were heated from 30 to 950 °C with the heating rate of 5 °C/min. Before the reduction, the samples were heated in Ar flow at 200 °C for 1 h to remove physically adsorbed water.

TPD of NH_3 was conducted using an Autochem II 2920 instrument after reduction *in situ* at 500, 700 or 850 °C. Typically, *ca.* 100 mg of sample was pretreated in situ at 200°C for 1 h to remove the physisorbed species on the surface. The NH_3 adsorption was performed with a flowing gas mixture containing 10% NH_3 balanced with Ar (30 mL/min) at 80 °C for 1 h. After adsorption, a flow of Ar (30 mL/min) was passed through the sample at 80 °C for 1 h to remove the

physisorbed NH_3. Then, the analysis was performed in flowing Ar (30 mL/min) from 40 to 950 °C (20 °C/min). Desorption was also followed by MS to identify the species desorbed. The number of acid sites was calculated from the area under the NH_3 peak. The calibration of the instrument was done using injections of a known volume of 10% NH_3/Ar gas.

Thermogravimetric analysis (TGA) was carried out with a Sensys Evo analyser from SETARAN coupled with a MS spectrometer, under Ar flow (20 mL/min), from room temperature to 850 °C, at a heating rate of 5 °C/min.

2.3 Catalyst reduction

Typically, 40 mg of Co-Al spinel were reduced under dynamic conditions for 4 hours in 5% H_2-Argon mixture at 500, 700 or 850 °C with a heating rate of 5 °C /min.

2.4 Furfural reduction

Reduction of furfural (FA) was carried out in a 100 mL stainless steel autoclave (Autoclave engineers). Typically, a solution of 10 g/L of FA in 40 mL of 2-propanol (IPA) was placed in the reactor with 40 mg of previously reduced catalyst. Then the reactor was purged with hydrogen, and pressurised at 20 bar (unless otherwise indicated). Once the desired temperature was reached, stirring was initiated (1000 rpm) and samples were withdrawn periodically to follow the reaction during 8 hours.

Two different reuse experiments were carried out, all of them at the optimum conditions. For the first, semi-batch, reuse set of experiments, the reaction was set as usual and each 2 hours, the reaction was stopped, depressurized, cooled down, the reaction vessel was opened, and 6 mL of IPA + 340 uL of FA were added. This procedure was repeated 5 times for a total of 6 runs. For the second reuse, the reaction was run for 8 hours, once stopped the catalyst was thoroughly washed with IPA, dried, calcined and reduced at 700°C with 5% H_2/Ar prior reuse.

The products were identified and characterised with CG-MS, calibrations curves were performed using commercial standards of FA, FFA, THFA, 1-pentanol (2-pentanol calibration curve was assumed to be equivalent) and 1,5-pentanediol (1,2-pentanediol and 1,4-pentanediol calibration curves were assumed to be equivalent). Possible gaseous products formed such as pentane were not monitored in our system; however, the mass balance in most of the cases was around 95%.

FA conversion and product yields were calculated on molar bases, tipically:

$$Yield\ of\ X = \frac{C_X(g/L) \times M_{W_{FA}}(g/mol)}{C_{FA_i}(g/L) \times M_{W_X}(g/mol)}$$

Where C_x is the determined concentration in grams litre of the given compound, M_{WFA} is FA molecular weight, C_{FAi} is initial concentration in grams litre of FA, and M_{Wx} is the molecular weight of the given compound.

For the second recycle the yield was calculated out of the initial FA quantity. And for the semi-batch out of the total FA added.

3. RESULTS AND DISCUSSION

3.1 Catalyst characterization

The textural properties of the CoAl oxide catalysts reduced at different temperatures were studied by low temperature N_2 adsorption analysis. The N_2 adsorption–desorption isotherms of all the samples exhibited a type IV isotherms with a hysteresis loop apparently between H1 and H3 (upon the IUPAC

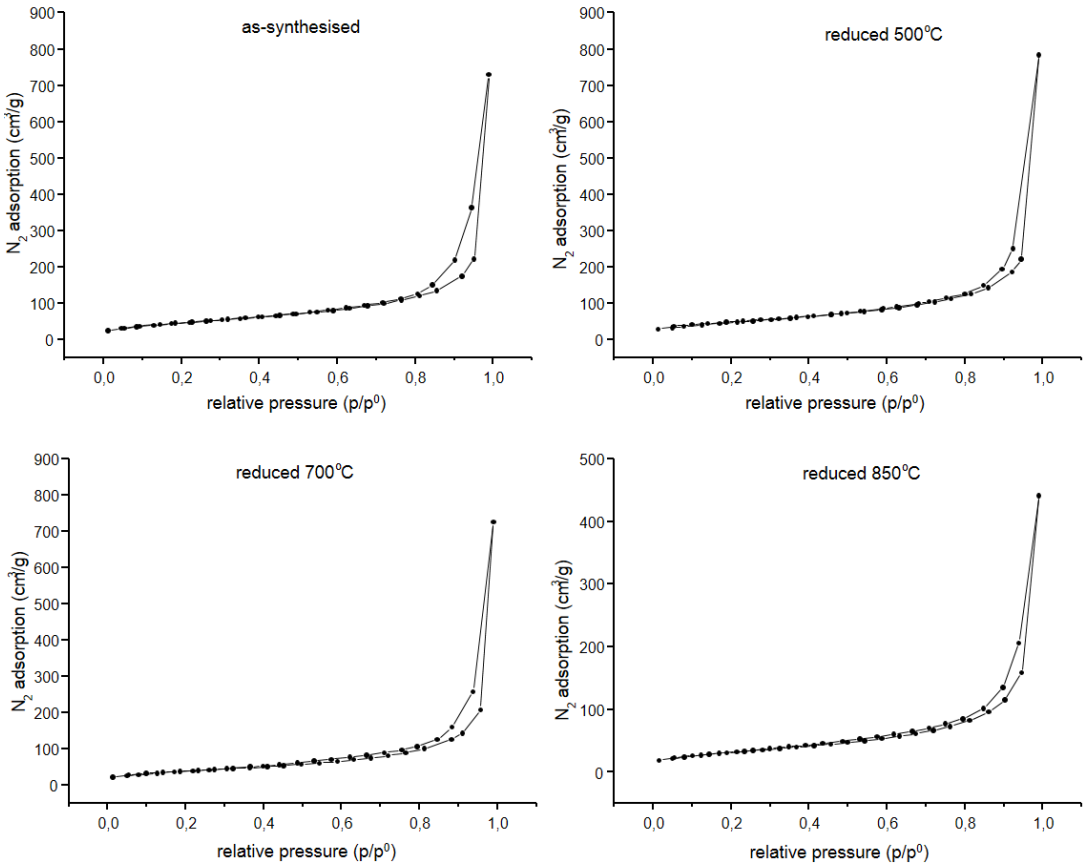

Figure 4.1. N_2 adsorption–desorption isotherms of the as-synthesised sample and reduced at different temperatures.

classification[18]), since the adsorption and desorption branches are rather parallel and the hysteresis loop is not closed until $P/P_0 = 1$ (Figure 4.1). This may indicate the presence of both mesoporous channels made by aggregates or agglomerates and **Table 4.1.** BET area, pore volume, pore diameter and Co crystallite size of the as-synthesised sample and reduced at different temperatures.

Sample	SBET (m^2/g)	Vp (cm^3/g)	Average pore diameter (nm)[a]	Co^0 Crystallite size (nm)[b]
As-synthesized	174	1.21	10.68	-
Red. 500 °C	170	1.13	10.68	-
Red.700 °C	139	1.12	13.37	1.8±0.4
Red. 850 °C	112	0.68	14.64	9±1

[a] Average pore size was calculated based on DFT model due to the pore shape presented in the samples
[b] Average crystallite size calculated through integration of all the diffraction planes using the through double Voigt approach with TOPAS program. The instrumental resolution function (pseudo-Voigt) has been estimated with LaB_6 (NIST 660a)

the existence of slit-shaped pores. The BET surface area, total pore volume and average pore diameter of the cobalt aluminates are summarized in Table 4.1. Both as-synthesized sample and the spinel reduced at 500 °C presented similar specific surface areas (174 m^2/g and 170 m^2/g, respectively) and pore volumes. The specific surface area decreased along with the increase of reduction temperature of the catalyst, dropping, about a 36%, from 174 m^2/g of the as-synthesized spinel to 112 m^2/g. Similarly, the pore volume decreased upon the thermal treatment from 1.21 cm^3/g in the as-synthesized sample to 0.68 cm^3/g in the spinel reduced at 850 °C.

The XRD patterns of both the as-synthesized Co-Al spinel nanoparticles and the reduced materials revealed the presence of cobalt aluminum oxide species with the structure of spinel; however, it cannot be concluded that these patterns correspond to normal ($CoAl_2O_4$), inverse (Co_2AlO_4) or Co_3O_4 spinel, since they present the same crystalline structure (Fig. 4.2). The diffractogram corresponding to as-synthesized sample was fitted using the double Voigt approach (by means of TOPAS program), revealing the coexistence of two cubic structures (Fd-3m) which present different lattice parameters (data not shown). Additionally, the Co/Al ratio in the precursor solution of approximately 0.22 was confirmed in the solid by EDX (see Apendix I, Table C1); therefore, the formation of a spinel-Al_2O_3 solid solution may be expected. Taking these two facts into account, the coexistence of cubic γ-alumina (corresponding to the smaller lattice parameter, JCPDS 79-1553) and a

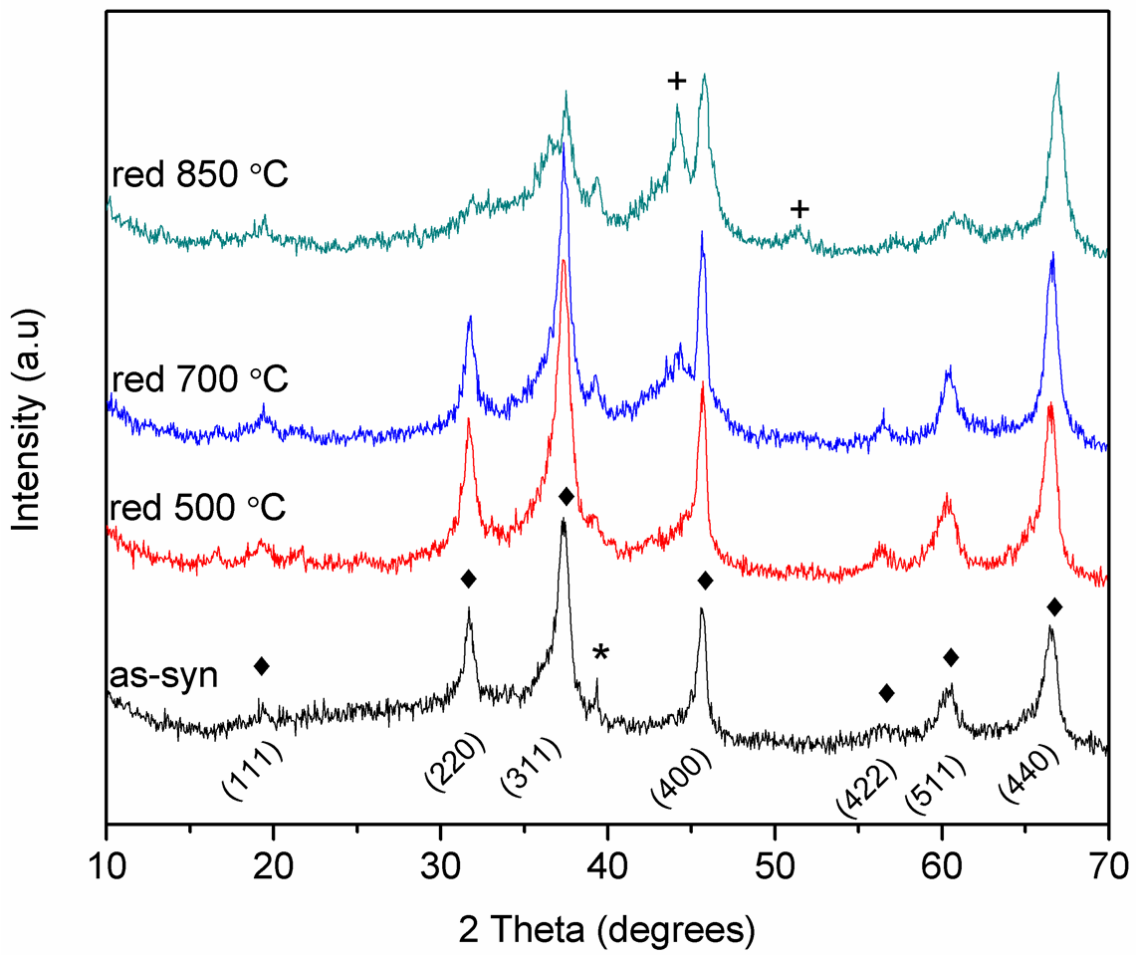

Figure 4.2. XRD diffraction patterns of the as-synthesised sample and reduced at different temperatures. (♦) CoAl-spinel (*) Al_2O_3 (+) metallic Co

cubic Co spinel (with higher lattice parameter) can be expected. However, further information is needed to confirm the type of spinel formed during the material synthesis. To resolve this uncertainty, a Raman spectrum of the as-synthesised spinel was acquired (Figure 4.3), finding the presence of five main bands (located at 192 (vs), 476 (m), 516(w), 615(w), and 683 (vs) cm^{-1}). According to the work of Mwenesongole[19] the presence of a band at 683 cm^{-1} and the absence of a band at 408 cm^{-1} might discard the presence of normal spinel ($CoAl_2O_4$), while the blue-green colour of the sample also might discard the presence of Co_3O_4 spinel, clearly suggesting the presence of an inverse Co spinel (Co_2AlO_4, JCPDS 38-814).

Upon sample reduction at different temperatures, some differences in XRD patterns can be envisaged, and the intensity of some diffraction peaks varied along with temperature (Fig. 4.2). For instance, peaks at 2θ angles 46º and 67º (corresponding to 400 and 440 planes, respectively) increased the relative intensity while those peaks at 32º and 37º (corresponding to 220 and 331 planes, respectively) experimented a decrease in intensity. We initially attributed this to the

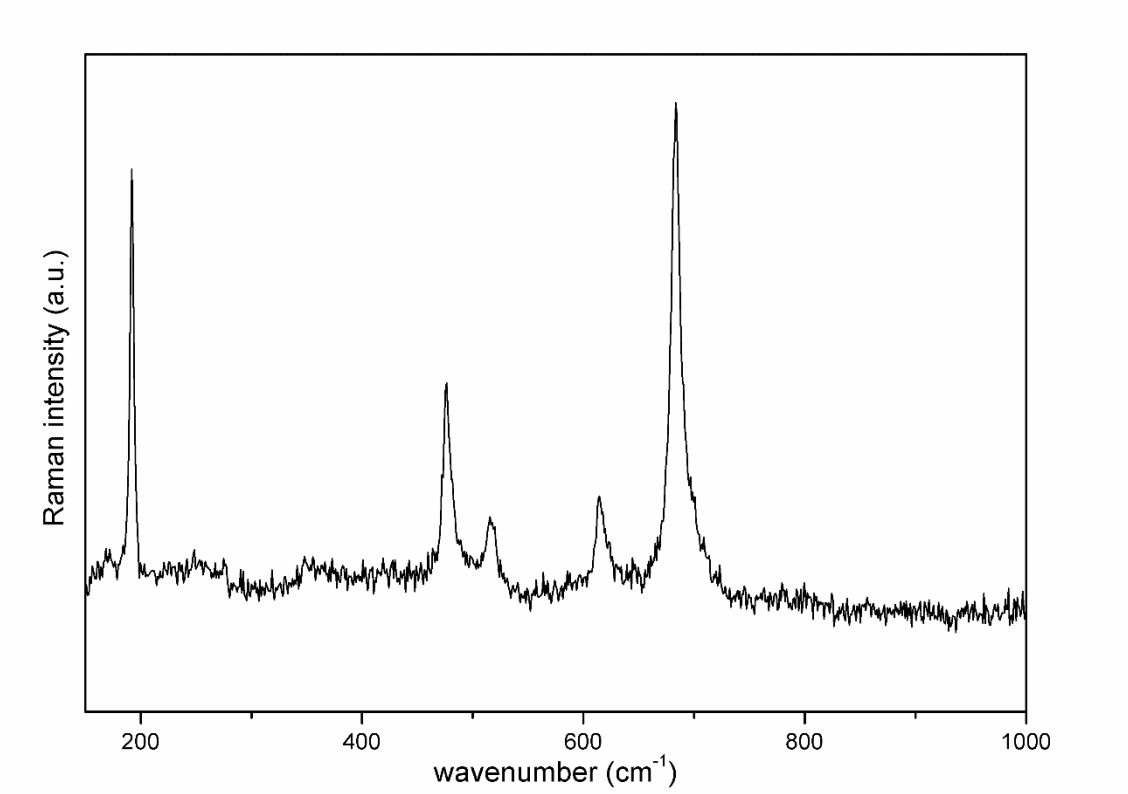

Figure 4.3. Raman spectrum of the as-synthesised sample, laser 785 nm.

partial destruction of the crystalline structure of Co_2AlO_4 spinel during reduction, while γ-Al_2O_3 remained intact, hence increasing its relative intensity. Additionally, when the sample was reduced at 700 °C and 850 °C, new peaks corresponding to a cobalt bearing face centered cubic structure (FD-3m-(225) JCPDS 89-4307) developed as showed in Figure 4.2. This agrees with spinel degradation upon reduction at higher temperatures, segregating part of the cobalt from the spinel structure, which was, then, subsequently reduced. Further, the intensity of the Co peaks increased at 850 °C compared to sample reduced at 700 °C, suggesting the growth of the segregated Co particles as could be confirmed with Scherrer equation (Table 4.1).

TPR analysis gives information about the reduction process in the Co-Al spinel and changes in the sample structure. The TPR profile of the sample showed two major signals (Fig. 4.4). A small broad peak in the 300 °C and 550 °C region can correspond to the reduction of Co^{3+} to Co^{2+} possibly from Co_2AlO_4 spinel or even from small amounts of Co_3O_4 indiscernible by XRD. Further, as discussed above, XRD analysis did not show presence of metallic Co when the sample was reduced at 500 °C, suggesting the absence of CoO in the as-synthesised sample. In addition, TPR displayed a higher reduction peak in the 600 – 900 °C region, which was

attributed to the reduction of Co_2AlO_4 spinel. This peak exhibited an asymmetric shape, suggesting the presence of at least three different reducible species in different coordination environments.

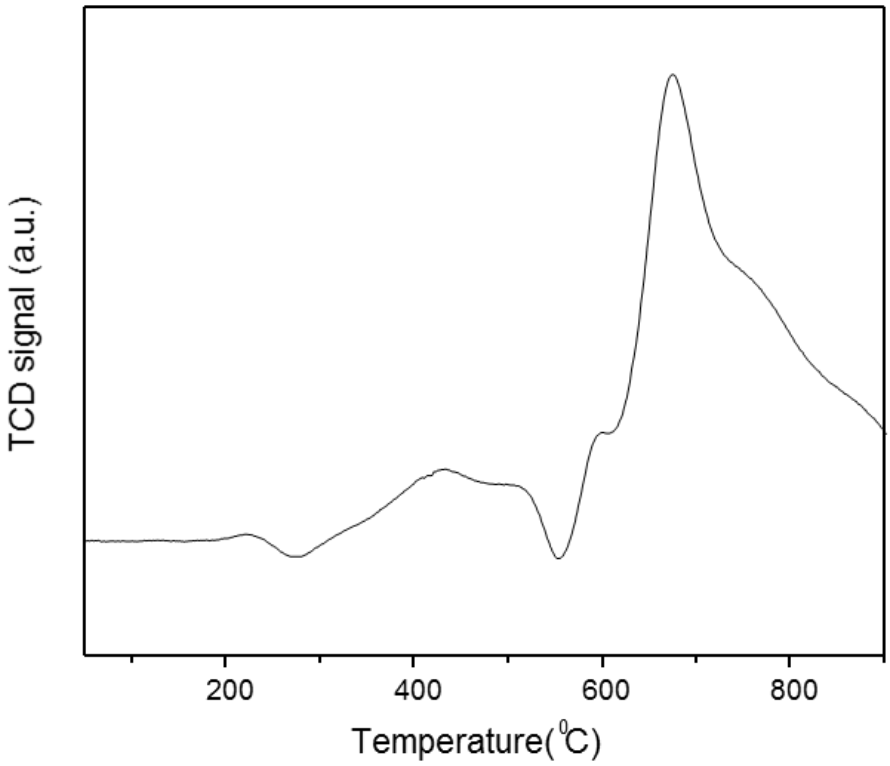

Figure 4.4. TPR profile of the as-synthesised sample.

The peak centered at 675 °C could be attributed to the reduction of the formed Co^{2+} in the first reduction step (from Co_3O_4 to CoO) and/or the reduction of unsaturated Co^{2+} in the spinel to zero valence cobalt, since XRD analysis already revealed metallic Co in the sample reduced at 700 °C. On the other hand, those shoulders showed at 760 °C and 870 °C could be attributed, respectively, to: i) the reduction of saturated structural Co^{3+} of lower accessibility or presenting higher structural interactions with aluminium, and ii) the subsequent Co^{2+} reduction forming more Co^0 (as observed by XRD). This also agrees with the decrease of intensity of the Co_2AlO_4 diffraction lines in that sample reduced at 850 °C.

Thermal programmed desorption of ammonia (TPD-NH_3) was monitored with mass spectrometry (MS) to calculate the concentration of acid sites at the surface of the material after the reduction in situ of the catalyst. Notably, the TPD profiles were different depending on the catalysts reduction temperature. For instance, the profile of those catalysts reduced at 700 and 850 °C presented two peaks (Fig. 4.5), whereas the catalyst reduced at 500 °C presented three peaks. Only the peak at the lowest temperature, between 100 and 500 °C, corresponds to desorption of

ammonia, as evidenced by MS (m/z = 16, 17), while the peak at higher temperature corresponds to desorption of ions corresponding to m/z = 44. This peak occurred at temperatures higher than 600 °C and decreased notably as the reduction temperature increased; initially we attributed this peak to CO_2 evolution from the presence of organic phase not completely burned during synthesis. However, this assumption was completely discarded after TG-MS analysis results, where CO_2 evolution was found to occur at lower temperatures (< 400 °C) (TGA – see appendix C Fig. C1); thus, any possible organic phase present in the sample should be removed at all the reduction temperatures used in the pretreatment of the sample.

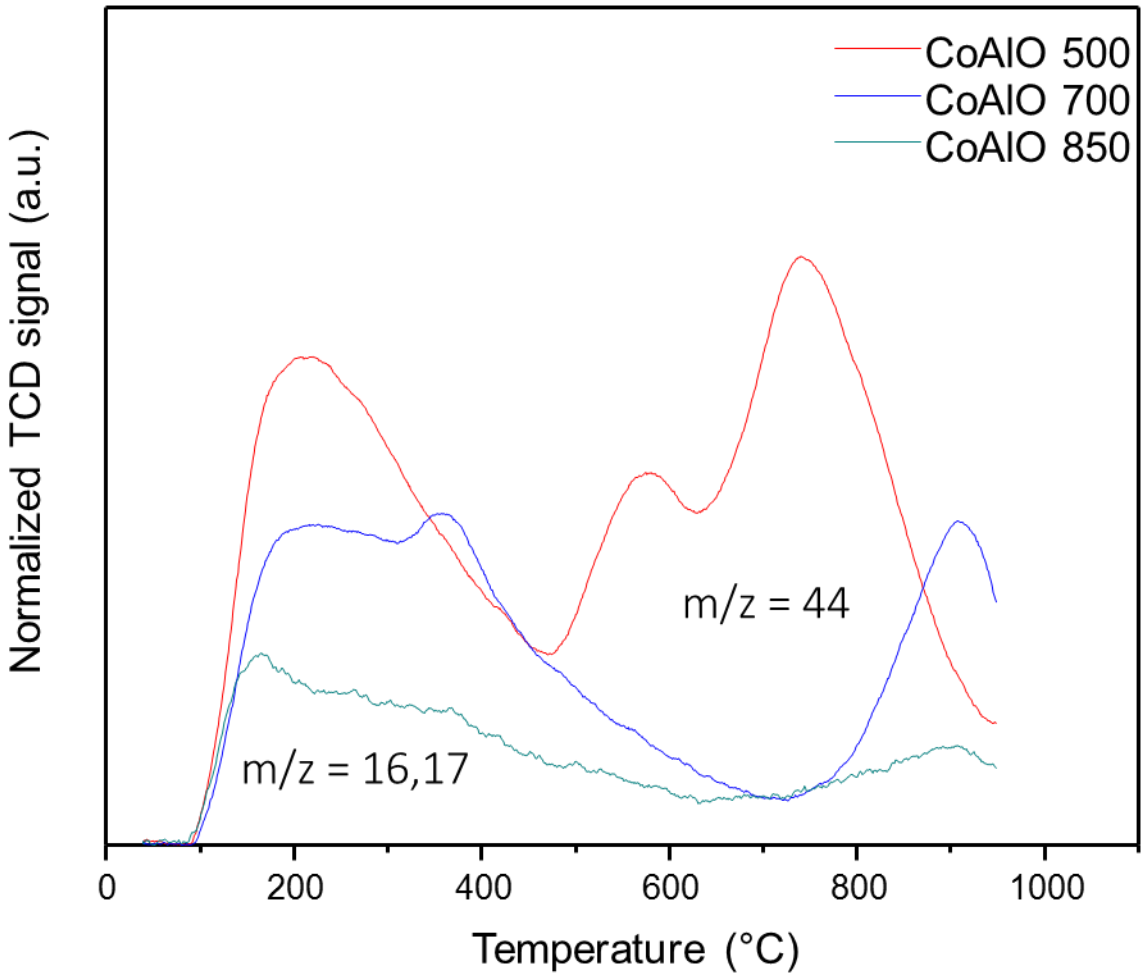

Figure 4.5. NH_3-TPD profile of the sample reduced at 500, 700, and 850°C.

Notably, the contribution of those peaks corresponding to m/z = 44 decreased with the increasing reduction temperature and, interestingly, hydrogen evolution (m/z =2) was also detected, whereas N_2 evolution (m/z = 28) was not observed at any time, suggesting that this peak may correspond to N_2O formed from NH_3 oxidation at expenses of the surface oxygens of the sample. This would also agree

with the marked intensity decrease of this peak as the reduction temperature increases. Hence, considering this information, only the peak at the lowest temperature was used to calculate the amount of acid sites in the samples (Table 4.2).

Table 4.2. Acid sites density by TPD-NH_3

Sample	NH_3 desorption (mmol/g) (50-600 ºC)		Total $NH_{3des.}$ evolved (mmol/g)	Acid sites density (μmol/m^2)
	I (≈200 ºC)	II (≈350 ºC)		
Red. 500 ºC	0.89 (210)	--	0.89	5.2
Red. 700 ºC	0.48 (207)	0.25 (377)	0.73	5.3
Red. 850 ºC	0.27 (156)	0.38 (326)	0.65	5.8

In brackets: temperature maximum peak

3.2 Catalytic performance for furfural reduction

3.2.1 Influence of reaction conditions

Initially, Co-spinel reduced at 850 °C, was tested for the reduction of furfural at a reaction temperature of 150 °C. As observed in Fig. 4.6, complete furfural conversion was achieved within 2 h and, initially, FFA is formed. As previously reported, FA reduction to FFA is rapidly achieved.[9] Afterwards FFA, is further hydrogenated, remaining only 17.8 % after 8 h, to form THFA and 1,5-PeD in a yield of 50.5 % and 16.7 %, respectively (Table 4.3, Entry 2). Contrary to what is normally reported for monometallic catalysts[15,20–22], the Co-spinel was capable of producing 1,5-PeD. This is an interesting remark which led us to go deeper into the reaction mechanism.

At first sight, the reduction of the FFA furan ring seems to be more favoured than FFA hydrogenolysis. Further, it was observed that THFA hydrogenolysis was not achieved at the working conditions, indicating that rather parallel and competitive reduction to either 1,5- PeD or THFA may undergo. This will be studied in more detail below. In addition, traces of 1-pentanol, 2-pentanol, and 1,2-PeD were detected (Scheme 4.1 shows some of the potential products that can be formed through FA hydrogenation).

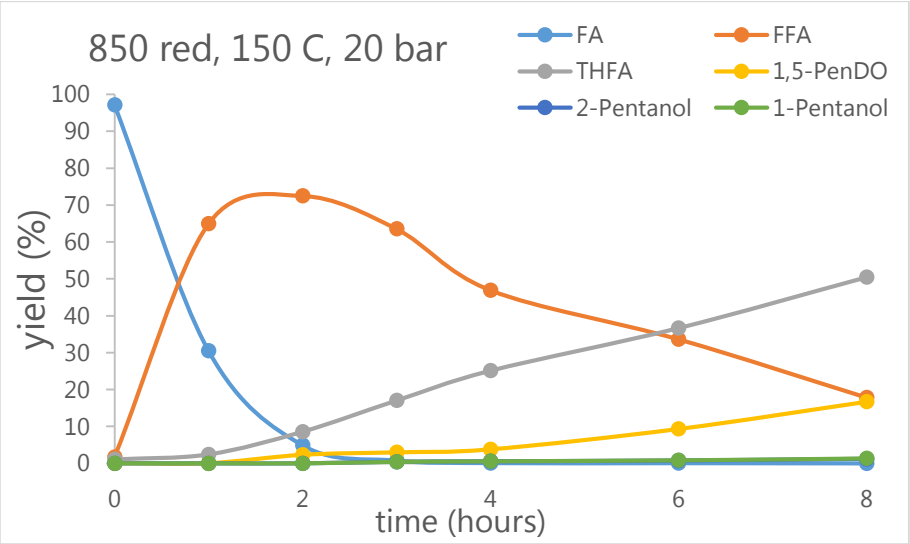

Figure 4.6. Furfural reduction during 8 hours. Conditions: 150°C, 20 bar H_2, 1000 rpm, 40 mg catalyst (reduced at 850 °C).

Different temperature, pressure, and catalyst loadings were tested. Results are summarized in Table 4.3 and the reaction evolution with time for all the conditions presented in the table can be found in appendix C (Fig C2-C8).

Variation of the reaction temperature had large impact in both the FA conversion and products selectivity. Thus, when the reaction temperature was decreased from 150 to 130°C (Table 4.3, Entry 1) the reduction of FA to FFA severely decreased (See also Fig C2). In this case, only a 58 % of furfural was converted after 8 h of reaction, achieving FFA in 48 % yield.

Table 4.3. Furfural reaction products after 8 hours of reaction at different reaction conditions. FA: furfural, FFA: furfuryl alcohol, THFA: thetrahydrofurfuryl alcohol, pdiol: pentanediol

	T reacc	cat (mg)	H_2 (bar)	2-PENTANOL	1-PENTANOL	FA	FFA	THFA	1.2-PDIOL	1.5-PDIOL	SUM
1	130	40	20	0.00	0.00	42.39	48.07	0.00	0.00	0.00	90.46
2	150	40	20	2.03	2.01	0.00	17.80	50.46	1.30	16.71	90.31
3	150	40	10	0.00	0.00	0.87	68.23	4.68	0.00	0.00	73.79
4	150	40	40	2.99	3.39	0.00	0.00	68.71	0.00	24.17	99.29
5	150	20	20	0.00	0.00	0.00	50.02	19.54	0.00	5.07	74.65
6	150	80	20	2.69	3.03	0.00	2.75	48.75	4.07	15.25	76.58
7	170	40	20	8.45	4.21	0.00	0.00	20.80	8.70	14.39	56.57
8	150	-	20	0.00	0.00	73.52	21.73	0.00	0.00	0.00	95.26

On the contrary, when the reaction was performed at 170 °C (Table 4.3, Entry 7), FA was rapidly reduced to FFA, which was then subsequently reduced to produce a

mixture of THFA, pentanol, 1,2-PeD and, 1,5-PeD. Here is important to notice that only a 57 % of the total products are identified by GC-MS, pointing out that the desired products might be further hydrogenated to form pentanes (steps 11 and 13 from Scheme 4.1) or even polymerise at high temperatures (step 1 from Scheme 4.1).[9]

Decreasing the catalyst content to 5 wt.% also caused a decrease in the FA reduction rate (Figure C6, Appendix C), obtaining complete FA conversion after 4 h of reaction, compared to 2 h needed to achieve total FA conversion with a catalyst loading of 10 wt.%. Further, FFA reduction occurred at lesser extent. After 8 h of reaction, a 50 % of the FFA remained and only a 20 % of THFA was formed, while only 5 % of 1,5-PeD was formed (Table 4.3, Entry 5). On the other hand, when the loading of catalyst was increased to 20 wt.%, the reduction of FA occurred faster; however, the use of higher catalyst amount did not increase 1,5-PeD yield (Table 4.3, Entry 6). Additionally, increasing the initial hydrogen pressure to 40 bar led to the increase of 1,5-PeD yield up to 24 % (table 4.3, entry 4 and Fig. C5 in Appendix C), probably due to an increase in hydrogenation rates of the reaction steps 4 and 5 (scheme 4.1).

Finally, a blank test, without catalyst, was performed. For it, 2-propanol (IPA) and furfural (FA) were added to the reactor which, then, was pressurized with H_2 (20 bar) and the reaction elapsed for 8 hours with stirring at 150 °C. In this case, a 26 % of FA reacted forming 22 % of FFA (table 4.3, entry 8), showing that some hydrogenation of FA can be given in the reaction conditions; nonetheless conversion of FA is poor, pointing to the need of a catalyst for further FFA hydrogenation.

3.2.2 Influence of the catalyst temperature reduction

As previously mentioned, looking at the TPR profile (Fig 4.4) it can be observed that Co present in the inverse spinel structure can be partially reduced when reduction temperature is carefully elected. Hence, we studied the different catalytic properties of spinel as synthesized, reduced at 500, 700 and 850 °C (Table 4.4, entries 1-4, see Appendix C for the graphs). Without reduction, the spinel showed poor activity, only obtaining a 44 % of FFA after 8 h of reaction. When the catalyst was reduced at 500°C, FFA was rapidly formed with a yield of ca. 80% after 1 h of reaction; although, any further hydrogenation of FFA was rather slow, PeDs being obtained in a yield of *ca.* 6%. Reducing the spinel at 700 °C resulted in a notable increase of the FFA reduction rate, while the yield of 1,5-PeD reached 22 %.

However, despite reduction at higher temperatures (i.e. 850 °C) led to rapid FA hydrogenation to FFA, a decrease in the 1,5-PeD yield was observed compared to the catalyst reduced at 700 °C.

Table 4.4. Furfural reaction products after 8 hours of reaction at different reaction conditions. FA: furfural, FFA: furfuryl alcohol, THFA: thetrahydrofurfuryl alcohol, pdiol: pentanediol. *Entry 8 started with THFA instead of FA

	T red	H_2 (bar)	2-PENTANOL	1-PENTANOL	FA	FFA	THFA	1.2-PDIOL	1.5-PDIOL	SUM
1	850	20	2.03	2.01	0.00	17.80	50.46	1.30	16.71	90.31
2	0	20	0.00	0.00	61.11	43.99	0.00	0.00	0.00	105.10
3	500	20	0.00	0.00	0.00	23.73	27.42	1.38	4.70	57.25
4	700	20	3.39	3.22	0.00	0.00	50.42	3.33	22.03	82.41
5	700	-	0.00	0.00	83.97	17.60	0.00	0.00	0.00	101.57
6	700	30	3.58	3.45	0.00	0.00	62.15	0.00	29.77	98.98
7	700	40	1.23	1.31	0.00	0.00	57.01	0.01	12.45	73.66
8*	700	30	0.00	0.00	0.00	0.00	94.69	0.00	0.00	94.69

At a first glance, it seems that the first limiting step for obtaining higher yields of PeDs is the hydrogenation rate of FFA. In this regard, the higher the FFA hydrogenation rate the higher the PeD yield.

As found by XRD and TPR, the reduction temperature of the spinel plays an important role on its structure which is mirrored in the catalytic features. Two effects may be responsible for the improved catalytic performance for FFA hydrogenation in the catalyst reduced at 700 ºC. On the one hand, the presence of metallic Co nanoparticles is needed to undergo the reaction toward the more hydrogenated products, i.e. PeD. According to X-ray diffractograms, when sample was reduced at 500 ºC, no formation of metallic Co nanoparticles was found, and reduction towards PeDs resulted disfavoured. On the contrary, those catalysts reduced at 700 ºC and 850 ºC showed peaks corresponding to Co nanoparticles. By XRD it was found that the crystallite size of the formed metallic Co was smaller on the catalyst reduced at 700 ºC (crystallite size of 1.8 nm) than that of catalyst reduced at 850 ºC (crystallite size of 8.8 nm). Thus, the dispersion and size of the formed Co nanoparticles on the surface of the catalyst reduced at 700 ºC favoured the subsequent hydrogenation reactions.

Acidity measurements performed by NH_3 desorption (TPD-NH_3) did not show any trend that could explain the differences in the catalytic behaviour of the catalyst.

As the spinel reduced at 700 ºC showed the highest PeD yield, the influence of the H_2 pressure (Table 4.4, entries 5-6) was evaluated using this catalyst to foster 1,5-PeD yield. As previously found, an increase in pressure also increased the hydrogenation rates, producing the highest 1,5-PeD yield (*ca.* 30 %) at 30 bar of initial H_2 pressure. However, at 40 bars both THFA and 1,5-PeD yields decreased and the unknown products yield increased. Hence, analogously to temperature, pressure also needs to be controlled thoroughly since increases reaction rates to the desired products but also favours the formation of unwanted by-products. Then we defined 30 bars of H_2 and 150 ºC as the optimum reaction conditions.

Additionally, in order to get insights into the reaction mechanisms, FFA (Fig. 4.7) hydrogenation was performed at the optimal conditions, i.e. 150 ºC, 30 bar and 700 ºC as reduction temperature of the catalyst. When FFA was used as substrate, the reaction led to the formation of both THFA and 1,5 PeD in a similar yield, achieving a maximum 1,5-PeD yield of ca. 50 % at 4 h, which also coincides with the THFA maximum formed. After 4 h of reaction, THFA and 1,5-PeD concentration decreased slightly, to form further reduced products such as 1-pentanol (Table 4.4, entry 8). Notably, when looking at the reaction evolution, the formation profile of THFA and 1,5-PeD with time resulted rather similar, suggesting that formation of 1,5-PeD occurs directly via hydrogenation of FFA and not following a subsequent THFA hydrogenation. In this case, formation of 1,5-PeD from THFA seems not to take place or to occur in a very slow rate.

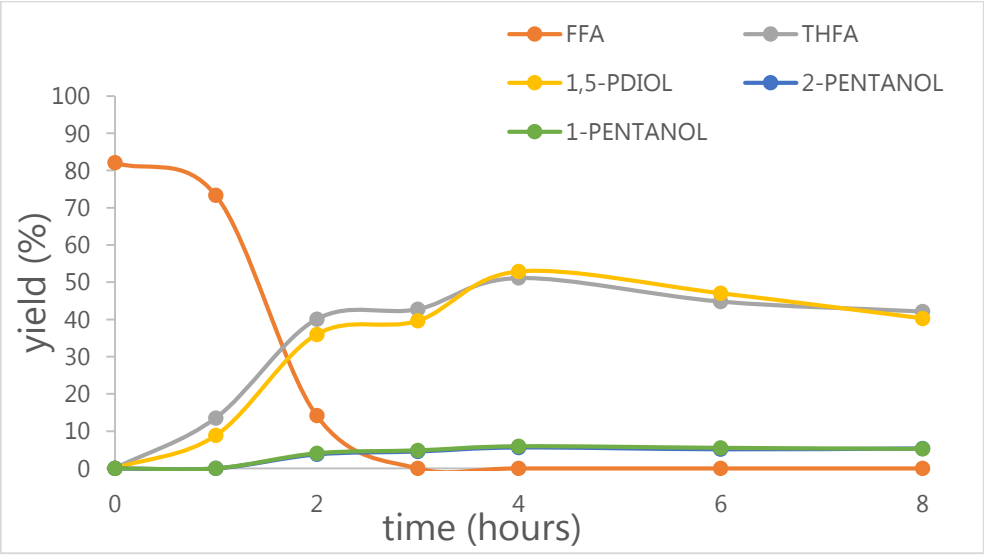

Figure 4.7. Furfuryl alcohol reduction during 8 hours. Conditions: 150 ºC, 30 bar H_2, 1000 rpm, 40 mg catalyst (reduced at 700ºC).

To further confirm this hypothesis, the reaction was then performed using THFA as substrate. Similarly to that reported by Lu et.al[12] with Pt-supported Co-spinel, our Co-spinel catalyst was found not to be able to catalyse THFA hydrogenolysis (Table 2, entry 8). Dumesic et. al[23]. reported that hydrogenolysis of C-O bonds proceeds *via* acid-catalyzed ring-opening, while the metal site activates hydrogenation. Hence, promoting spinel acidity might increase 1,5-PeD through THFA hydrogenolysis, but we do not have experimental data about this fact and will have to be further studied for confirmation.

3.2.3 Catalyst reuse

Finally, the reuse of catalyst was tested. For this, the reaction was run as usual and, after every 2 hours, the reaction was stopped, cooled down, the reactor was opened and FA and IPA were added to the reaction mixture. This was done for 6 runs (Fig 4.8).

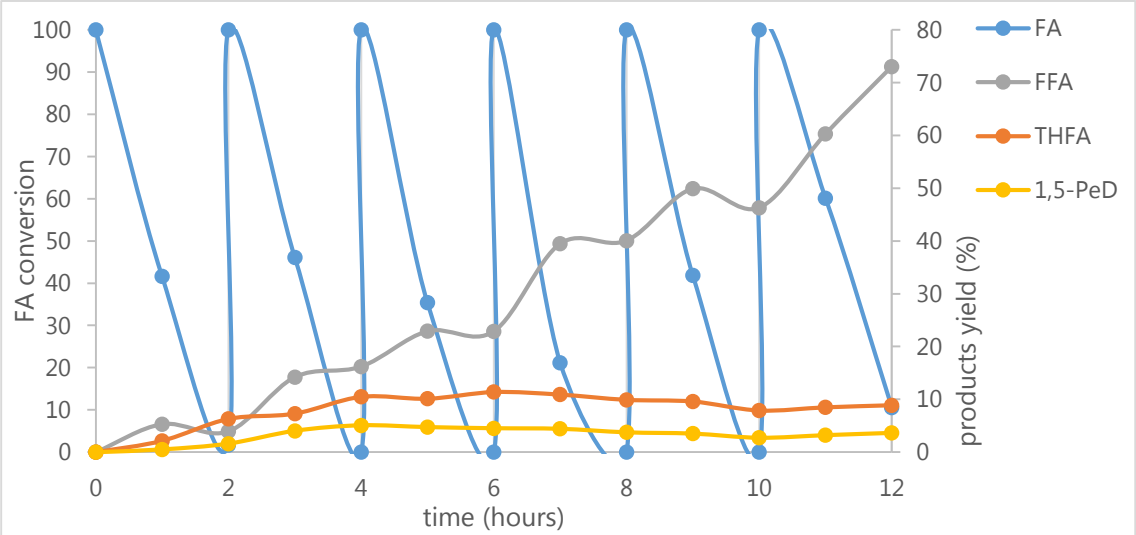

Figure 4.8. Semi-batch furfural reduction during 6 runs. Conditions: 150 ºC, 30 bar H_2, 1000 rpm, 40 mg catalyst (reduced at 700ºC).

In all the 6 runs, the FA was reduced within 2 hours and FFA was continuously formed. However further hydrogenation of FFA to either THFA or 1,5-PeD was produced only during the first two runs, achieving only 9 % of THFA and 4 % of 1,5-PeD out of the total amount of added FA. Co-spinel showed activity without deactivation for 6 runs for FA reduction but no THFA or 1,5-PeD was formed after the second run. So, after the second round the catalyst was neither able to hydrogenate the furan ring or catalyse hydrogenolysis of FFA. In order to reactivate the catalyst, a second reuse experiment was done. First, a reaction was carried out at the optimal conditions. Once the reaction finished (8 h) the reaction was stopped, and the catalyst was washed, dried, reduced, and reused for a second

run. During the second run, the catalyst was able to reduce all the FA, mainly forming FFA and just *ca.* 3% of THFA, but no 1,5-PeD was detected. So also here a partial deactivation of the catalyst was observed, which cannot be reactivated with reduction prior its second usage.

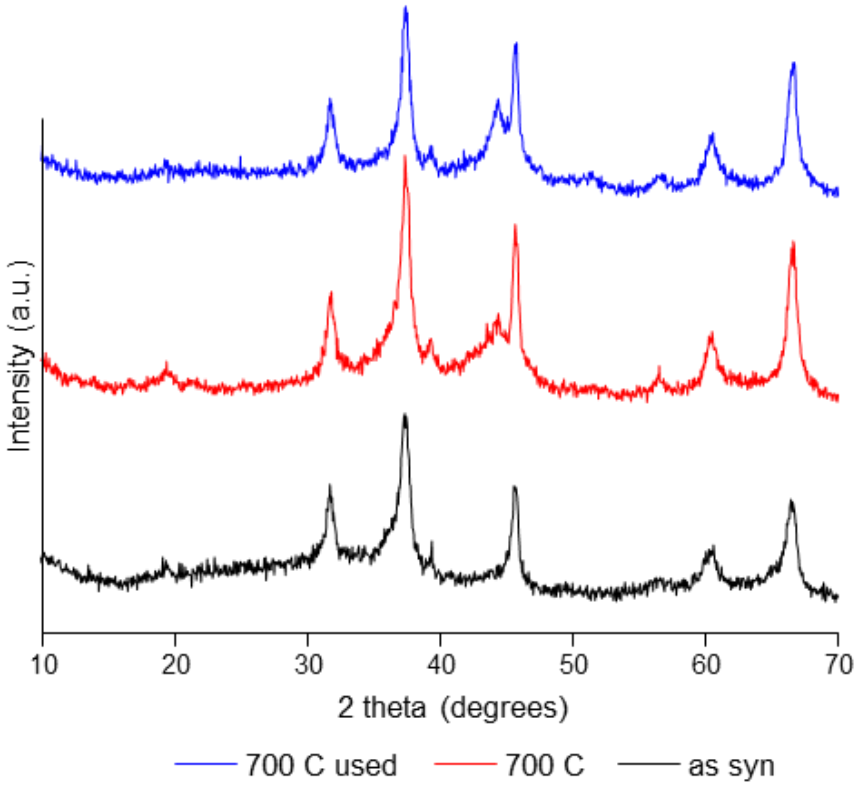

Figure 4.9. XRD of the fresh sample, reduced at 700 C, and reduced at 700 C after a single run.

Usually, one of the drawbacks of metallic catalysts, and in this particular case Co-based catalysts lies in its lack of stability. Our first hypothesis about the lability of these materials was based on the poisoning of the active centers, which was discarded due to the non-recovery of activity after thermal re-activation. In the same way, BET surface measurements did not reveal deactivation by fouling, since the surface area a pore volumes were rather similar to those presented by the fresh catalyst (data not shown). Additionally, the XRD pattern of the used sample (Figure 4.9) did not reveal any remarkable change in the crystalline structure; however, it was detected an increase of crystallite size of the metallic Co from 1.8 nm (in the fresh catalyst) to *ca.* 7 nm in the used one. Hence, a plausible explanation for the catalyst deactivation might be found in the sintering of the material surface produced during reaction and/or leaching of the metallic Co.

4. CONCLUSIONS

We have proved the activity of a non-noble metal catalyst, such as Co-Al catalyst for the production of PeD directly from furfural. These materials are able to achieve 30 % yield of 1,5-propanediol from furfural if the reduction temperature of the catalyst is carefully selected. We showed here the importance of selecting a proper catalyst pretreatment, since it greatly influences the catalytic properties. Here it was shown, for instance, how the formation and size of metallic Co nanoparticles on the surface of the catalyst, during the material reduction, have proved to be vital to increase furfuryl alcohol hydrogenation rate. For this 700 ºC was selected as the best reduction temperature for the reaction to achieve the highest 1,5-propanediol yield. Additionally, more reaction parameters were studied, e.g. catalyst loading, hydrogen pressure loading, and reaction temperatures. Finally, it was also proved that these type of Co-Al, which are remarkably able to catalyse furfuryl alcohol hydrogenolysis, do not catalyse tetrahydrofurfuryl alcohol hydrogenolysis.

In summary, a nice strategy to prepare 1,5-pentanediol from furfural without the need of precious or toxic metal was presented in this chapter. To the best of our knowledge, it is the first time that such a fact is reported.

5. REFERENCES

1 T. and P. G. Werpy, *Natl. Renew. Energy Lab.*, 2004, 76.

2 R. Mariscal, P. Maireles-Torres, M. Ojeda, I. Sádaba and M. López Granados, *Energy Environ. Sci.*, 2016, **9**, 1144–1189.

3 G. W. Huber, S. Iborra and A. Corma, *Chem. Rev.*, 2006, **106**, 4044–4098.

4 A. Corma, S. Iborra and A. Velty, *Chem. Rev.*, 2007, **107**, 2411–2502.

5 M. J. Climent, A. Corma and S. Iborra, *Green Chem.*, 2011, **13**, 520–540.

6 J. C. Serrano-Ruiz and J. A. Dumesic, *Energy Environ. Sci.*, 2011, **4**, 83–99.

7 P. Gallezot, *Chem. Soc. Rev.*, 2012, **41**, 1538–1558.

8 S. G. Wettstein, D. Martin Alonso, E. I. Gürbüz and J. a. Dumesic, *Curr. Opin. Chem. Eng.*, 2012, **1**, 218–224.

9 Y. Nakagawa, M. Tamura and K. Tomishige, *Catal. Surv. from Asia*, 2015, **19**, 249–256.

10 D. Sun, S. Sato, W. Ueda, A. Primo, H. Garcia and A. Corma, *Green Chem.*, 2016, **18**, 2579–2597.

11 H. Adkins and R. Connor, *J. Am. Chem. Soc.*, 1931, **53**, 1091–1095.

12 W. Xu, H. Wang, X. Liu, J. Ren, Y. Wang and G. Lu, *Chem. Commun. (Camb).*, 2011, **47**, 3924–3926.

13 S. Liu, Y. Amada, M. Tamura, Y. Nakagawa and K. Tomishige, *Green Chem.*, 2014, **16**, 617–626.

14 J. Wu, G. Gao, J. Li, P. Sun, X. Long and F. Li, *Appl. Catal. B Environ.*, 2017, **203**, 227–236.

15 M. Audemar, C. Ciotonea, K. De Oliveira Vigier, S. Royer, A. Ungureanu, B. Dragoi, E. Dumitriu and F. Jérôme, *ChemSusChem*, 2015, **8**, 1885–1891.

16 J. Lee, S. P. Burt, C. A. Carrero, A. C. Alba-Rubio, I. Ro, B. J. O'Neill, H. J. Kim, D. H. K. Jackson, T. F. Kuech, I. Hermans, J. A. Dumesic and G. W. Huber, *J. Catal.*, 2015, **330**, 19–27.

17 T. Karhunen, A. Lähde, J. Leskinen, R. Büchel, O. Waser, U. Tapper and J. Jokiniemi, *ISRN Nanotechnol.*, 2011, **2011**, 1–6.

18 K. S. W. Sing, *Pure App. Chem.*, 1985, **57**, 603–619.

19 A. E. Mwenesongole, University of pretoria, 2008.

20 O'Driscoll, J. J. Leahy and T. Curtin, *Catal. Today*, 2015, **279**, 194–201.

21 X. Chen, L. Zhang, B. Zhang, X. Guo and X. Mu, *Sci. Rep.*, 2016, **6**, 28558.

22 P. N. Romano, J. M. A. R. de Almeida, Y. Carvalho, P. Priecel, E. Falabella Sousa-Aguiar and J. A. Lopez-Sanchez, *ChemSusChem*, 2016, **9**, 3387–3392.

23 M. Chia, Y. J. Pagán-Torres, D. D. Hibbitts, Q. Tan, H. N. Pham, A. K. Datye, M. Neurock, R. J. Davis and J. A. Dumesic, *J. Am. Chem. Soc.*, 2011, **133**, 12675–12689.

Chapter 5:

Summary and outlook

1. SUMMARY

As it was mentioned few lines ago in the introduction, biorefinery is a broad topic in constant development with numerous cases of success and failure. Here three different up-to-date strategies for biomass transformation into valuable chemicals have been presented. Albeit, initially, these three strategies do not have straight-forward connection among them, biorefineries cannot be understood without taking profit of all biomass fractions. So the technologies described in this thesis can be fitted in a larger context depending of the desired needs or final product.

Thus, for instance, one could imagine a plant where: once fermentation of a woody hydrolysate with lactic acid bacteria (**Chapter 2**) has finished, lactic acid is extracted and afterwards the present furfural is also extracted (if somebody has more imagination, could also think about transforming xylose into furfural previously) and used for hydrogenation (**Chapter 4**).

Or, on the other hand, in an alternative imaginary plant, one could take profit of the fractionation capabilities of biomass acetylation (**Chapter 3**). Once cellulose acetate has been prepared (and upgraded to AMF) the acetylated hemicellulose units (presumably short oligomers or monomers) can also be converted to furfural and be upgraded to pentanediols (**Chapter 4**).

Being this said, a brief discussion of the main achieved facts on each chapter will be disclosed in the following lines.

In **Chapter 2,** an integrated biomass-to-lactic acid process has been presented. For this, fractionation of woody biomass with ionic liquids was first demonstrated. And afterwards the produced pulps were hydrolysed, finally the hydrolysate was used as carbohydrate source by lactic acid bacteria. Lactic acid bacteria fermentation resulted in successful conversion of glucose into optically pure D-lactic acid. Recalling the requirements for ILs exploitation for biomass treatments mentioned in the introduction, an IL which meets most of these conditions has been studied (e.g. water tolerant, reusable…); here, also biocompatibility has been studied and demonstrated.

Chapter 3 presents a new interesting approach for the production of a furanic compound from biomass. For this, acetylation of cellulose is posed as an alternative entry point to cellulose hydrolysis. By doing this, cellulose solubility is modified, enlarging the solvent list which can solubilise it. Taking benefit of it, acetic acid is used as solvent and then "acetolysis" of cellulose acetate leads to the formation of acetylated HMF, the so-called acetoxymethoxyfuraldehyde (AMF). Not only this, in this chapter cellulose acetate is prepared from different biomass sources and successfully transformed to AMF.

Finally, in **chapter 4** upgrading of furfural is studied. In this chapter is demonstrated that Co aluminate nanoparticles facilitate, the not easy, formation of 1,5-pentanediol from furfural. Also, in this chapter the influence of the reduction temperature of the catalyst is studied, giving some insight on the segregation of metallic Co nanoparticles, which will ultimately favour 1,5-pentanediol formation.

2. OUTLOOK

Even in chapter 2 an integration of different technologies has been demonstrated, this whole thesis shed light into different early stage approaches inside the biorefinery picture. So, prior any potential application, obviously, techno-economic assessments needs to be done. However, from the scientific point of view also some new ideas appear as an appealing extension of the work presented here.

In **chapter 2** a nice combination of extraction-hydrolysis-fermentation is presented. So immediately springs to mind increasing final product yield (lactic acid). This could be done in different ways: i) increasing ionic liquid fractionation capability, this could solely be done by adjusting treatment conditions (e.g. longer extraction time, adjusting temperature, reducing particle size, biomass loading…) or tuning the ionic liquid extraction capabilities so they adapt to biomass source. Also during the hydrolysis step, increasing the biomass/liquid ratio would potentially yield more glucose in solution. However, this may also lead to higher inhibitory compounds content in solution and surely will lead to higher humins formation.[1] Finally, other fermentation systems rather than batch could be studied for fermentation, for instance fed-batch.

Chapter 3 presents a fresh view for continuous biomass processing. If one thinks about the obtained furanic compound as an end product, solvent tuning might help to separation of product and solvent. Also, increasing cellulose acetate/solvent ratio will give a more appealing exploitation of this technology. On the other hand, taking AMF as an intermediate product, acetic acid appears as an interesting solvent for oxidation of AMF into the appreciated furandicarboxylic acid. Also, one could think about AMF reduction into dimethylfuran or 2,5-dimethyltetrahydrofuran, valuable liquid fuels (or blends). Finally, for this process a development of a heterogeneous catalyst would increase value of this process and possibly increase final product yield.

Finally, to complement the work done in **Chapter 4** several aspects could be addressed. Firstly optimizing reaction conditions, for instance as Liu et. al. proposed,[2] a two steps reaction may lead to higher 1,5-PeD content. Also, improving the catalyst design would increase 1,5-PeD yield For instance, it was shown that the employed Co-aluminates do not catalyse ring opening of THFA, thus increasing the acidity of

the catalyst may help to catalyse hydrogenolysis of THFA[3] and increase final 1,5-PeD yield.

3. REFERENCES

1 I. Van Zandvoort, Y. Wang, C. B. Rasrendra, E. R. H. Van Eck, P. C. A. Bruijnincx, H. J. Heeres and B. M. Weckhuysen, *ChemSusChem*, 2013, **6**, 1745–1758.

2 S. Liu, Y. Amada, M. Tamura, Y. Nakagawa and K. Tomishige, *Green Chem.*, 2014, **16**, 617–626.

3 M. Chia, Y. J. Pagán-Torres, D. D. Hibbitts, Q. Tan, H. N. Pham, A. K. Datye, M. Neurock, R. J. Davis and J. A. Dumesic, *J. Am. Chem. Soc.*, 2011, **133**, 12675–12689.

Appendices:

Additional Figures and Index

Appendix A – Additional figures from chapter 2

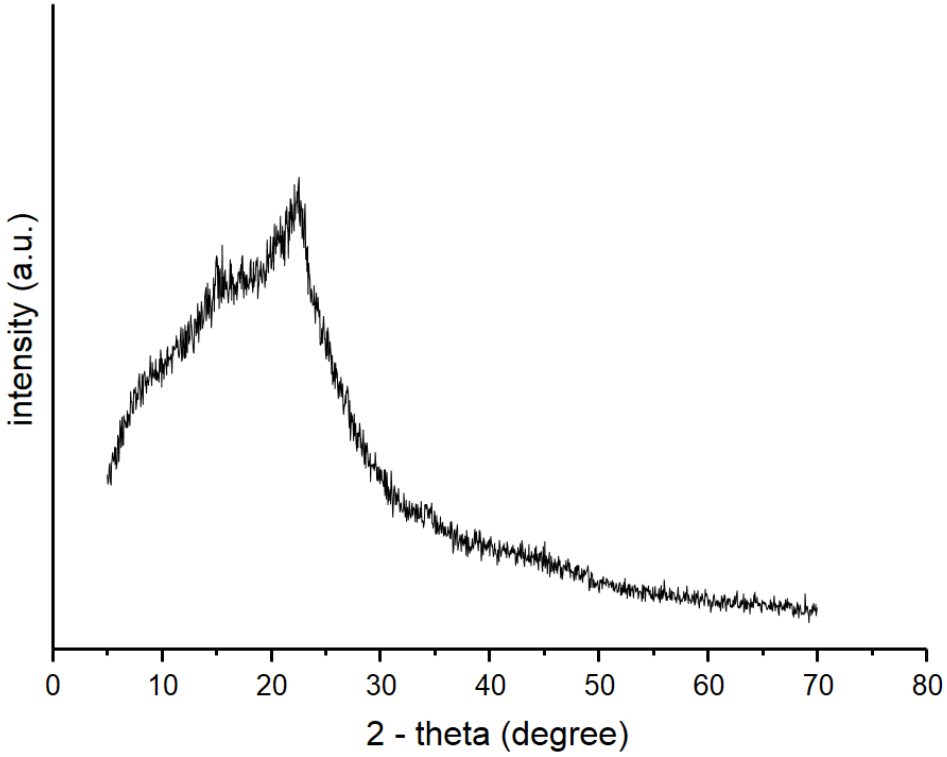

FIG A1. XRD of a recovered sample after hydrolysis

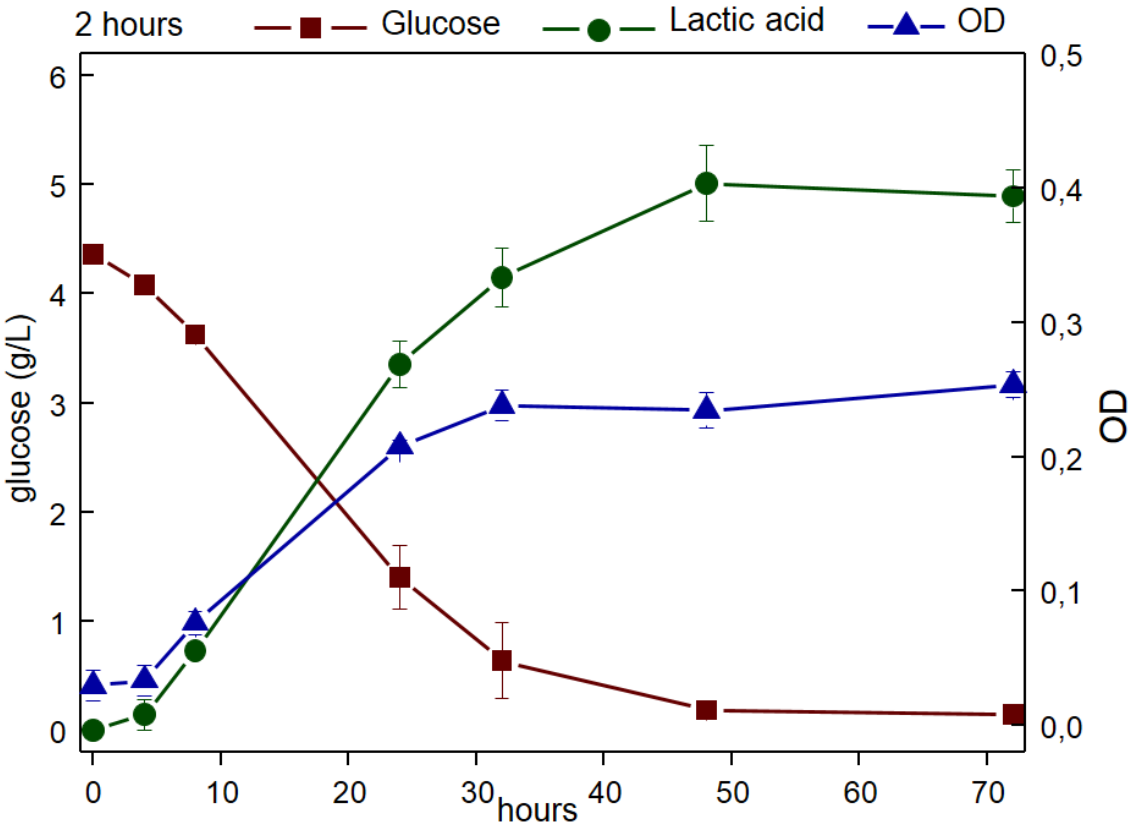

Fig A2. Lactic acid production by *L. delbrueckii* from cellulose hydrolysate after 2 hours of treatment

Appendices: Additional figures and index

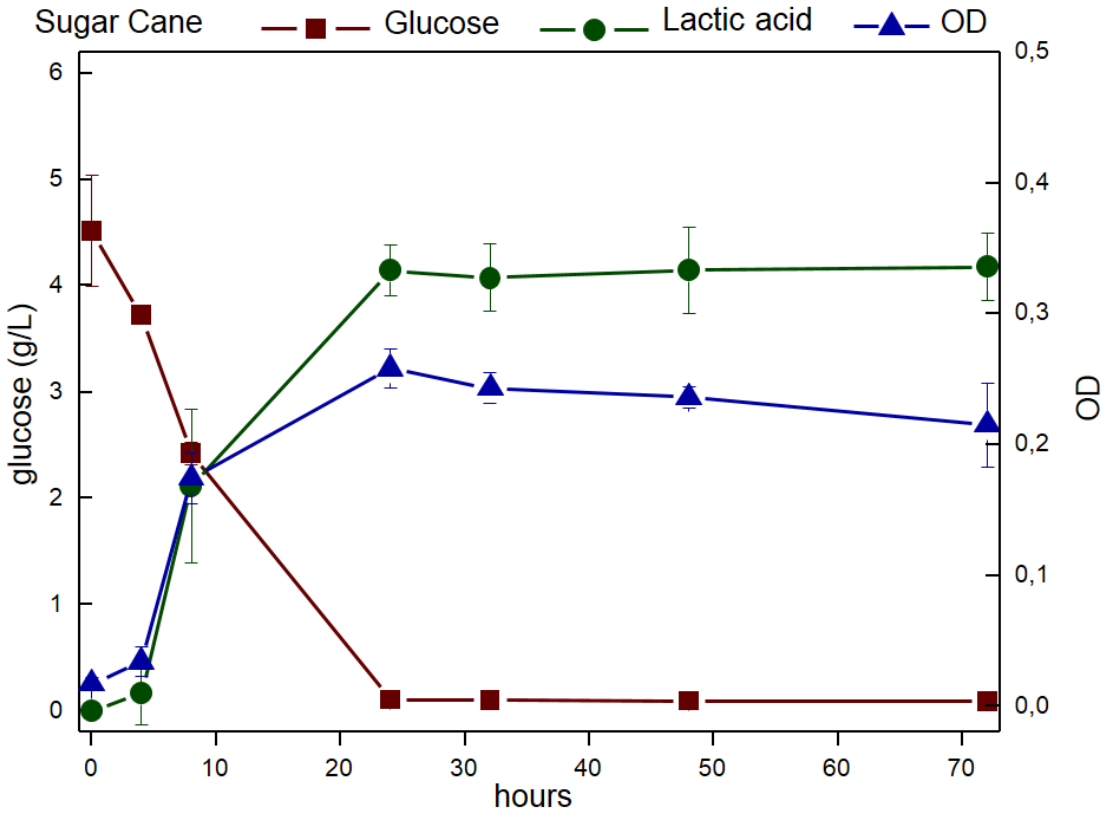

Figure A3. Lactic acid production by *L. delbrueckii* from SCB hydrolysate

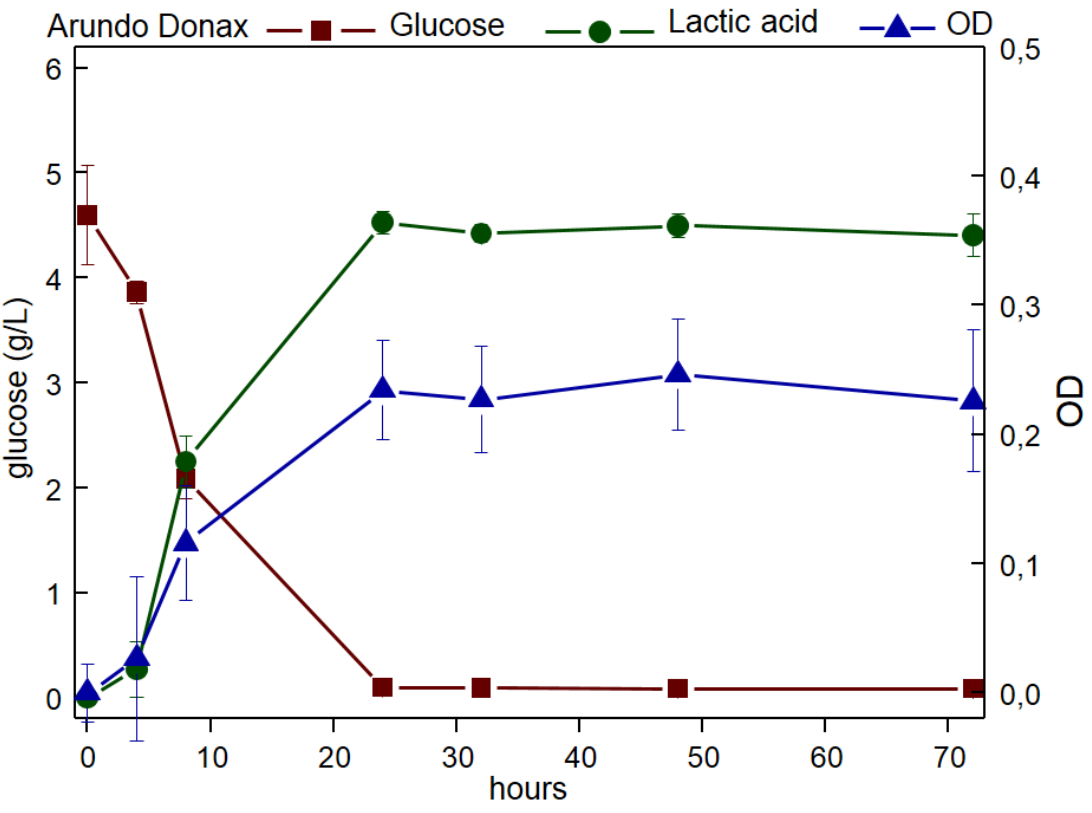

Figure A4. Lactic acid production by *L. delbrueckii* from AD hydrolysate

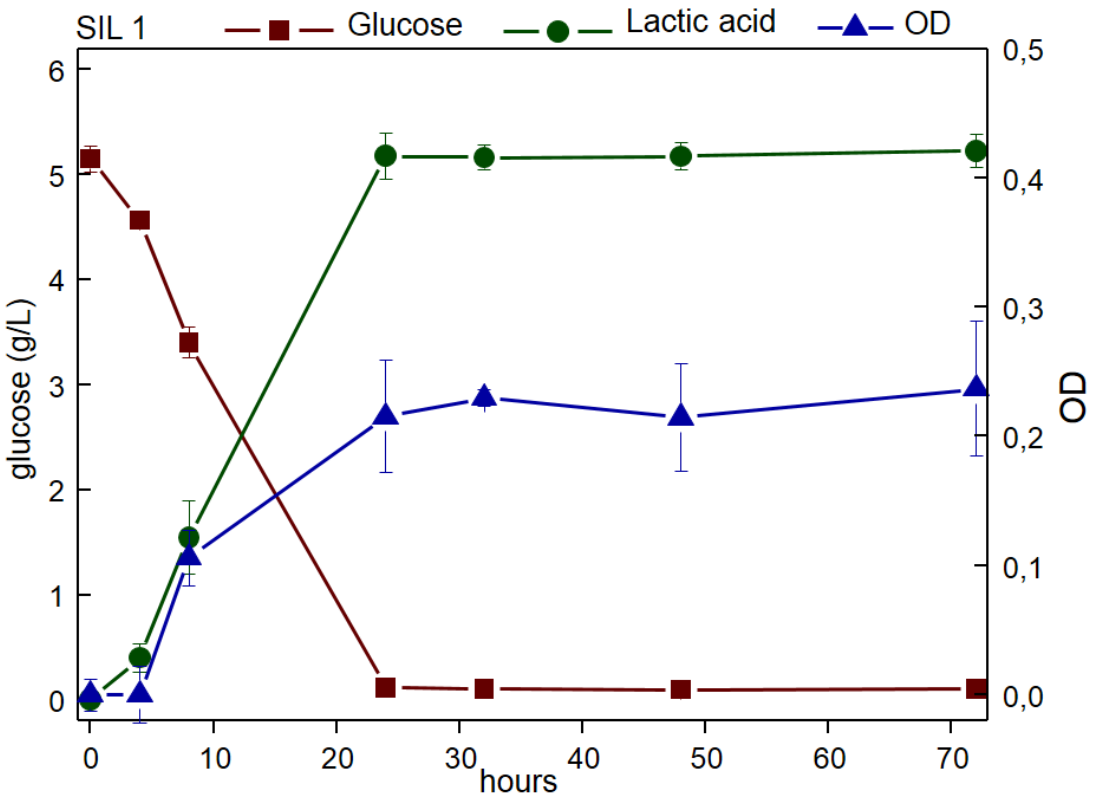

Figure A5. Lactic acid production by *L. delbrueckii* from SIL1 hydrolysate

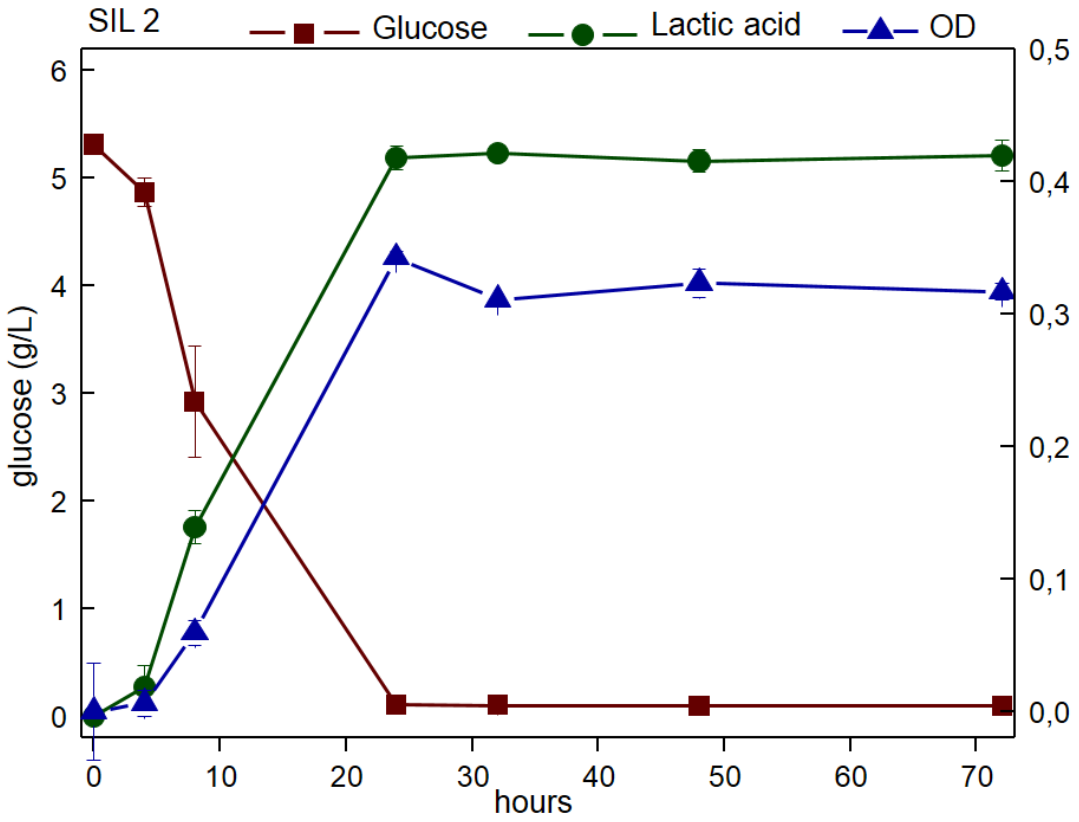

Figure A6. Lactic acid production by *L. delbrueckii* from SIL2 hydrolysate

Appendices: Additional figures and index

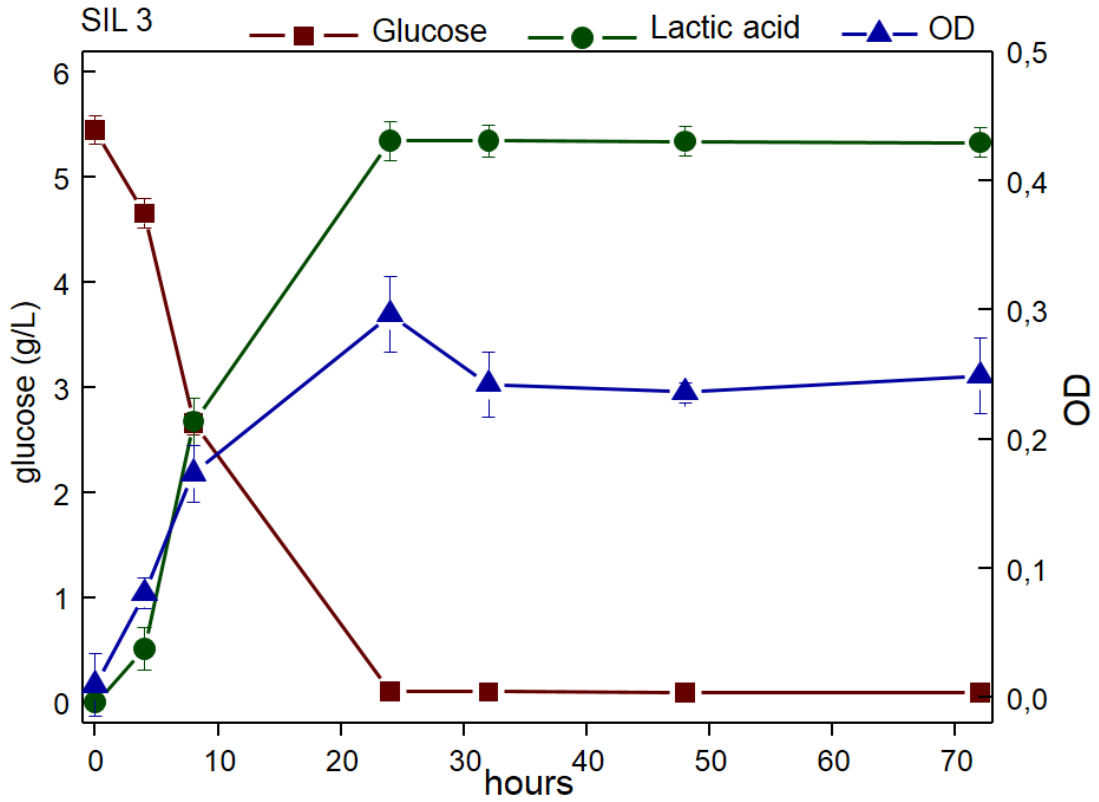

Figure A7. Lactic acid production by *L. delbrueckii* from SIL3 hydrolysate

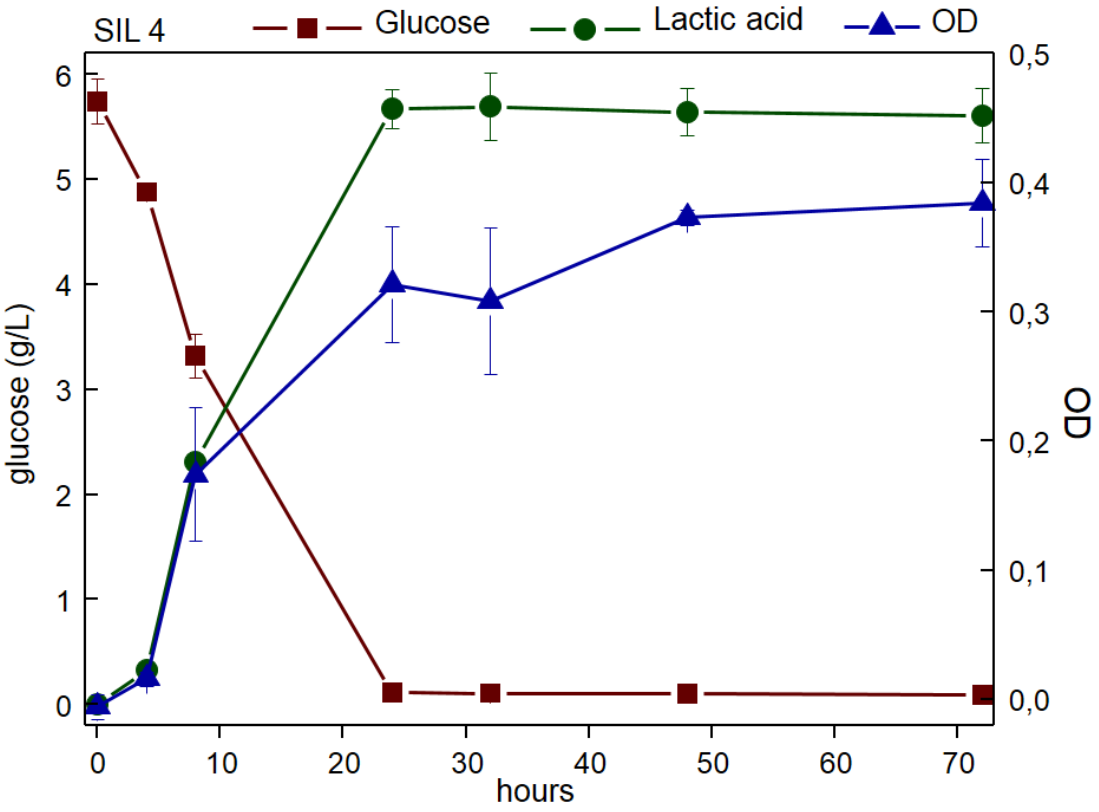

Figure A8. Lactic acid production by *L. delbrueckii* from SIL4 hydrolysate

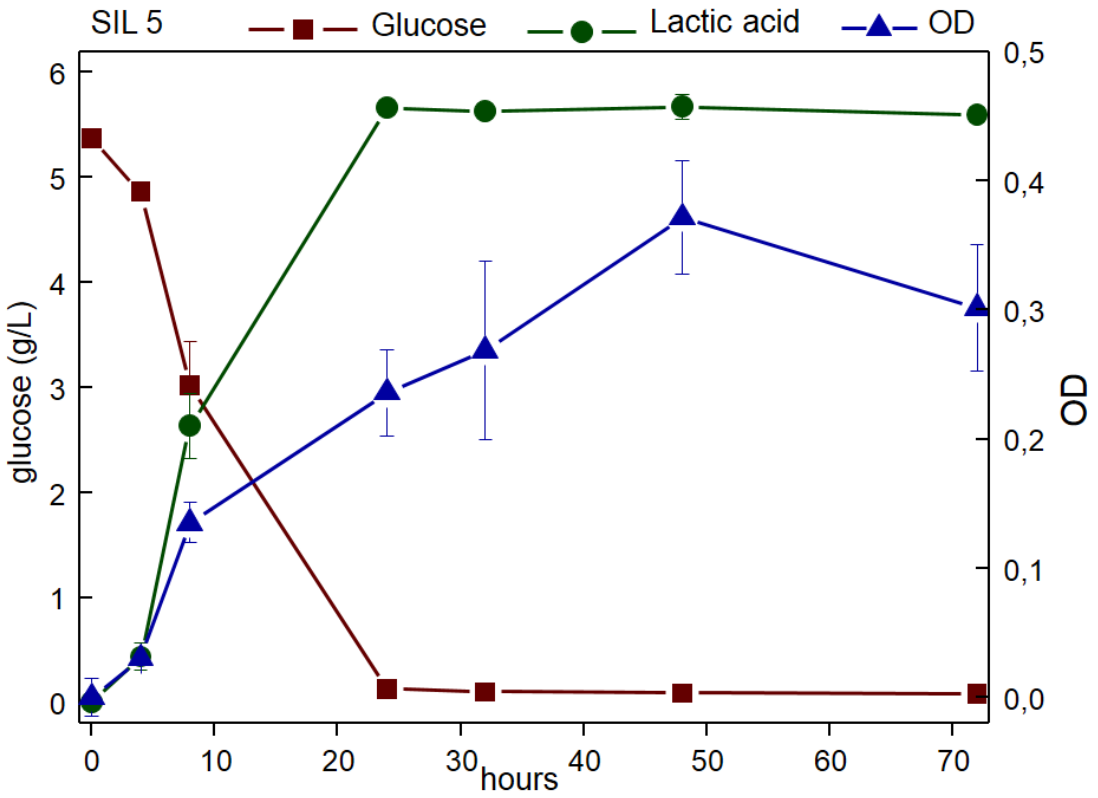

Figure A9. Lactic acid production by *L. delbrueckii* from SIL5 hydrolysate

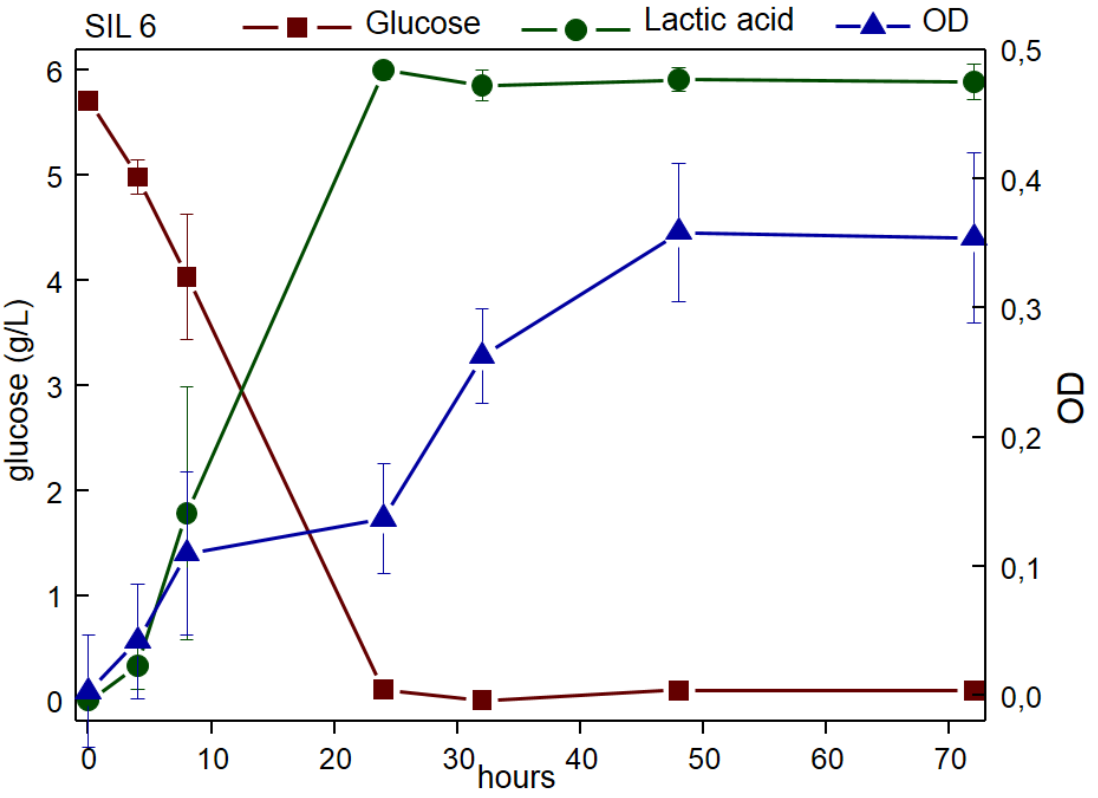

Figure A10. Lactic acid production by *L. delbrueckii* from SIL6 hydrolysate

Appendices: Additional figures and index

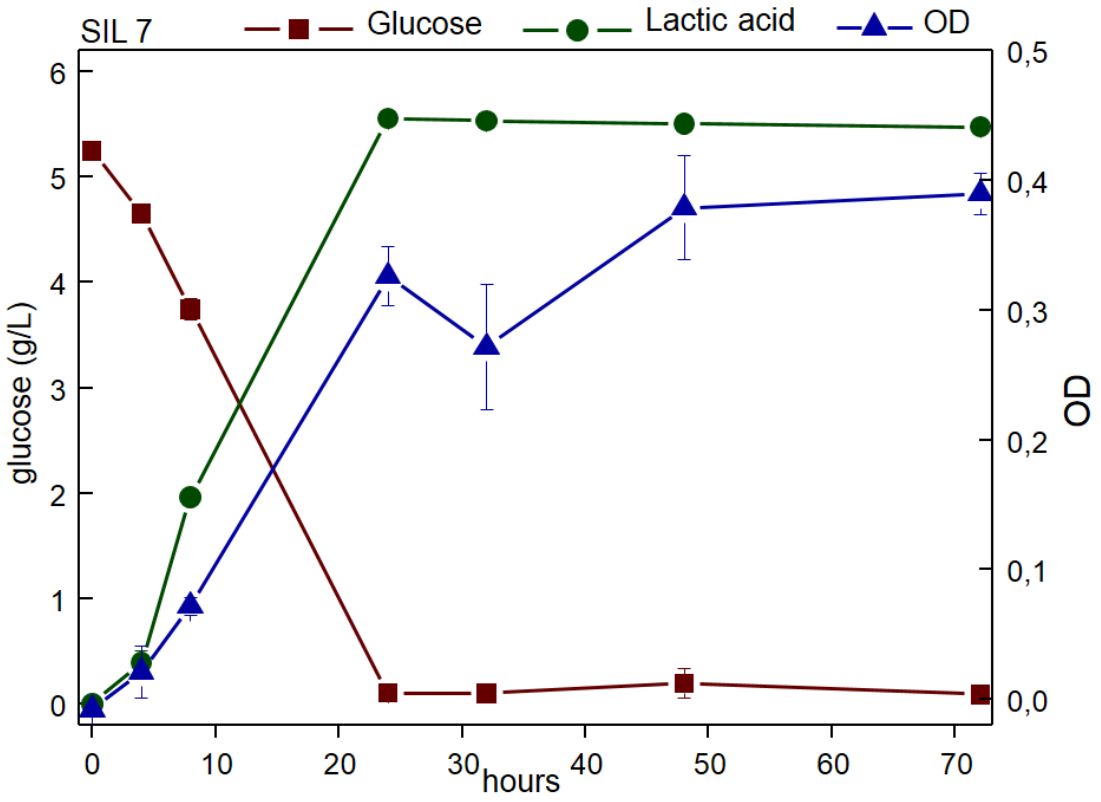

Figure A11. Lactic acid production by *L. delbrueckii* from SIL7 hydrolysate

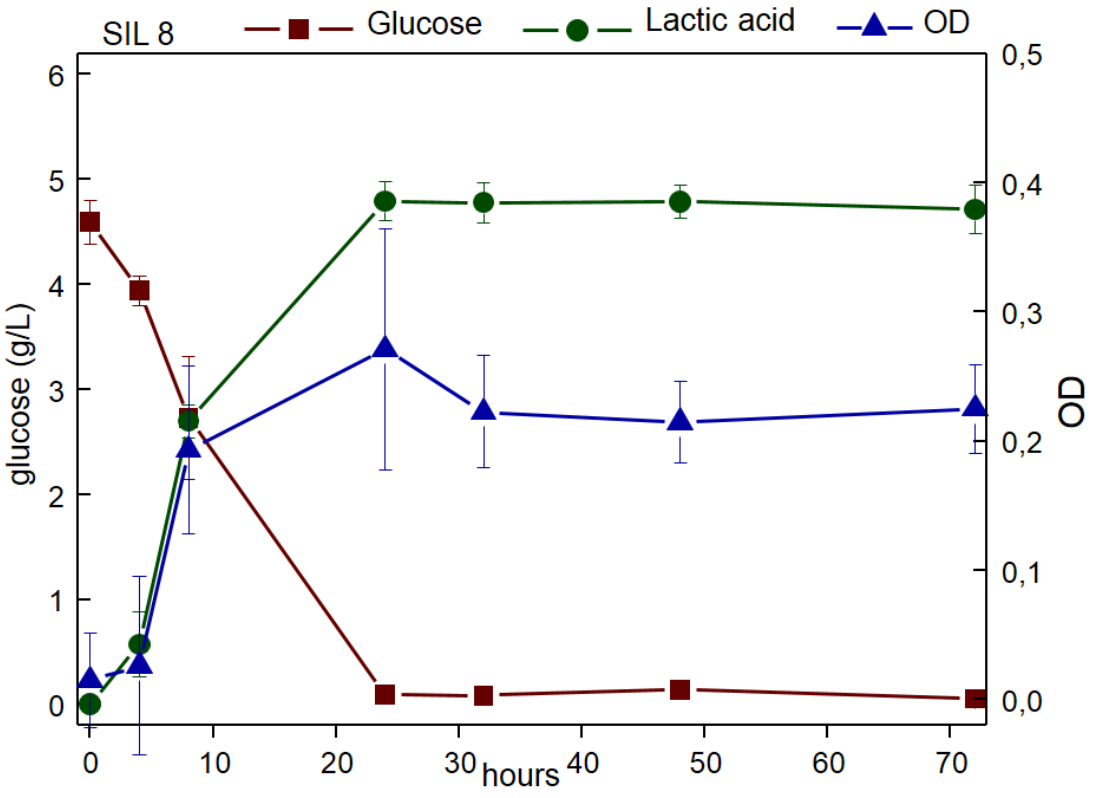

Figure A12. Lactic acid production by *L. delbrueckii* from SIL8 hydrolysate

Appendix B – Additional figures from chapter 3

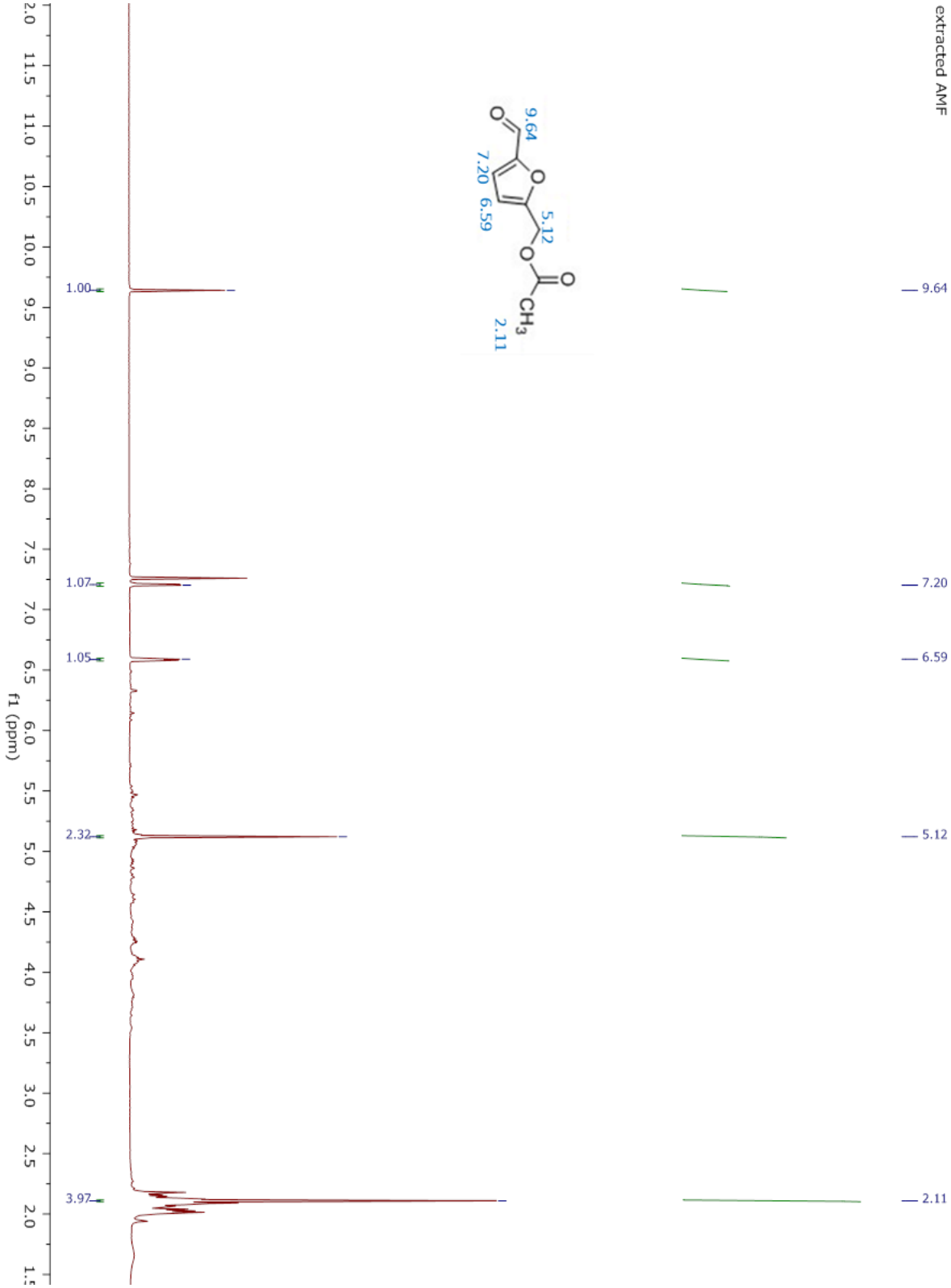

Fig B1. ^{1}H-NMR of crude AMF from the 2h time on stream experiment

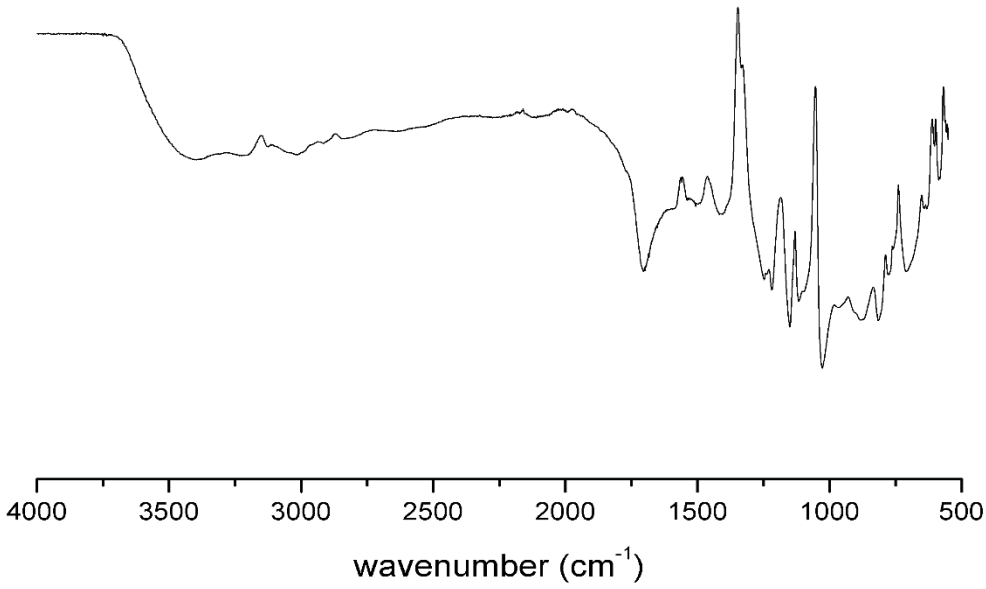

Fig B2. FTIR spectra of recovered humic material (after reacting 3 g/L of AMF in 15 mL of acetic acid for 6 hours at 220 ºC)

The bands at 1506, 1218, 1026, 956 and 774 cm^{-1} can be attributed to the presence of the furan ring (AMF condensation), while bands at 760 and 710 cm^{-1} can be allotted to the aromatic nature of humins.

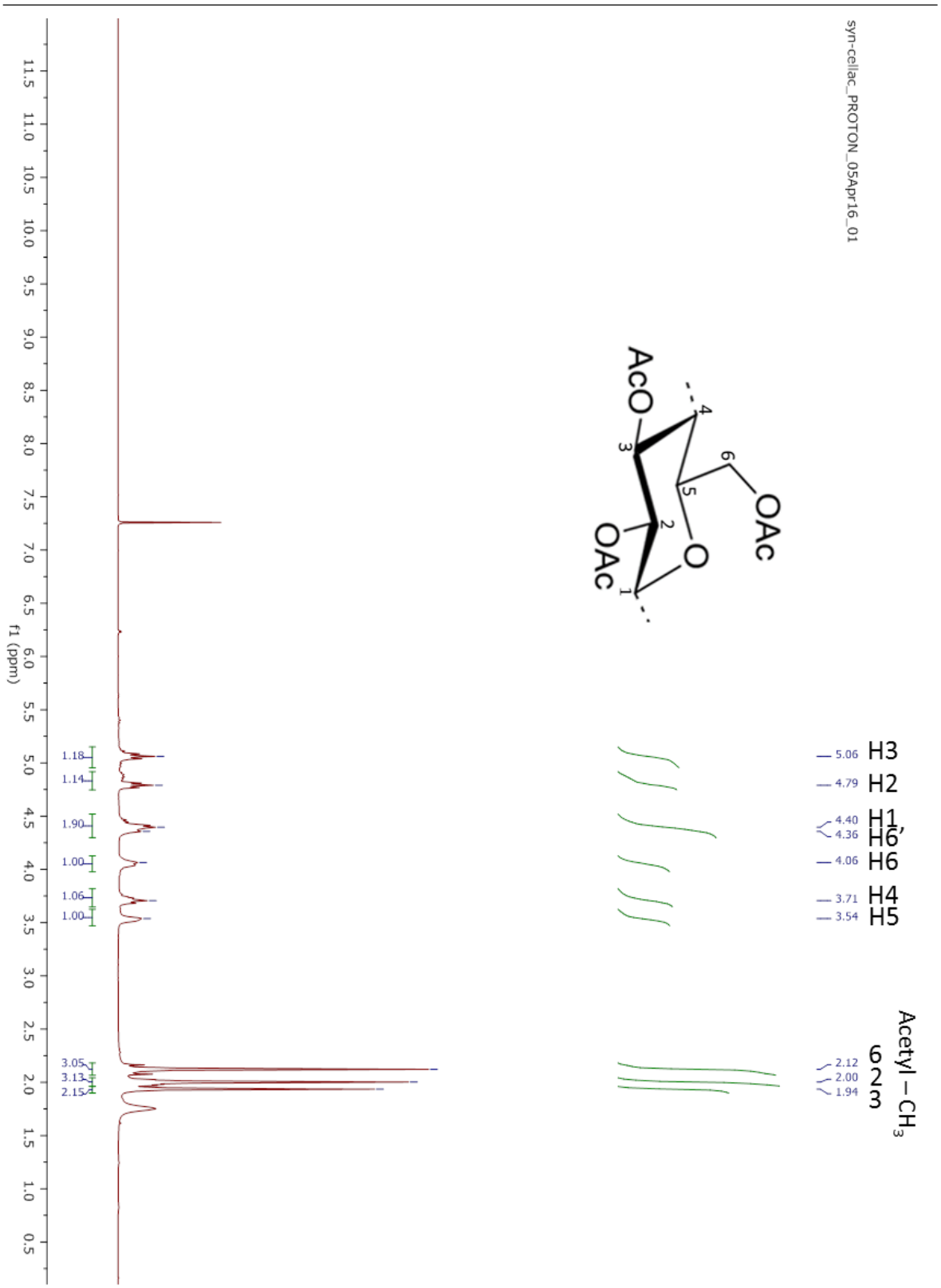

Fig B3. ^{1}H-NMR of acetylated cellulose

Appendices: Additional figures and index

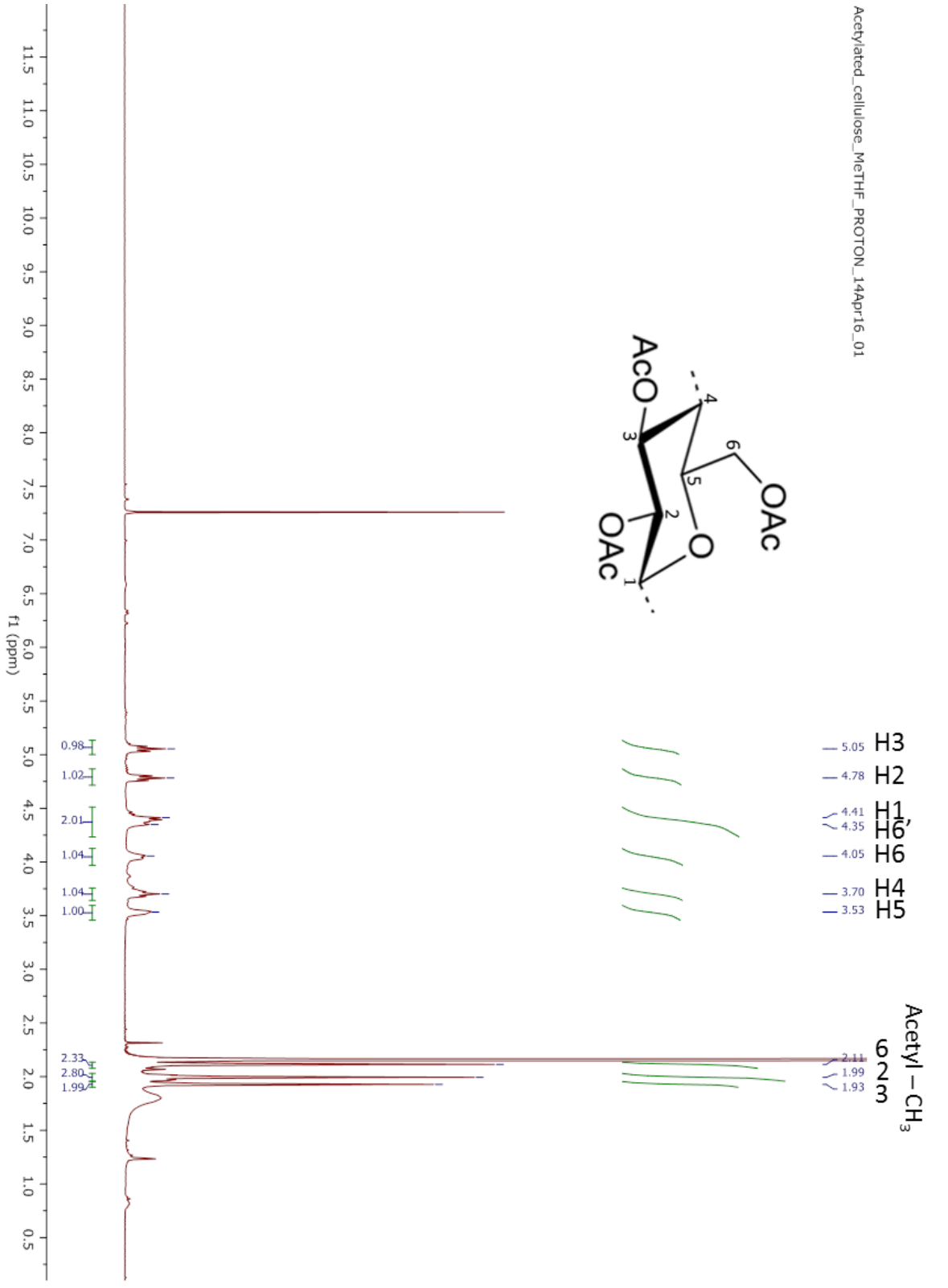

Fig B4. ^{1}H-NMR of acetylated beech wood

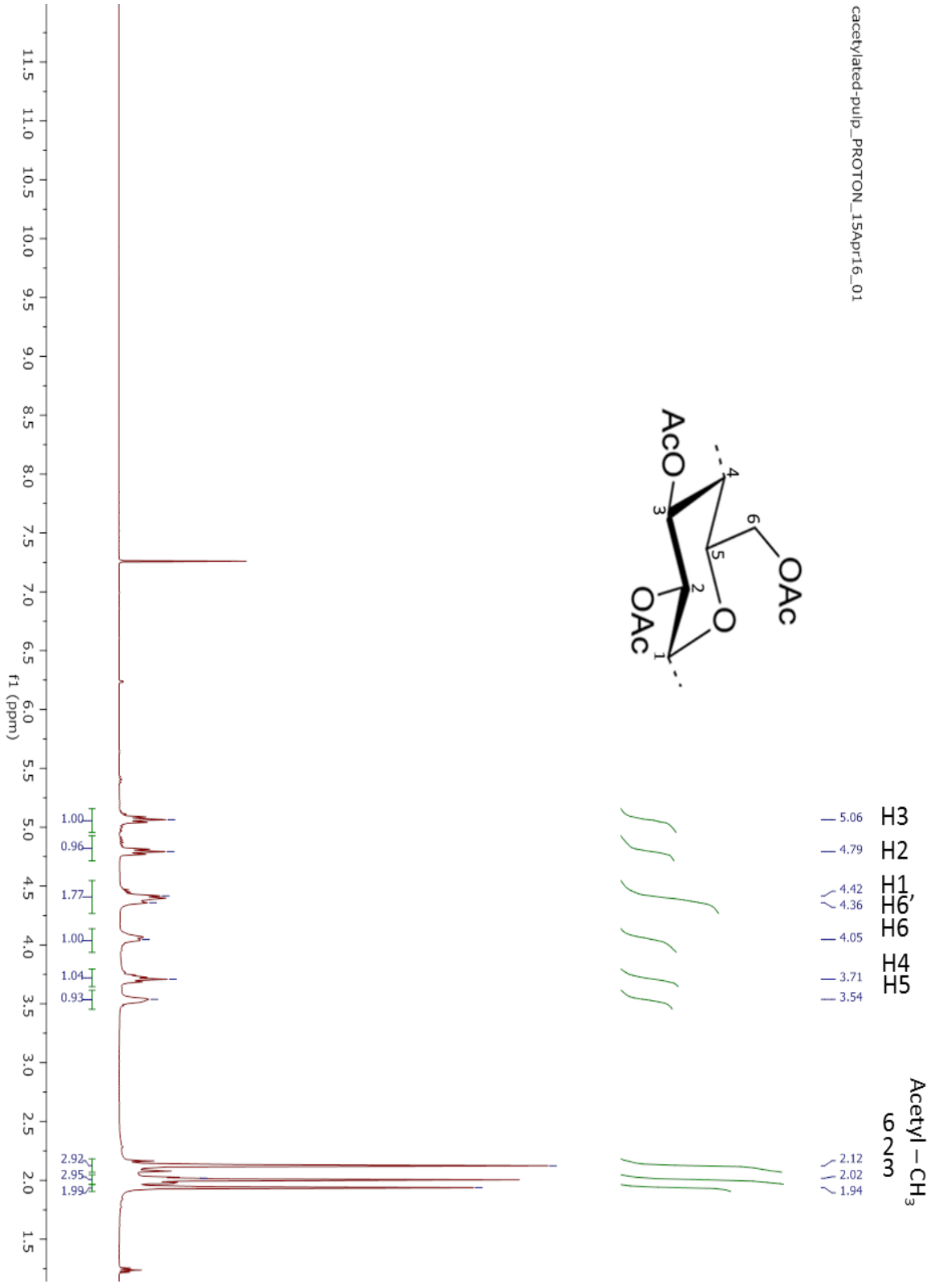

Fig B5. ^{1}H-NMR of acetylated organocat pulp

Appendices: Additional figures and index

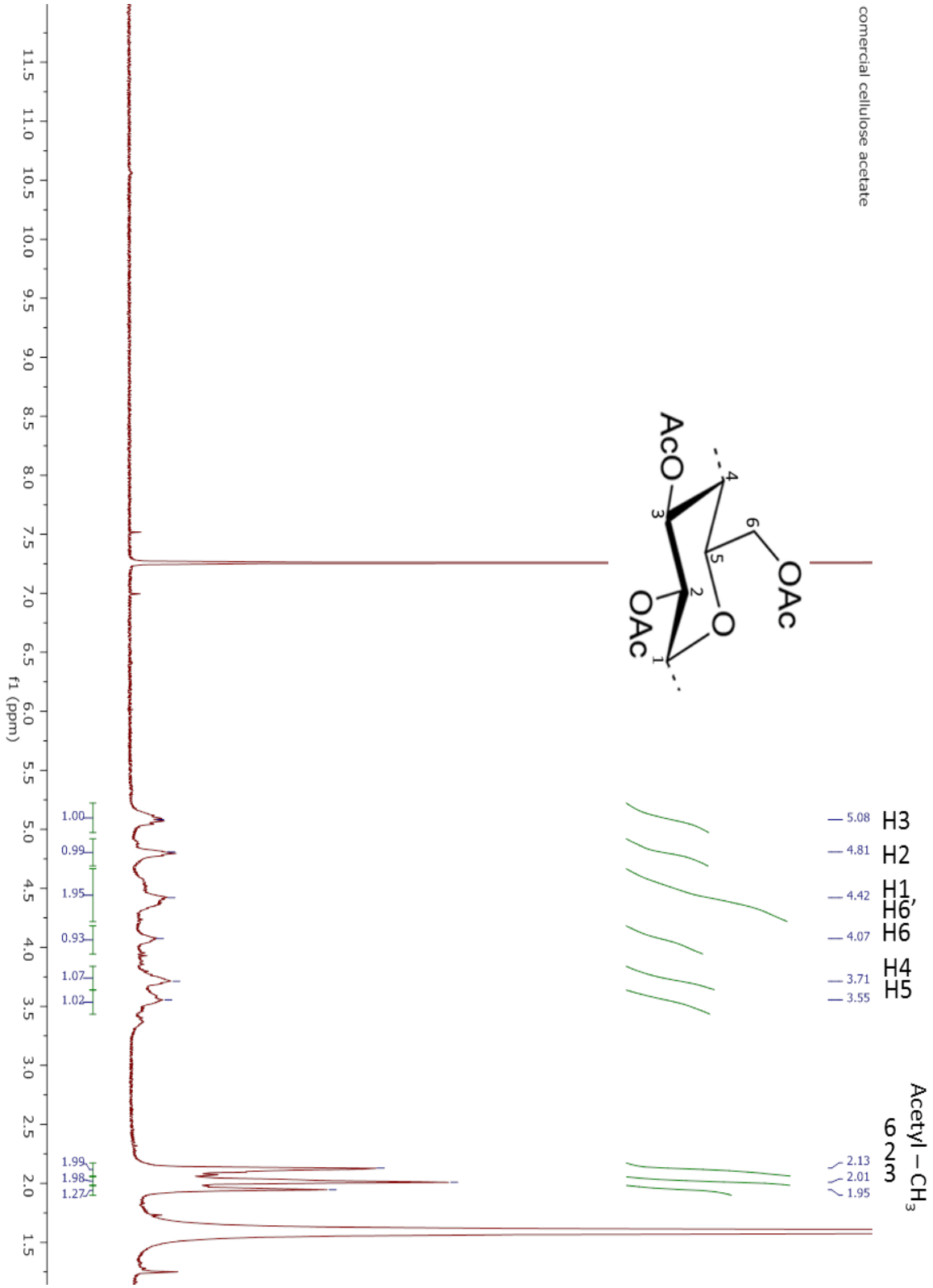

Fig B6. ^{1}H-NMR of commercial cellulose acetate

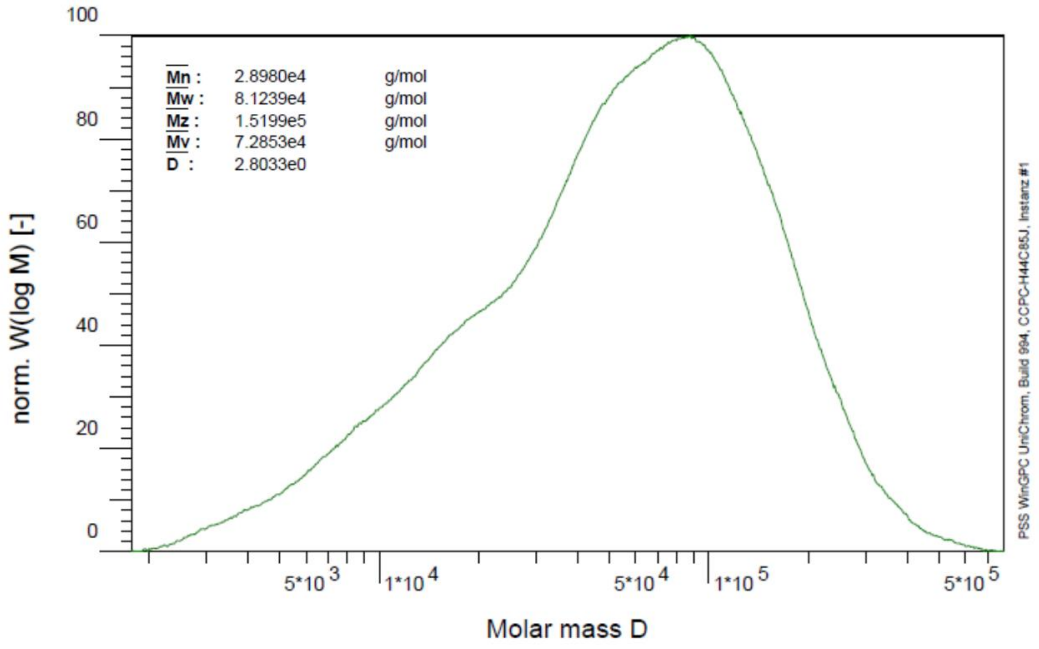

Fig B7. GPC of commercial cellulose acetate

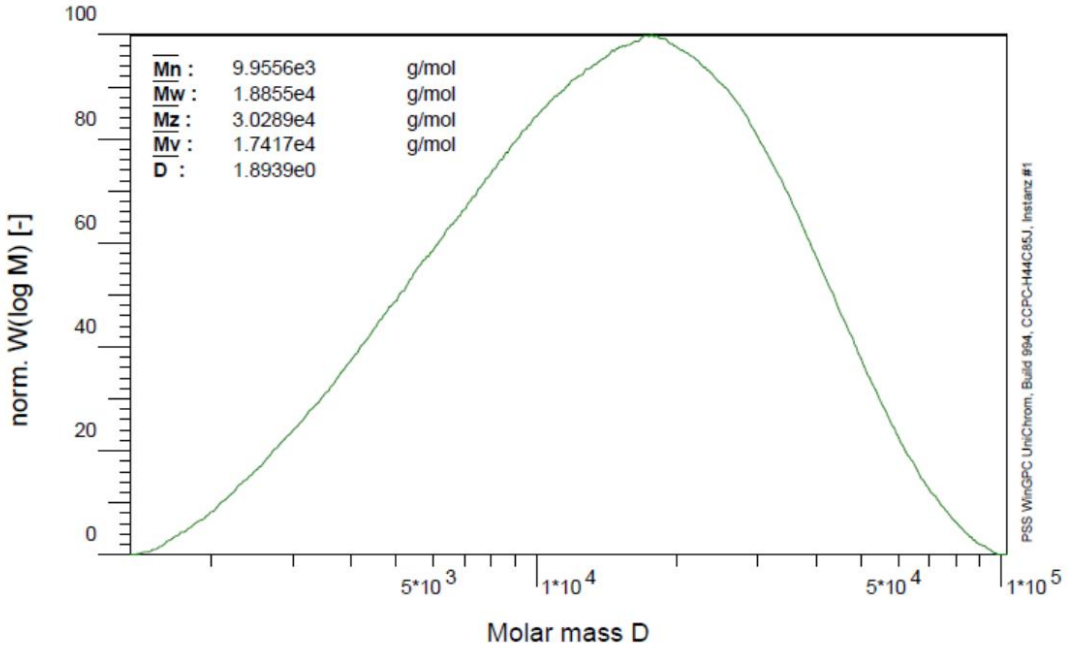

Fig B8. GPC of acetylated cellulose

Appendices: Additional figures and index

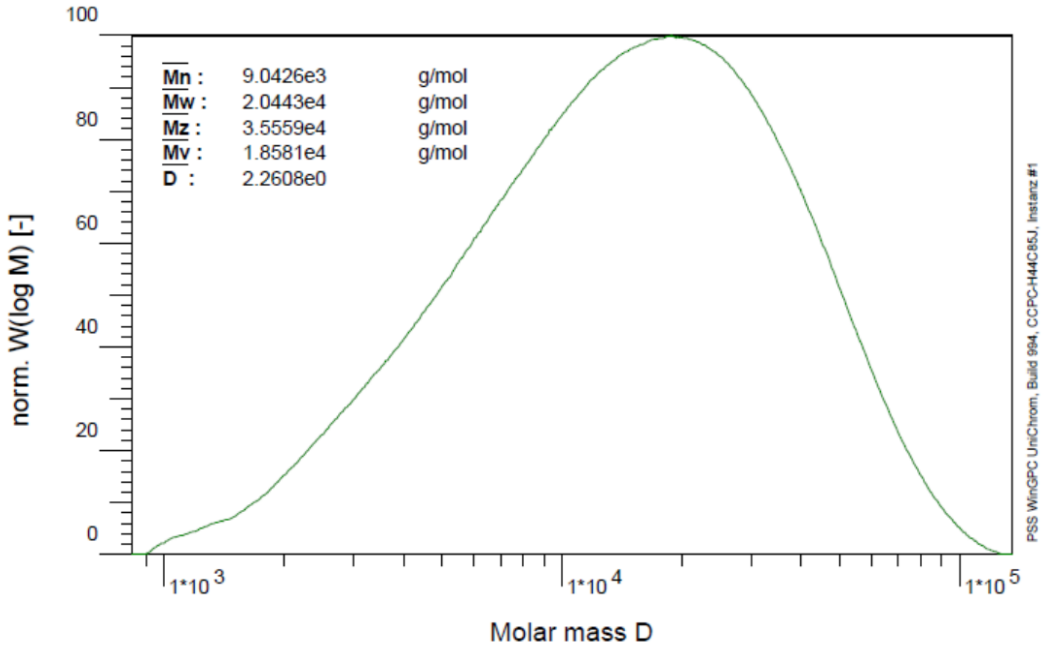

Fig B9. GPC of acetylated Organocat pulp

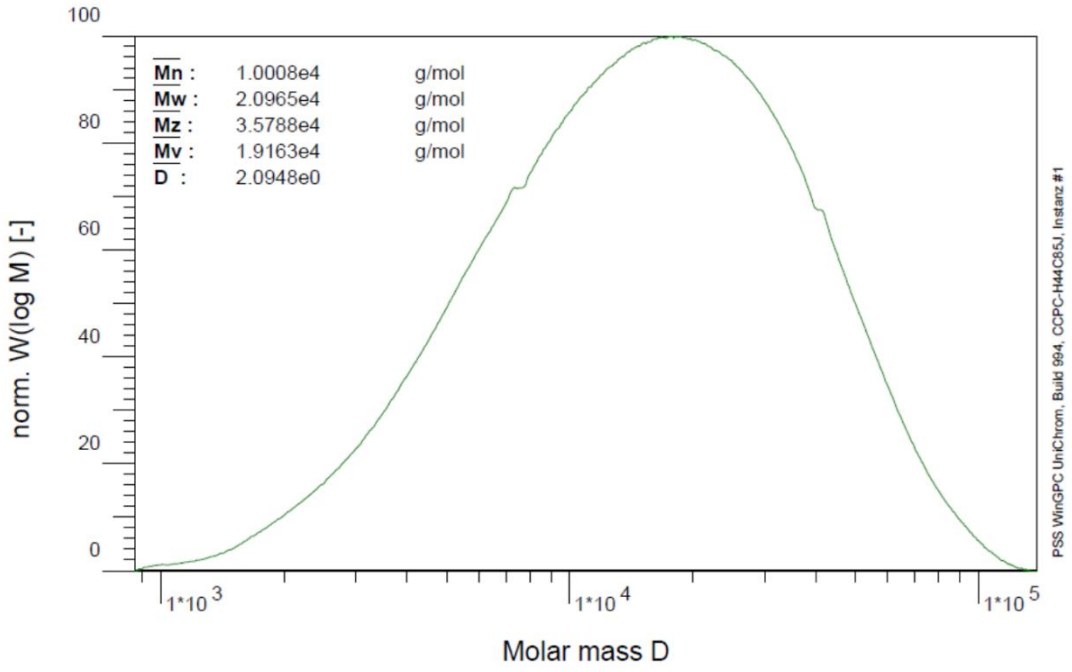

Fig B10. GPC of acetylated beech wood

Appendix C – Additional figures and table from chapter 4

Table C1. Elemental composition of the as-synthesized Co-Al spinel nanoparticles determined with energy dispersive X-ray spectroscopy (EDX)

Element	Weight %	Atomic %
C	9.11	13.17
O	33.46	47.67
Al	37.03	31.28
Co	20.39	7.89

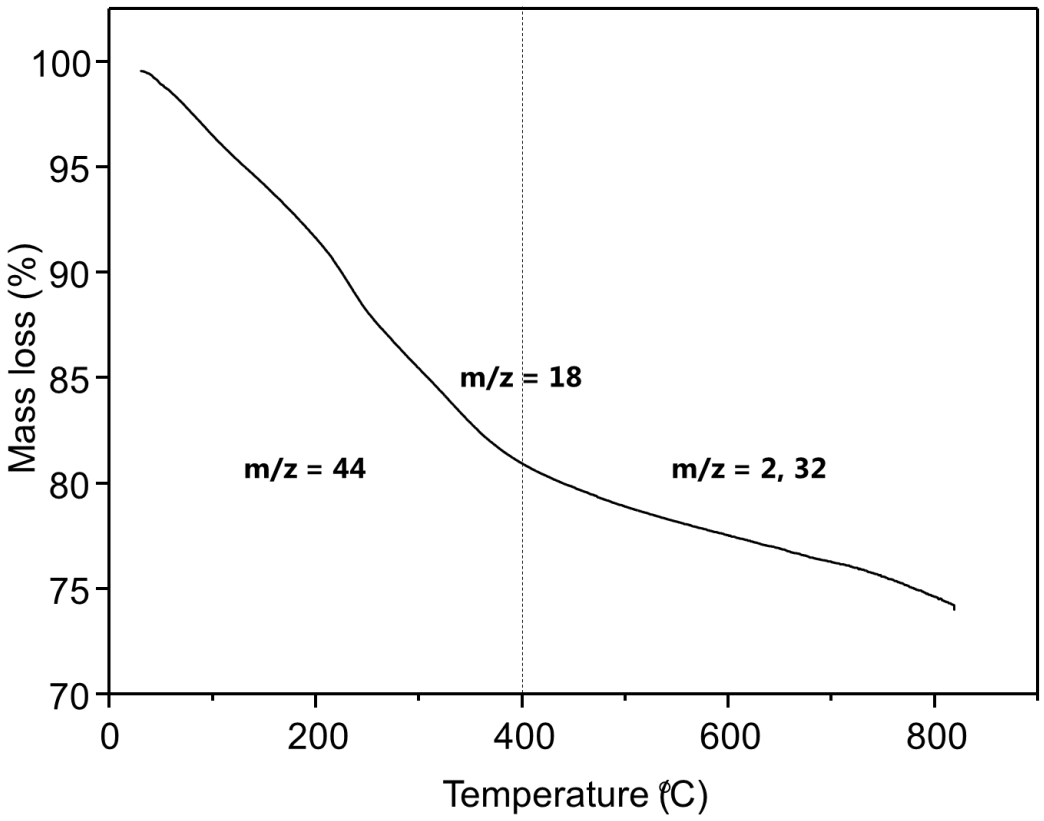

Figure C1. TGA profile of the as-synthesised sample

Appendices: Additional figures and index

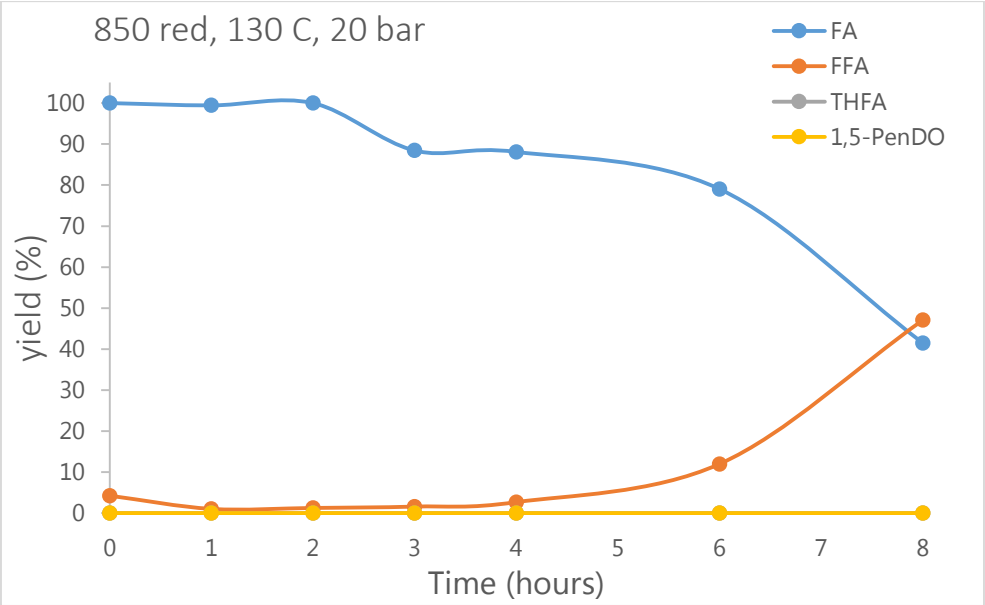

Figure C2. Furfural reduction during 8 hours. Conditions: 130 C, 20 bar H_2, 1000 rpm, 40 mg catalyst (reduced at 850°C)

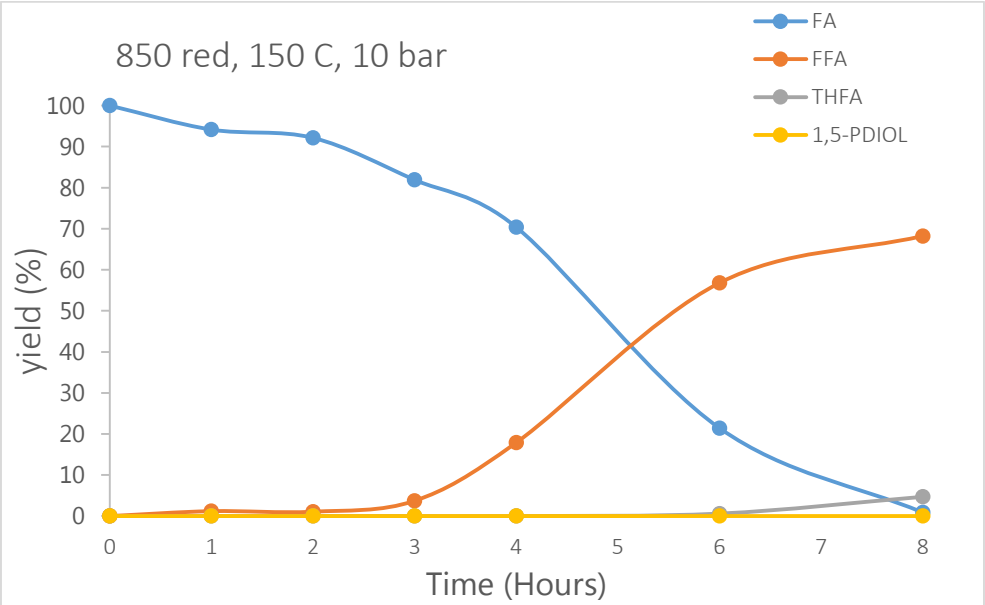

Figure C3. Furfural reduction during 8 hours. Conditions: 150 C, 10 bar H_2, 1000 rpm, 40 mg catalyst (reduced at 850°C)

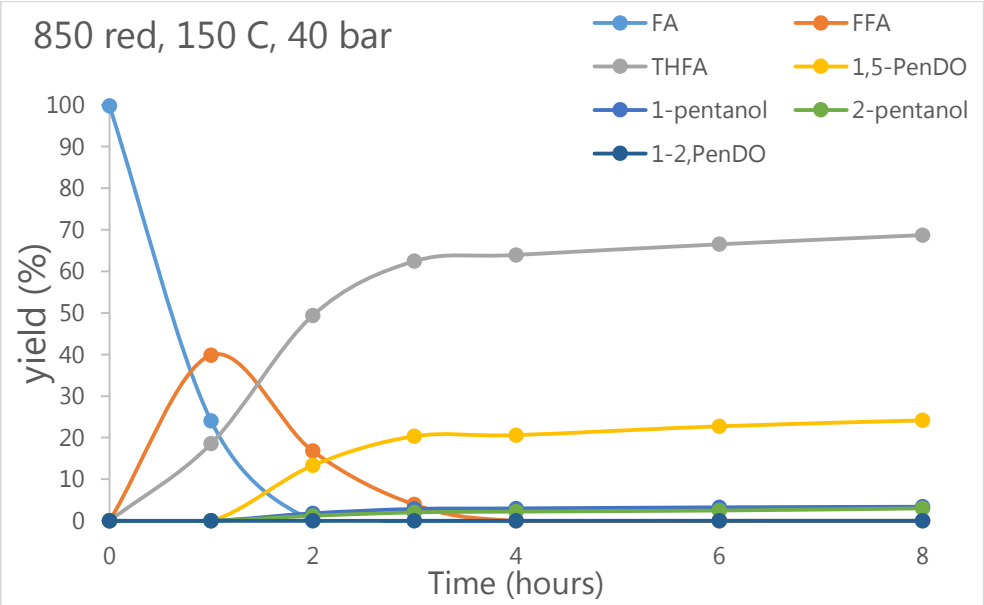

Figure C4. Furfural reduction during 8 hours. Conditions: 150 C, 40 bar H_2, 1000 rpm, 40 mg catalyst (reduced at 850°C)

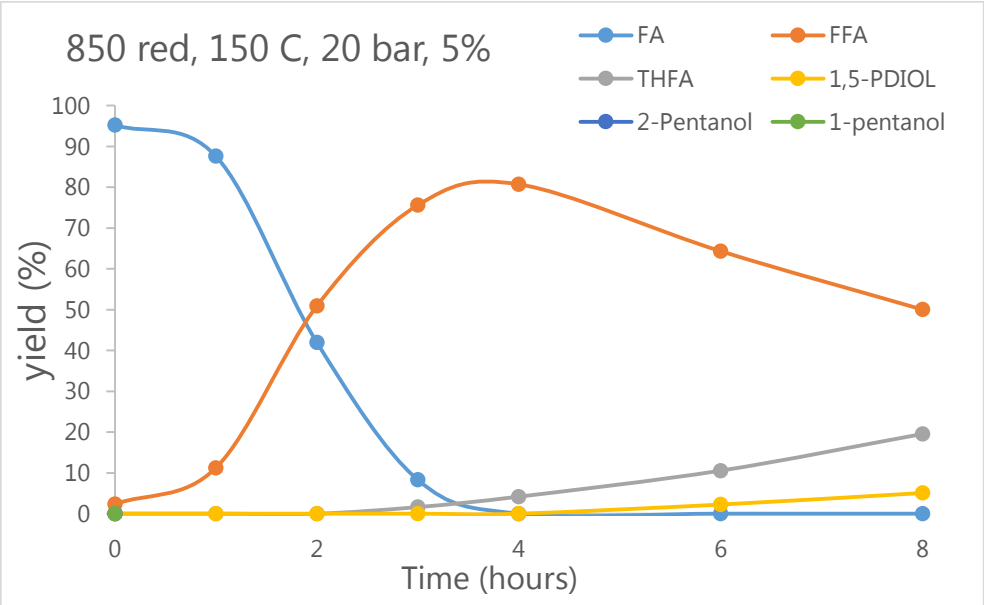

Figure C5. Furfural reduction during 8 hours. Conditions: 150 C, 40 bar H_2, 1000 rpm, 20 mg catalyst (reduced at 850°C)

Appendices: Additional figures and index

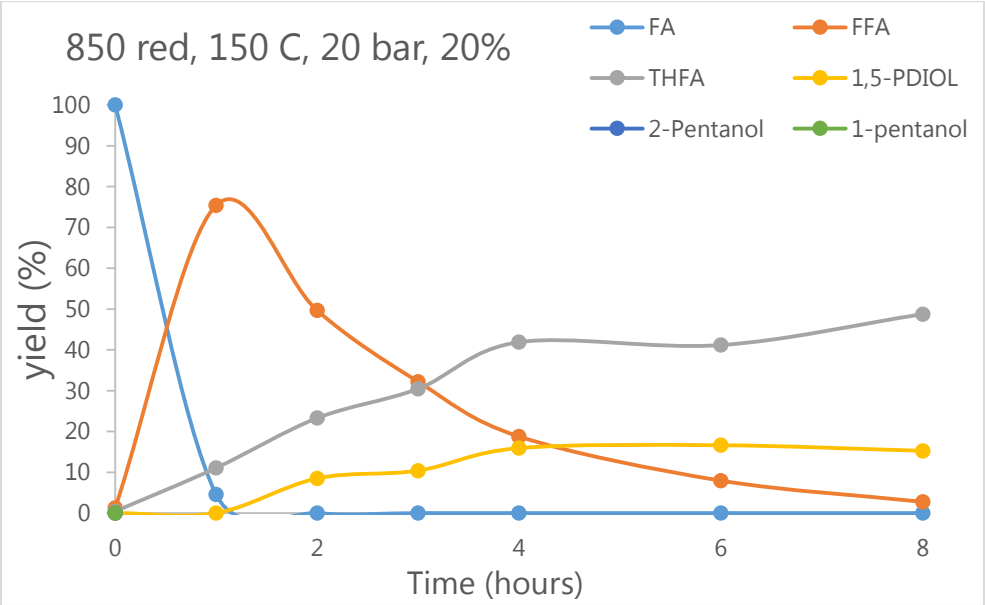

Figure C6. Furfural reduction during 8 hours. Conditions: 150 C, 40 bar H_2, 1000 rpm, 80 mg catalyst (reduced at 850°C)

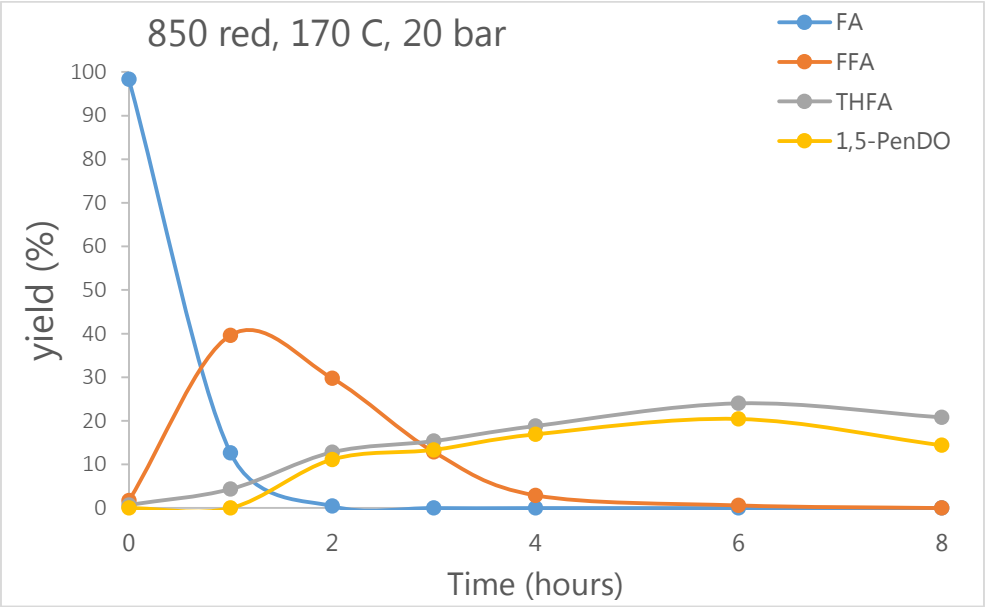

Figure C7. Furfural reduction during 8 hours. Conditions: 170 C, 20 bar H_2, 1000 rpm, 40 mg catalyst (reduced at 850°C)

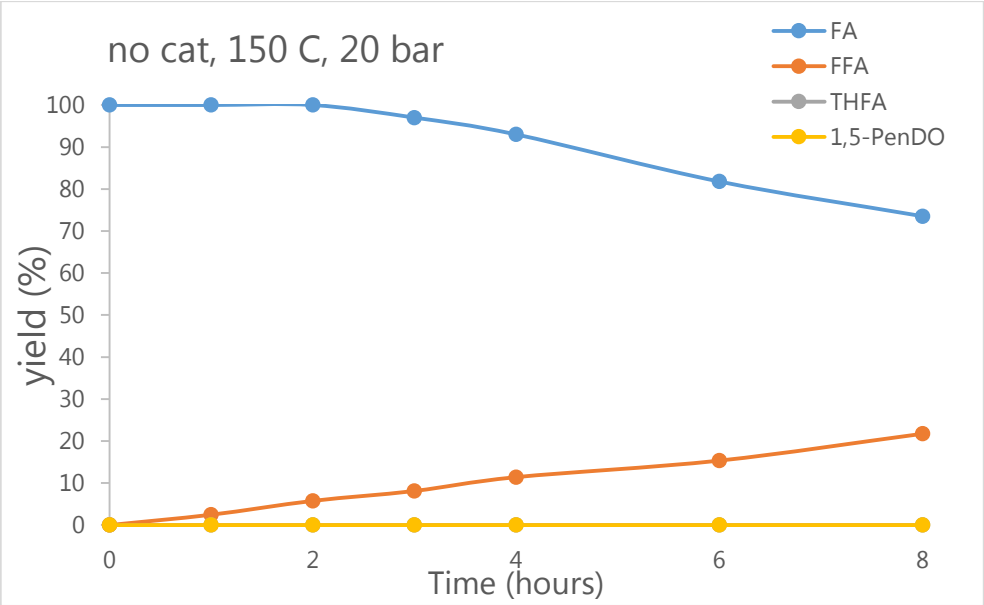

Figure C8. Furfural reduction during 8 hours. Conditions: 150 C, 20 bar H_2, 1000 rpm, without catalyst

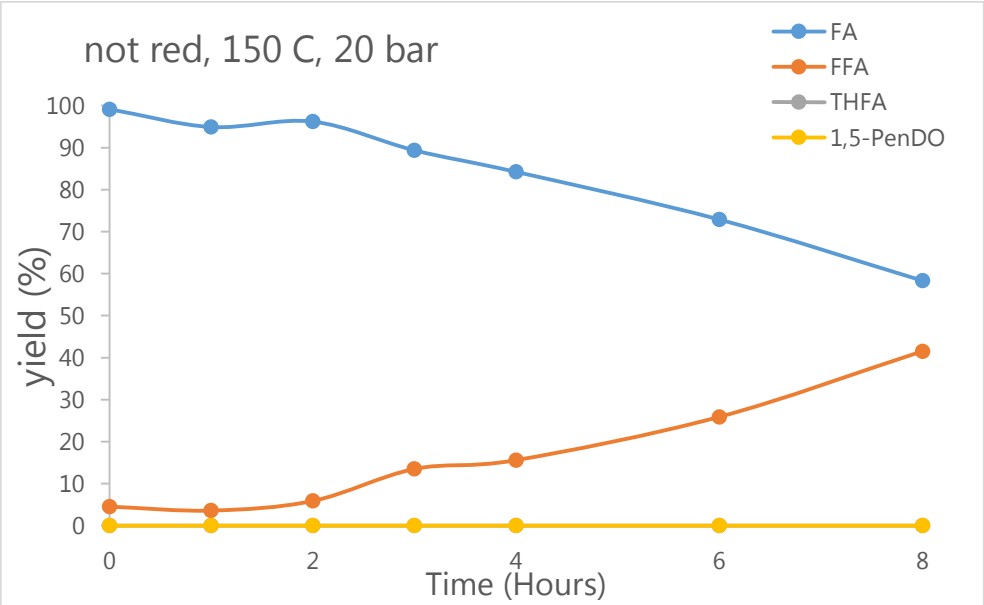

Figure C9. Furfural reduction during 8 hours. Conditions: 170 C, 20 bar H_2, 1000 rpm, 40 mg catalyst (without reduction)

Appendices: Additional figures and index

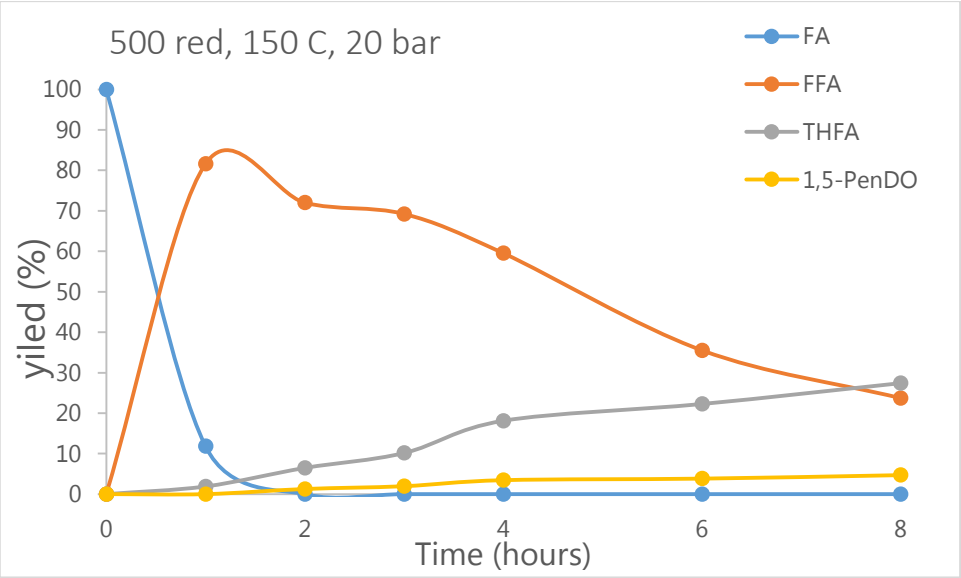

Figure C10. Furfural reduction during 8 hours. Conditions: 150 C, 20 bar H_2, 1000 rpm, 40 mg catalyst (reduced at 500°C)

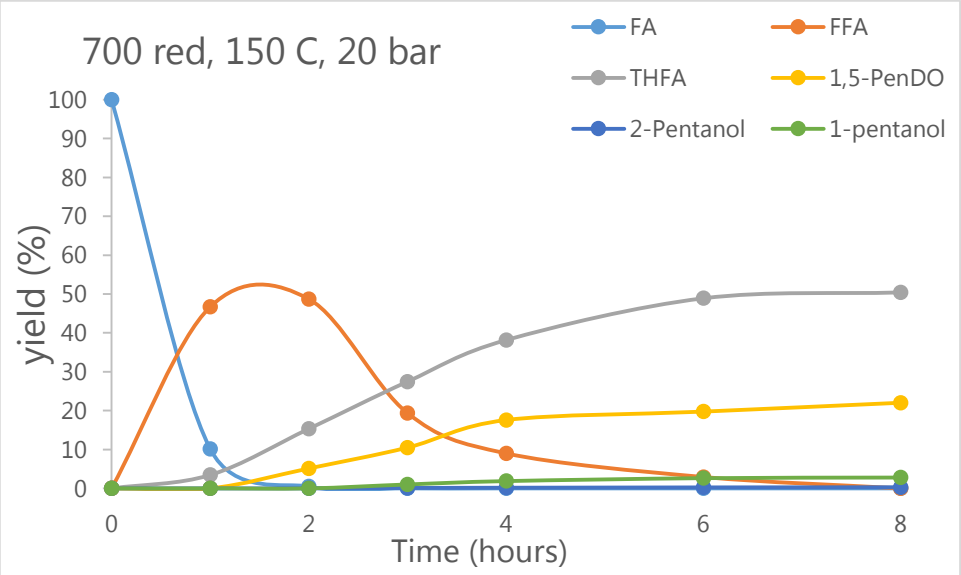

Figure C11. Furfural reduction during 8 hours. Conditions: 150 C, 20 bar H_2, 1000 rpm, 40 mg catalyst (reduced at 700°C)

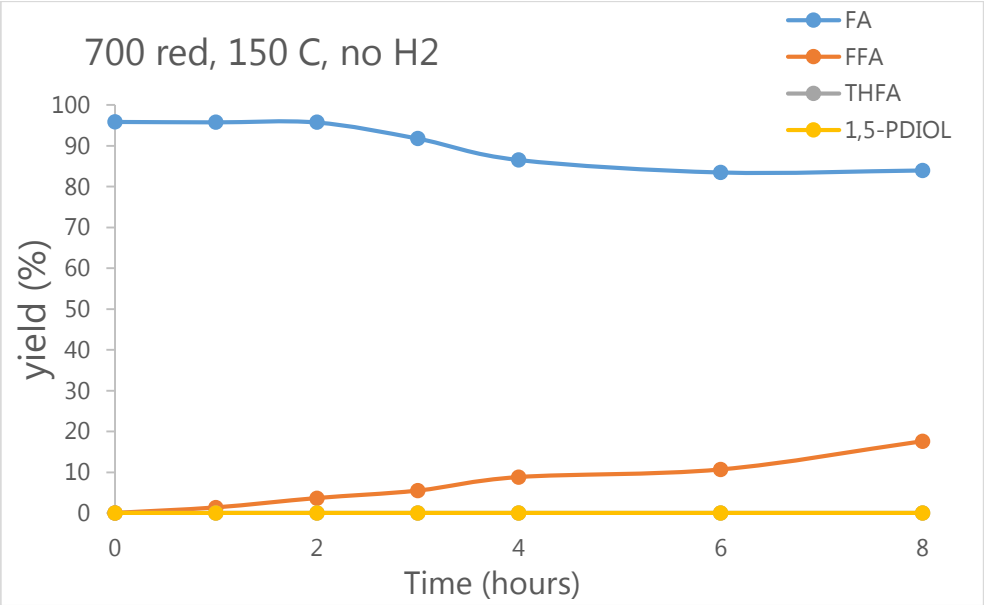

Figure C12. Furfural reduction during 8 hours. Conditions: 150 C, 0 bar H_2, 1000 rpm, 40 mg catalyst (reduced at 700°C)

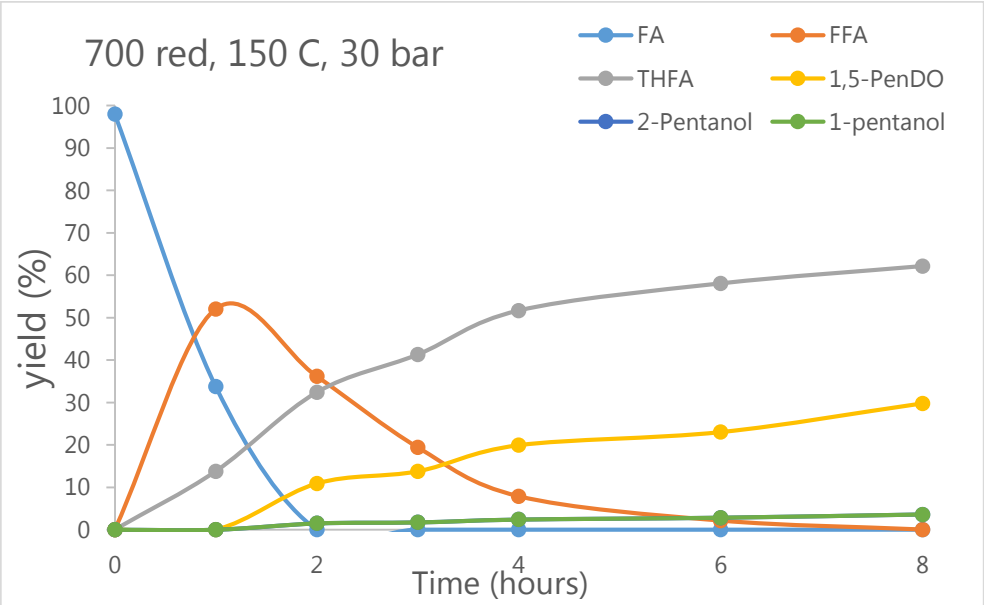

Figure C13. Furfural reduction during 8 hours. Conditions: 150 C, 30 bar H_2, 1000 rpm, 40 mg catalyst (reduced at 700°C)

Appendices: Additional figures and index

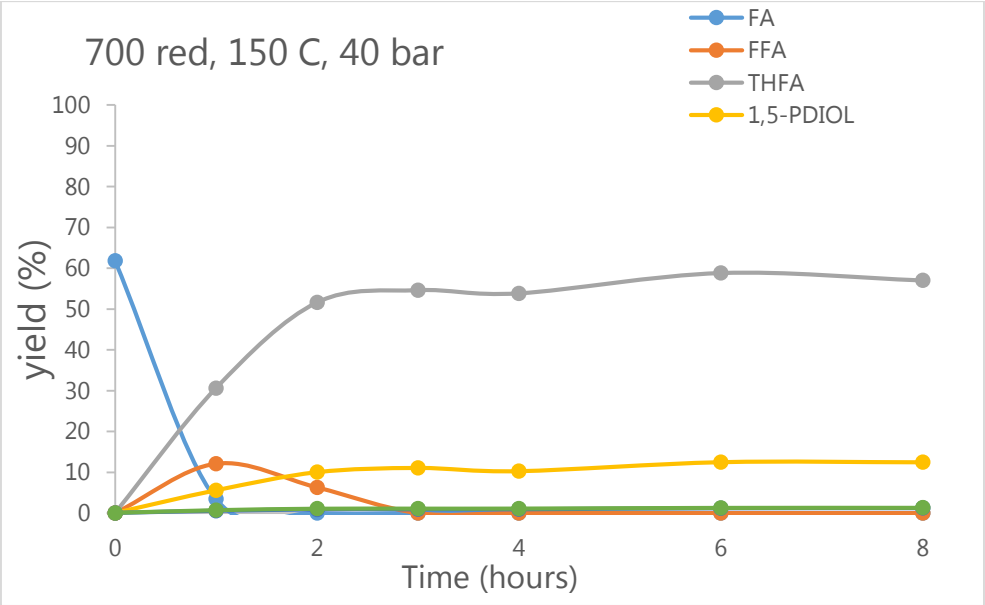

Figure C14. Furfural reduction during 8 hours. Conditions: 150 C, 40 bar H_2, 1000 rpm, 40 mg catalyst (reduced at 700°C)

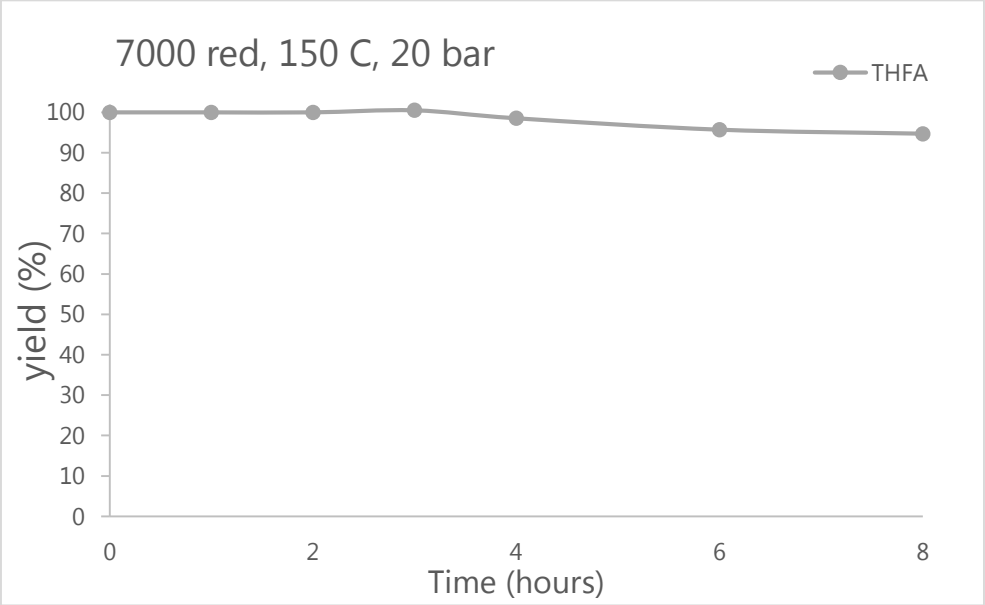

Figure C15. THFA reduction during 8 hours. Conditions: 150 C, 30 bar H_2, 1000 rpm, 40 mg catalyst (reduced at 700°C)

Appendix D – Index of figures

Appendix E – Index of tables

Appendix F – Index of scheme